AMERICAN UNIVERSITY OF BEIRUT

EFFECT OF SAND COLUMNS ON THE DRAINED LOAD RESPONSE OF SOFT CLAYS

by
YARA SALAH MAALOUF

A thesis
submitted in partial fulfillment of the requirements
for the degree of Master of Engineering
to the Department of Civil and Environmental Engineering
of the Faculty of Engineering and Architecture
at the American University of Beirut

Beirut, Lebanon
June 2012

AMERICAN UNIVERSITY OF BEIRUT

EFFECT OF SAND COLUMNS ON THE DRAINED LOAD RESPONSE OF SOFT CLAYS

by

YARA SALAH MAALOUF

Approved by:

Dr. Shadi Najjar, Assistant Professor Civil and Environmental Engineering	Advisor
Dr. Salah Sadek, Professor Civil and Environmental Engineering	Co-Advisor
Dr. Ghassan Chehab, Assistant Professor Civil and Environmental Engineering	Member of Committee

Date of thesis defense: June 11, 2012

AMERICAN UNIVERSITY OF BEIRUT

THESIS RELEASE FORM

I, Yara Salah Maalouf

☐ authorize the American University of Beirut to supply copies of my thesis to libraries or individuals upon request.

☐ do not authorize the American University of Beirut to supply copies of my thesis to libraries or individuals for a period of two years starting with the date of the thesis defense.

_____
Signature

_____
Date

ACKNOWLEDGMENTS

I am deeply grateful to my advisor Dr. Shadi Najjar for all his help, assistance, knowledge and patience throughout these four years spent at AUB.

The simple and efficient technical ideas provided by Mr. Helmi Al-Khatib were extremely helpful. Truly, I express my deep gratitude and thankfulness to him.

Special thanks to Mrs. Zakia Deeb for her administrative assistance.

Finally, deep thanks are dedicated to my husband and parents who continuously supported and encouraged me throughout the course of my tuition period.

ABSTRACT OF THE THESIS OF

Yara Salah Maalouf for Master of Engineering
Major: Civil Engineering

Title: Effect of Sand Columns on the Drained Load Response of Soft Clays

Compacted sand columns constitute an economical and environmentally friendly technique to treat and reinforce weak soils to increase their load-carrying capacity and to allow the soil to support loads from overlying structures. This method has been used for almost 30 years to improve the quality of both fine and coarse grained soils by increasing the bearing capacity, accelerating consolidation and improving the settlement response of the foundation. The extent of improvement depends on the confinement ensured by the surrounding soil, the presence of reinforcing material around the columns (geosynthetics) and the properties of the sand columns. The inclusion of geosynthetic reinforcement enhances load transfer from the soil to the columns and reduces total and differential settlement.

The objective of this thesis is to study the performance of clay specimens that are reinforced with sand columns of different diameters, heights, and confinement conditions and which are loaded under fully drained conditions to represent long-term stability conditions. The study is comprised of a series of triaxial tests that will be performed on back-pressure saturated normally consolidated Kaolin specimens that are prepared from slurry. The parameters that are varied in the study are the diameter of the sand column (2cm and 3cm), the height of the column relative to the height of the clay specimen (0.75 and 1.0), and the type of sand column reinforcement (no sand column, unreinforced sand column, and sand column reinforced with a geotextile). All tested samples will be consolidated and tested at confining pressures of 100 kPa, 150 kPa, and 200 kPa to study the effect of sand columns on the load response of soft clays.

CONTENTS

ACKNOWLEDGEMENTS…… v

ABSTRACT…… vi

LIST OF ILLUSTRATIONS……. xii

Chapter

1. INTRODUCTION AND SCOPE OF WORK……. 1

1.1. Introduction ……. 1

1.2. Significance of Stone Columns ……. 4

1.3. Methods of Construction of Stone Columns …...……..... 6

1.3.1. Top Feed Construction / Wet Vibro Replacement Method…….. 7

1.3.1. Bottom Feed Construction / Dry Vibro Displacement Method…….. 7

1.4. Scope of Work……. 8

1.5. Organization of Thesis …...……. 11

2. LITERATURE REVIEW……... 12

2.1. Introduction…….……. 12

2.2. Studies Involving 1-g Tests……. 15

2.2.1. Hughes and Withers (1974)…… 16

2.2.2. Narasimha Rao et al. (1992)……... 17

2.2.3. Muir Wood et al. (2000)….……... 18

2.2.4. Malarvizhi and Ilamparuthi (2004)..……. 19
2.2.5. McKelvey et al. (2004)…...…… 20
2.2.6. Ayadat and Hanna (2005)……... 21
2.2.7. Ambily and Gandhi (2007)……... 23
2.2.8. Murugesan and Rajagopal (2008)…….…… 25
2.2.9. Gniel and Bouazza (2009)……... 26
2.2.10. Murugesan and Rajagopal (2010)……... 27
2.2.11. Cimentada et al. (2011)…… 29
2.2.12. Shahu and Reddy (2011)….……. 30
2.2.13. Fattah et al. (2011)….……... 31

2.3. "Undrained" Triaxial Tests ……..……. 32

2.3.1. Sivakumar et al. (2004)…… 32
2.3.2. Black et al. (2007)……..……. 36
2.3.3. Najjar et al. (2010)…… 37

2.4. "Drained" Triaxial Tests …… 44

2.4.1. Black et al. (2006)…… 45
2.4.2. Black et al. (2011)……..……. 46
2.4.3. Sivakumar et al. (2011)…… 48

2.5. "Partially Drained" Triaxial Tests …….……... 49

2.5.1. Juran and Guermazi (1988)……... 50
2.5.2. Andreou et al. (2008)……... 51

2.6. Summary……..... 52

3. TEST MATERIAL AND SAMPLE PREPARATION…….... 53

3.1. Introduction……...…….…….. 53

3.2. Test Materials……...…….…….. 53

3.2.1. Kaolin Clay …….. 53
3.2.2. Ottawa Sand ……... 63
3.2.3. Geotextile Fabric …….. 66

3.3. Preparation of Normally Consolidated Kaolin Samples ……... 69

3.3.1. Preparation of Kaolin Slurry ……. 69
3.3.2. One-Dimensional Consolidometers ……. 70
3.3.3. One Dimensional Consolidation of Kaolin Slurry ……... 73
3.3.4. Sample Preparation Prior to Placement in the Triaxial Cell …… 76

3.4. Preparation of Sand Columns ……... 78

3.4.1. Encased Sand Columns with Geotextile Fabric ……. 80
3.4.2. Ordinary Sand Columns ……... 82

3.5. Summary……... 84

4. TRIAXIAL TESTING……. 86

4.1. Introduction……... 86

4.2. General Steps in Performing Consolidated Drained (CD) Tests ..….. 86

4.3. Creating Specimen and Test Data Files …….. 87

4.4. Seating Stage ……... 92

4.4.1. Seating the Piston …….. 92
4.4.2. Adjust the External Load Sensor…… 94
4.4.3. Fill the Cell Chamber with Water ..…….. 94
4.4.4. Cell Pressure Selection …….. 96
4.4.5. Flushing the Drains …… 97
4.4.6. Maintain the Volume……... 99

4.5. Back Pressure Saturation Stage……... 100

4.6. Isotropic Consolidation Stage ……... 102

4.7. Drained Shearing Stage ……... 103

4.8. Test Tear Down ……..... 105

4.9. Summary ……... 106

5. TEST RESULTS AND ANALYSIS …… 107

5.1. Introduction……...…….…….. 107

5.2. Test Results……..….. 108

5.2.1. Unreinforced/Control Kaolin Specimens ..…….. 108

5.2.2. Kaolin Specimens Reinforced with Sand Columns…….. 118

5.2.2.1. Modes of Failure ..……..... 110

5.2.2.2. Stress-Strain Behavior..……. 116

5.2.2.3. Effect of Sand Columns on Deviatoric Stress at Failure……. 117

5.2.2.4 Effect of Sand Columns on Volume Change…. 121

5.2.2.5. Effect of Sand Columns on the Drained Secant Modulus……. 122

5.2.2.6. Effect of Sand Columns on the Drained Shear Strength……. 129

5.3. Summary of Main Findings ……...…….…….. 133

6. COMPARISON BETWEEN DRAINED AND UNDRAINED TESTS……. 136

6.1. Introduction……...…….…….. 136

6.2. Test Results……..….. 136

6.2.1. Analysis for Control Kaolin Specimens..…….. 138

6.2.2 Analysis for Ottawa Sand Specimens …….…….. 141

6.2.3 Undrained and Drained Response for Clay Reinforced with Ordinary Sand Columns …….…… 143

6.2.3.1. Comparison between the Stress Strain Behavior. 143

6.2.3.2. Comparison between the Deviatoric Stress at Failure……..…….. 146

6.2.3.3. Comparison between the Effective Shear Strength Parameters……. 149

6.2.3.4. Comparison between Secant Young's Modulus.. 153

6.2.4 Undrained and Drained Response for Clay Reinforced with Encassed Sand Columns …… 156

6.2.4.1. Comparison between the Stress Strain Behavior. 156

6.2.4.2. Comparison between the Deviatoric Stress at Failure…….. 159

6.2.4.3. Comparison between the Effective Shear Strength Parameters……. 161

6.2.4.4. Comparison between Secant Young's Modulus.. 164

6.3. Summary of Main Findings ……... 166

7. CONCLUSIONS, RECOMMENDATIONS, AND FURTHER RESEARCH……..... 169

7.1. Introduction……... 169

7.2. Conclusions…….. ……... 169

7.3. Recommendations ……... 173

7.4. Further Research ……..... 175

Appendix

1. DEVIATORIC STRESS AND VOLUMETRIC STRAINS VERSUS AXIAL STRAINS FOR PARTIALLY PENETRATING SAND COLUMNS…… 178

2. DEVIATORIC STRESS AND VOLUMETRIC STRAINS VERSUS AXIAL STRAINS FOR FULLY PENETRATING SAND COLUMNS…… 179

REFERENCES..... 180

ILLUSTRATIONS

Figure Page

1.1(a) Vibroflot/poker (b) Vibroflot motion with vibrator parts..... 6

1.2(a) Top feed construction (wet method), (b) Bottom construction (dry method) 8

2.1 Effect of s/d and Ø on axial capacity of stone column (Ambily and Ghandi 2007)..... 25

2.2Effect of s/d and cu on stress concentration ratio (n) (Ambily and Ghandi 2007) 25

2.3 Stress-strain relationship for uniform loading: (a) wet compaction; (b) previously frozen sand column..... 35

2.4 Stress-strain and load-settlement behavior, comparison between reinforced and unreinforced columns (a) uniform loading, (b) foundation loading..... 35

2.5 Stress-strain response under uniform undrained loading for (a) single column and (b) group of columns..... 37

2.6 Modes of failure of clay specimens (upper part) and sand columns (lower part) reinforced with (a) fully penetrating column; (b) column with penetration ratio of 0.75; and (c) column with penetration ratio of 0.5 40

2.7Modes of failure of clay specimens with (a) fully penetrating unreinforced column; (b) fully penetrating reinforced column; (c) unreinforced column with penetration ratio of 0.5; and (d) reinforced column with penetration ratio of 0.5 40

2.8 Deviatoric stress and excess pore water pressure versus axial strain for kaolin specimens reinforced with non encased sand columns ((σ'3)o=150 kPa) 42

2.9 Deviatoric stress and excess pore water pressure versus axial strain for kaolin specimens reinforced with encased sand columns ((σ'3)o=150 kPa) 42

2.10 Effective failure envelops for unreinforced and reinforced kaolin specimens 44

2.11 Load-settlement behavior for control and reinforced specimens (L/D = 6 and 10)..... 46

2.12 Settlement under unit cell consideration with increasing area replacement ratio..... 48

2.13 Bearing Pressure-settlement characteristics..... 49

2.14 Effect of drainage on response of reinforced soil specimens to triaxial compression..... 50

2.15 Variation of deviator stress and excess pore pressure with axial strain..... 51

3.1 e-log P for normally consolidated Kaolin clay 56

3.2 Variation of Cv with consolidation pressure for Kaolin clay 58

3.3 Displacement vs. Log time for consolidation pressure of 10, 20 and 50 kPa..... 59

3.4 Displacement vs. Log time for consolidation pressure of 100, 200, and 383 kPa..... 60

3.5 Displacement vs. square root of time for consolidation pressure of 10 kPa, 20 kPa, and 50 kPa..... 61

3.6 Displacement vs. square Root of time for consolidation pressure of 100 kPa, 200 kPa, and 383 kPa..... 62

3.7 Sieve analysis curve for Ottawa sand 64

3.8 Deviatoric stress and volumetric strain versus axial strain for Ottawa sand 65

3.9 Mohr Coulomb effective stress failure envelop for Ottawa sand 66

3.10 Preparation of cylindrical geotextile fabric of diameter (a)2cm and (b)3cm..... 67

3.11 Performing pull out test on geotextile fabric 68

3.12 Electric Mixer for preparing Kaolin slurry 70

3.13 Picture for custom fabricated 1-dimensional consolidometers 71

3.14 Photo for (a) Split PVC pipe and (b) Wrapped PVC pipe with duct tape 71

3.15 Custom fabricated 1-dimensional consolidometer..... 73

3.16 Water content and void ratio along the height of the sample after consolidation..... 75

3.17 (a) Kaolin specimen after removal from custom fabricated consolidometer, (b) dismantling of PVC pipe, and (c) Kaolin specimen after removal form PVC pipe. 76

3.18 (a) Kaolin specimen after trimming, (b) Installation of porous stones, (c) installation of filter paper around Kaolin specimen..... 77

3.19 (a) Brass tube with the rubber membrane. (b) Installation of Kaolin specimen on the cell chamber, (c) Insertion of glass cover around cell chamber 78

3.20 Wrapping the Kaolin specimen with PVC tubes prior to auguring 79

3.21 Custom fabricated auguring machine (a) 2cm -diameter auger (b) auguring of specimen by 2cm diameter augur, (c) Removal of Kaolin material by 3 cm diameter augur 79

3.22 Vibration of encased sand columns with geotextile fabrics, (a) 3cm column diameter and (b) 2 cm column diameter..... 81

3.23 Installation of 3-cm diameter encased sand column with geotextile fabric..... 82

3.24 (a) Freezing the sand columns (b) and (c) removal of geotextile fabric..... 83

3.25 Photographs (a) Predrilled 3-cm diameter hole, (b) Insertion of frozen sand column in clay, and (c) Reinforced Kaolin specimen with frozen sand column. 84

3.26 Photograph of vertical cross section of Kaolin specimen with ordinary sand column of diameter 2cm and height 10.65cm after column insertion..... 84

4.1 Automated triaxial equipment “TruePath” 87

4.2. Selection of sensor button 88

4.3. Selection of the cell pressure sensor 88

4.4 Initializing readings for the selected sensors 89

4.5 Entering file menu to select Specimen Data 90

4.6 Writing the specimen data information 91

4.7 Entering the control test parameters 91

4.8. Selection for the manual mode 92

4.9 Reduction of gap between the piston and the load button 93

4.10 Window for seat piston 93

4.11 Adjustment for the external load transducer 94

4.12 Filling the cell chamber with water 95

4.13 Steps for filling the cell chamber with water 96

4.14 Application of initial confining pressure 97

4.15 Flushing of the drains 98

4.16 Application of confining pressure 99

4.17 Window for back pressure saturation stage 101

4.18. View the curve during the saturation process 102

4.19 Window for “B” value check 102

4.20 Window for isotropic consolidation..... 103

4.21 Window for drained shear test 104

4.22 Window for unloading stage 106

5.1 Deviatoric stress and volumetric strain versus axial strain for unreinforced/control specimen at confining pressures of 100 kPa, 150 kPa, and 200kPa 109

5.2 Mohr Coulomb effective stress failure envelope for control/unreinforced Kaolin specimens 110

5.3 Example of external and internal modes of failure of test specimens (Hc/Hs = 0.75 and Ac/As = 7.9%, ordinary) 113

5.4 Example of external and internal modes of failure of test specimen (Hc/Hs = 0.75 and Ac/As = 17.8% encased). 114

5.5 Example of external and internal modes of failure of test specimen (Hc/Hs = 1.0 and Ac/As = 17.8% encased). 115

5.6 Deviatoric stress and Volumetric strain versus axial strain for Kaolin specimen reinforced with 2-cm sand columns (Ac/As=7.9%) 119

5.7. Deviatoric stress and Volumetric strain versus axial strain for Kaolin specimen reinforced with 3-cm sand columns (Ac/As=17.8%) 120

5.8 Variation of improvement in deviatoric stress at failure with confining pressure (dotted lines for the encased sand columns) 122

5.9 Relationship between improvements in deviatoric stress and reduction in volumetric strains at failure for (a) Ac/As=7.9% and (b) Ac/As=17.8% 124

5.10 Variation of (Esec)1% with effective confining pressure (dotted lines represent encased

columns)..... 125

5.11 Variation of (Esec) with strain for control and composite specimens..... 127

5.12 Predicted and measured variation of (Esec) with strain for control and composite specimens (Hc/Hs=1, Ac/As=17.8%, ordinary)..... 129

5.13. Variation of predicted stress concentration factors with axial strain..... 130

5.14 Drained failure envelopes for unreinforced and reinforced kaolin specimens 133

5.15 Mohr-Coulomb envelopes for the 3-cm sand columns for partially and fully penetrating columns..... 134

6.1 Deviatoric stress, excess pore pressure, and volumetric strain versus axial strain for control clay (Dotted lines indicate undrained tests and solid lines indicate drained tests). 141

6.2 Comparison between Mohr-Coulomb failure envelops for control clay specimens from CD and CU triaxial tests..... 142

6.3 Deviatoric stress, excess pore pressure, and volumetric strain versus axial strain for Ottwa sand (Dotted lines indicate undrained tests and solid lines indicate drained tests). 144

6.4 Comparison between Mohr-Coulomb failure envelops for Ottawa sand specimens from CD and CU triaxial tests..... 145

6.5 Comparison between the variation of the deviatoric stress, excess pore pressure, and volumetric strain with axial strain for drained and undrained loading conditions (ordinary sand columns, partial penetration). 146

6.6 Variation of deviatoric stress and volumetric strain with axial strain (ordinary sand columns, full penetration)..... 148

6.7 Improvement in the deviatoric stress at failure for (a) partially penetrating ordinary sand columns and (b) fully penetrating ordinary sand columns for drained and undrained tests..... 149

6.8 Mohr-Coulomb failure envelopes (samples with ordinary 2-cm sand columns)..... 152

6.9. Mohr-Coulomb failure envelopes (samples with ordinary 3-cm sand columns)..... 153

6.10 Variation of (Esec)1% with effective confining pressure for samples reinforced with ordinary sand columns 157

6.11 Comparison between the variation of the deviatoric stress, excess pore pressure, and volumetric strain with axial strain for drained and undrained loading conditions (encased sand columns, partial penetration). 159

6.12 Comparison between the variation of the deviatoric stress, excess pore pressure, and volumetric strain with axial strain for drained and undrained loading conditions (encased sand columns, full penetration). 160

6.13 Improvement in the deviatoric stress at failure for (a) partially penetrating encased sand columns and (b) fully penetrating encased sand columns for drained and undrained tests. 162

6.14 Mohr-Coulomb failure envelopes (samples with encased 2-cm sand columns)..... 164

6.15 Mohr-Coulomb failure envelopes (samples with encased 3-cm sand columns)..... 163

6.16 Variation of (Esec)1% with effective confining pressure for samples reinforced with encased sand columns. 167

Fig.A. 1 Deviatoric stress and volumetric strain versus axial strain for partially penetrating sand columns encased and non-encased for confining pressures of 100, 150 and 200kPa……..178

Fig.A. 2 Deviatoric stress and volumetric strain versus axial strain for fully penetrating sand columns encased and non-encased for confining pressures of 100, 150 and 200kPa……..179

CHAPTER 1

INTRODUCTION AND SCOPE OF WORK

1.1. Introduction

Granular columnar inclusions are generally used to improve the mechanical properties of soft clays. This is generally accomplished either by the use of sand drains/columns to accelerate the rate of consolidation of the soft clay, or by replacing part of the soft clay with stiff granular columns (ex. vibro-replacement). Najjar et al. (2010) state that when sand columns are used as vertical drains to accelerate the rate of construction, the possible positive reinforcing role that these columns can play with regards to improving the short term and long term bearing capacity of the clay/sand column system is usually neglected in design.

Since short term stability conditions generally govern the design of foundation systems that are supported on soft normally consolidated clay, the possible improvement that could be brought by the inclusion of sand columns to the undrained shear strength of the clay/sand column system is of major interest. Najjar et al. (2010) and Maakaroun et al. (2009) designed and implemented a laboratory testing program that is based on "undrained" triaxial tests (32 consolidated undrained tests with pore pressure measurement) on normally consolidated Kaolin specimens that were reinforced with partially and fully penetrating single sand columns. The parameters that were varied were the diameter of the sand columns, the depth of penetration of the columns, the type of columns (geotextile-encased versus non-encased) and the effective confining pressure. Results reported in Najjar et al. (2010) indicated that sand columns improved the undrained strength of the clay significantly even for area replacement ratios that were less than 18%. The increase in undrained strength was accompanied by a decrease in pore pressure

generation during shear and an increase in stiffness. However, the effective shear strength parameters were found to be relatively unaffected by the sand column reinforcement, except for fully penetrating columns with high area replacement ratios.

Sand columns in the field are expected to act as drains that will exhibit drained behavior when sheared. In the triaxial tests conducted in the study by Najjar et al. (2010), no drainage was allowed through the sand columns, which represented an extreme condition in undrained loading. This discrepancy in the drainage conditions between the field and the laboratory has mainly two contradicting implications. The first implication is that the sand columns in the laboratory could exhibit generation of negative pore water pressures, a behavior which may not be applicable to field conditions, where the sand columns are expected to be freely draining. The second implication is that the clay in the undrained laboratory testing program cannot exhibit any partial drainage through the sand columns, thus eliminating any possibility for pore pressures to dissipate through the sand columns. This behavior is also not applicable to practical field conditions in which the clay is expected to exhibit partial dissipation of pore pressure through the sand columns under typical construction loads. The two implications mentioned above are expected to have opposite effects with regards to expected improvements in the undrained shear strength of the clay-sand column composite.

Juran and Guermazi (1987) and Andreou et al. (2008) studied the effects of partial drainage and rate of loading on the improvement brought by the addition of sand columns to soft soils in a triaxial framework. Juran and Guermazi (1987) performed instrumented triaxial tests on identical soft silty soil specimens that were reinforced with identical compacted river-sand columns while allowing drainage of the sand column in one specimen (partially drained tests) and prohibiting drainage of the sand column in the other (undrained tests). Results indicated that

the maximum load carried by the “drained” column was about twice that carried by the “undrained” column. These results indicate that allowing drainage in sand columns (which is the practical case in the field) is expected to improve the shear performance of the composite system, compared to the case where the columns are undrained. Similar results were obtained by Andreou et al. (2008) who conducted triaxial compression tests on a kaolin clay reinforced with single sand columns using drained, undrained, and partially drained tests. Results indicated that the maximum deviatoric stress carried by the reinforced sample under drained conditions (drained loading at 0.003 mm/min) is twice that of the undrained condition (undrained loading at 0.3mm/min). An increase in the rate of loading from 0.003 to 0.3mm/min while allowing drainage lead to a reduction in the strength of the reinforced sample compared to the fully drained case; however, the measured strength remained higher than that of the reinforced undrained sample.

The “undrained” triaxial tests conducted by Najjar et al. (2010) on soft clays that were reinforced with sand columns represent an extreme condition of undrained loading in the field. Based on the limited results presented in Juran and Guermazi (1987) and Andreou et al. (2008), it can be concluded that (1) results from “undrained” triaxial tests on reinforced clay specimens could underestimate the degree of improvement in shear strength of the clay-sand column system compared to the expected field condition, (2) the more realistic case of partial drainage through the sand column may lead to an added improvement in the short-term bearing capacity of the clay/sand column composite, and (3) the drained strength of the clay/sand column composite could provide an upper bound for the bearing capacity.

The objective of the research in this thesis is to investigate the behavior of clay/sand column composites at the extreme loading condition represented by the fully drained case, where

the drained shear strength of the clay/sand column composite is the parameter of interest. The results of such fully drained tests could bracket the range of loading conditions that could exist in practical field applications involving the use of sand/stone columns in soft clays. There is a need for a focused and comprehensive test program that aims at investigating the load response of clay/sand column composites under fully drained conditions. Results of such a testing program could fill a gap in the current knowledge on the long-term shearing behavior of reinforced soft clays and could provide an upper bound for the shear strength of these composites in practical field applications.

1.2. Significance of Stone Columns

The wide-spread development of urban cities and the expansion of industrial projects have urged investors and developers to look for available land for future construction. However, the majority of available future expansion sites are generally located in areas where the ground conditions are not favorable for carrying typical structural loads. Examples of soft lands include water front sites, recently deposited alluvium areas, and filled ground locations. In spite of the unfavorable ground conditions for these sites, a considerable number of projects are being constructed on weak soils provided that ground improvement techniques are implemented to improve the mechanical properties of the soil. Typical ground improvement techniques include installation of vibro-stone columns, preconsolidation using prefabricated or sand column vertical drains, drilling or driving piles into competent strata, and preloading of fill with/out vacuum. Soil improvement techniques that involve the use of stone/sand columns were adopted in European countries in the early 1960’s and their use spread thereafter following their successfully implementation in different countries.

Contrary to pile foundations which are designed to bypass weak layers of soil to transfer superstructure loads into competent strata, the use of stone/sand columns in clayey soils will take advantage of the surrounding weak soil and improve its load carrying capacity. Upon application of load, stone columns generally expand and bulge, thus exerting lateral pressure to the weak surrounding clay. In addition, and contrary to conventional piles, stone columns will reduce the dissipation of excess pore water pressure during loading.

The positive effect of the stone columns can be improved by encasing the columns with geotextiles to provide additional lateral support to the stone column. The installation of geosynthetics around the perimeter of the stone column can reduce the bulging of the sand column during loading, thus increasing the stiffness and bearing capacity of the sand column. This will in turn increase the ability of the hybrid clay sand column system to sustain the applied loads. Murugesan and Rajagopal (2006) recommend encasing stone columns with geogrids especially when the clay is very soft with undrained shear strength that is below 20 kPa.

Finally, vibro stone columns are seen as environmentally friendly (McKelvey et al. 2000). The stone column is possibly the most "natural" foundation system in existence. They are also more durable than any other foundation system that would involve the use of cement or steel. As a result, reinforced sand columns can be considered as one of the vital ground improvement techniques that can be adopted for improving and enhancing the load carrying capacity of the weak clayey soils. Sand columns have been successfully used in different structures such as under liquid storage tanks, earthen embankment, low rise buildings, industrial ware houses, and under raft foundations.

1.3. Methods of Construction of Stone Columns

Stone columns construction necessitates a partial replacement (10% to 35%) of unsuitable surface soil with a compacted vertical column of granular material that usually fully penetrates the weak soil. Typical column lengths range from 3m to 15m with diameters ranging from 0.5m to 1.5m. Stone columns can support loads up to 300 kN (Hughes and Withers 1970). There are two methods for constructing stone columns: 1) Wet method, known as top feed method or vibro-replacement method, and 2) Dry method, known as bottom feed method, or vibro-displacement method. The term vibroflot or poker is used to describe the probe which penetrates the weak soil (Fig. 1.1.a). Rotation of the eccentric weight within the body of the probe causes lateral vibration at the tip of the probe, thus inducing a lateral force varying approximately from 12 to 28 tons (Fig. 1.1.b). The probe usually varies in diameter from 0.3m to 0.5m with a length of 2m to 5m. The vibrator is suspended from the boom of crane where a 10 m probe can easily be handled with a 40 ton crane with a 12m boom length.

(a)

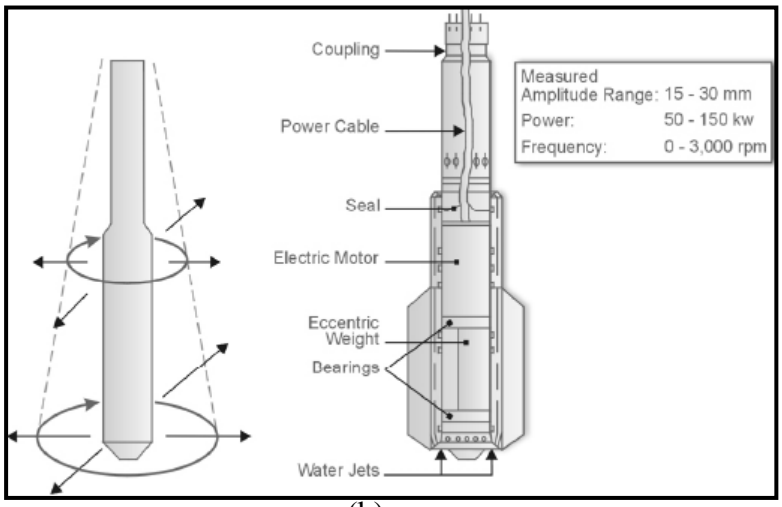

(b)

Fig. 1.1(a) Vibroflot/poker (b) Vibroflot motion with vibrator parts

1.3.1. Top Feed Construction / Wet Vibro Replacement Method

In the vibro replacement (wet) method (Fig. 1.2.a). A hole is formed in the ground by jetting a probe down to the desired depth. Jetting water is used to remove soft material, stabilize the probe hole, and guarantee that the stone backfill reaches the tip of the vibrator. The uncased hole is flushed out and then crushed stones with diameter ranging from 20 mm to 100 mm are added from the top in increments of 0.3m to 1.2m. The stones are then densified by means of a vibrator that is located near the bottom of the probe. Successive lifts are placed and densified until a column of stone is formed up to the ground surface.

The wet process is generally used when the borehole stability is questionable, and it is used for sites with a high water table. This method is the currently the most commonly used technique. Special consideration must be given to the construction of stone columns in silts and sensitive clays which undergo large strength losses when subjected to vibrations during stone column construction. According to Baumann and Bauer (1974), all contractors indicated that saturated silty soils tend to lose strength during stone column construction due to a build-up in pore pressure.

1.3.2. Bottom Feed Construction / Dry Vibro Displacement Method

The main difference between the vibro-replacement and vibro-displacement methods (Fig. 1.2.b) is the absence of jetting water during the initial formation of the hole in the vibro-displacement method. This method uses the same vibrator probe as in the wet vibro-replacement method but with the addition of a hopper at the top of the probe and a supply tube along the length of the probe to bring the crushed stone directly to the tip of the poker. This dry technique is suitable for partially saturated soils which can remain stable as the probe penetrates the

ground. Sometimes air is used as a jetting medium in order to facilitate the extraction of the probe since the probe will occasionally adhere to the walls of the hole. The lack of flushing water in this method eliminates the generation of flushing fluid, and this in turn will widen the range of the sites that can be improved with dry-displacement method.

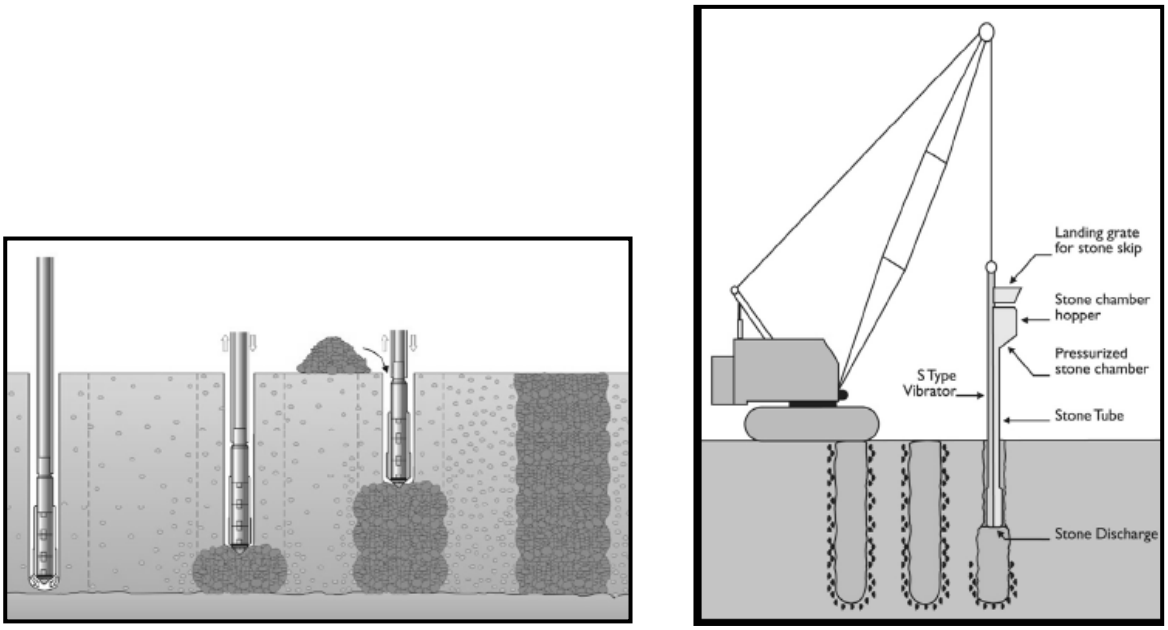

(a) (b)

Fig. 1.2(a) Top feed construction (wet method), (b) Bottom construction (dry method)

1.4. Scope of Work

The proposed study involves conducting drained triaxial tests on 7.1-cm diameter clay specimens that are reinforced with 2cm or 3cm-diameter sand columns that are installed with or without a geosynthetic encasement. Both fully penetrating and partially penetrating columns will be used to investigate the effect of column height on the improvement in drained shear strength. The consolidated drained triaxial tests will be performed on slurry-consolidated back-pressure saturated kaolin specimens at confining pressures ranging from 100 to 200 kPa.

Normally consolidated Kaolin samples with a diameter of 7.1cm and a length of 14.2cm will be prepared from slurry conditions. Sand columns of different diameters will then be installed in the Kaolin specimens to model different area replacement ratios (area of sand column/area of specimen). Two diameters of sand columns will be studied. The first diameter (2cm) will result in an area ratio of 7.9% and the second diameter (3cm) will result in an area ratio of 17.8%. Table 1.1 summarizes the proposed testing program.

A procedure for specimen preparation will be implemented to obtain normally consolidated kaolin specimens that are close to 100% saturation. Initially, dry Kaolin clods will be mixed with water at a water content of 100% using an electric mixer. The resulting slurry will be then poured into each of four prefabricated consolidometers that consist of 4 PVC pipe segments, each with a height of 35cm, an external and internal diameter of 7.3cm and 7.1cm respectively, and a wall thickness of 0.1cm. The pipe segment designed to function as a split mold, thus eliminating the need for extruding the soil sample after consolidation. The two PVC sections are held in place using high-strength duct tape. The soil specimen is loaded with a loading system consisting of dead weights similar to those used in 1-D consolidation tests. The dead weights are seated on a circular steel plate that transfers the load to the top of the soil specimen through a circular steel rod with a diameter of 1cm. A perforated circular steel piston with a diameter of 7.1cms (same as inner diameter of PVC pipe) is fixed to the bottom of the steel rod to act as a loading plate which transmits the load to the Kaolinite slurry. The soil is separated from this loading plate with a porous stone and a filter paper to provide a freely draining boundary at the top of the soil specimen. At the end of consolidation, the Kaolin PVC specimen will be removed from the apparatus.

Table 1.1. Testing program

Test No.	Confining pressure σ_3, (kPa)	Diameter of sand column (cm)	Area replacement ratio: A_c/A_s (%)	Height of sand column (cm)	Column height penetration ratio, (H_c/H_s)	Column height diameter ratio, (H_c/D_c)
1	100	0	0	0	0	-
2		2	7.9	10.75	0.75	5.37
3		2 (ESC)	7.9	10.75	0.75	5.37
4		2	7.9	14.2	1	7.10
5		2 (ESC)	7.9	14.2	1	7.10
6		3	17.8	10.75	0.75	3.58
7		3 (ESC)	17.8	10.75	0.75	3.58
8		3	17.8	14.2	1	4.73
9		3 (ESC)	17.8	14.2	1	4.73
10	150	0	0	0	0	-
11		2	7.9	10.75	0.75	5.37
12		2 (ESC)	7.9	10.75	0.75	5.37
13		2	7.9	14.2	1	7.10
14		2 (ESC)	7.9	14.2	1	7.10
15		3	17.8	10.75	0.75	3.58
16		3 (ESC)	17.8	10.75	0.75	3.58
17		3	17.8	14.2	1	4.73
18		3 (ESC)	17.8	14.2	1	4.73
19	200	0	0	0	0	-
20		2	7.9	10.75	0.75	5.37
21		2 (ESC)	7.9	10.75	0.75	5.37
22		2	7.9	14.2	1	7.10
23		2 (ESC)	7.9	14.2	1	7.10
24		3	17.8	10.75	0.75	3.58
25		3 (ESC)	17.8	10.75	0.75	3.58
26		3	17.8	14.2	1	4.73
27		3 (ESC)	17.8	14.2	1	4.73

Note: (ESC) indicates geosynthetic-encased sand columns

For test specimens that require the installation of sand columns, a hole with a diameter that is equivalent to the respective diameter of the sand column is augured gently into the specimen using a fabricated hand augur apparatus. The sand is then installed into the pre-drilled hole in layers. In the case where the sand column will be encased with a geotextile, the sand material is filled in layers into the fine geosynthetic material that has the shape of the respective column (diameter 2 or 3cm, and a length of 14.2cm). The sand column is then inserted into the predrilled hole.

Finally, the specimen is installed in the automated triaxial machine "TruePath" to be back-pressure saturated, consolidated under the specified confining pressures (100 kPa, 150 kPa, or 200 kPa), and then sheared under drained conditions. The variation of the deviatoric stress and volumetric strain with the axial strain will be analyzed to investigate the advantages of inserting sand columns of different characteristics in soft clays, particularly with regards to increasing the load carrying capacity during drained loading.

1.5. Organization of Thesis

The thesis consists of 7 chapters. A literature review which includes the major experimental and analytical studies related to the reinforcement of soft clays with stone columns is presented in CHAPTER 2. In CHAPTER 3, the properties of the materials used in the testing program are presented together with the methodology used in the clay sample preparation and construction of the reinforced and unreinforced sand columns. A step by step procedure for operating the automated triaxial equipment is discussed and presented in a detailed manner in CHAPTER 4 while the test results are presented and analyzed in Chapter 5. A comparison between drained and undrained tests is presented in CHAPTER 6. Finally, conclusions and

recommendations are presented in CHAPTER 7.

CHAPTER 2

LITERATURE REVIEW

2.1. Introduction

This chapter includes the major experimental and theoretical studies conducted to investigate the behavior of stone or sand columns in clays.

Since the 1970's, researchers have discussed the use of stone columns to increase the bearing capacity and the rate of settlement of weak cohesive soils (mainly clays). Examples of experimental studies in which sand columns were used to model the behavior of stone columns include the work done by Hughes and Withers (1974), Juran and Guermaizi (1987), Juran and Riccobono (1991), NarasimhaRao et al. (1992), Muir Wood et al. (2000), Sivakumar et al. (2004), McKelvey et al. (2004), Ayadat and Hanna (2005), and Black et al. (2006, 2007). In some studies, single sand columns were tested by direct loading of the columns while in others, both single sand columns and column groups (up to 4 columns per group) were loaded together with the surrounding clay using either model foundations or top plates of typical triaxial cells.

The majority of the studies mentioned above were conducted in large one dimensional loading chambers which do not allow for the control of drainage in the soil specimens during loading. Since most of these tests generally entailed partial drainage, the analysis of the test results was restricted to improvements in the general load carrying capacity of the sand column or the clay-sand column hybrid system. Juran and Riccobono (1991), Sivakumar et al. (2004) and Black et al. (2006, 2007) performed tests under full triaxial conditions in which the loading rate and the drainage conditions were controlled during shear. In some tests, the reinforced clay samples were sheared slowly to establish drained conditions, but more generally, soil specimens

were sheared undrained. Baumann and Bauer (1974),Alamgir et al. (1996), and Murugesan and Rajagopal (2006) performed finite element analyses to investigate the effect of granular columns on the load deformation response of reinforced clay.

Results of the experimental and finite element investigations listed above indicate that the mode of failure of clay specimens that are reinforced with circular single sand columns is characterized by lateral bulging of the sand column particularly in the top 4 to 5 diameters along the height of the column. Specimens with short partially-penetrating columns appeared to fail below the reinforced portion of the clay, causing no significant improvement in the load carrying capacity of the specimen. Based on the above observations, several researchers proposed the idea of the "critical column length" that is between 4 to 8 times the diameter of the column beyond which the sand column will not improve the capacity of the clay (Hughes and Withers 1974; NarasimhaRao et al. 1992; Muir Wood et al. 2000; and McKelvey et al. 2004).

For fully penetrating sand columns, results from experimental studies indicate that the insertion of sand columns in soft clays increases the load carrying capacity of the soft clays, reduces the settlement, and decreases the generation of excess pore water pressure during undrained loading. The extent of improvement in the above factors was shown to be dependent on the undrained shear strength of the clay, the angle of internal friction of the column material, and the geometric characteristics of the sand columns (diameter and spacing). Limited results involving tests conducted on both single columns and column groups indicate that for undrained loading, the relative increase in strength due to the presence of sand columns is independent of the column configuration (no column group effect) and is only dependent on the area replacement ratio of the reinforcement (Black et al. 2007).

In some field applications involving sand drains, geosynthetic filter materials are used to

separate the sand columns from the surrounding clay. Malarvizhi and Ilamparuthi (2004), Ayadat and Hanna (2005), and Murugesan and Rajagopal (2006) studied the effect of encapsulating sand columns with geofabrics of different strengths and stiffnesses. Although the main focus of these experimental research studies was to investigate the behavior of stone columns and not sand drains, the results obtained indicated that encasing the columns with geotextiles or geogrids provided additional lateral support to the granular column and reduced the bulging of the column during loading, increasing the stiffness and bearing capacity of the clay-sand column system.

Below is a summary of the research studies which targeted the behavior of clays that were reinforced with granular columns in a laboratory setting under 1-g and triaxial conditions.

2.2. Studies Involving 1-g Tests:

Historically, experimental research studies have been designed to investigate the behavior of sand/stone column-reinforced clay systems in the laboratory using 1-g tests that are conducted in one dimensional loading chambers (Hughes and Withers 1974, Narasimha Rao et al. 1992, Muir Wood et al. 2000, Malarvizhi & Ilamparuthi 2004, McKelvey et al. 2004, Ayadat and Hanna 2005, Ambily & Gandhi 2007, Murugesan & Rajagopal 2008, Gniel & Bouazza 2009, Murugeson & Rajagopal 2010, Cimentada et al. 2011, Shahu and Reddy 2011, and Fattah et al. 2011). In these studies, tests were conducted on clay specimens reinforced with partially or fully penetrating, encased or ordinary, stone or sand columns that were installed as single columns or as column groups. The loading mechanisms involved either direct column loading or foundation/plate loading at loading rates that varied from “slow” to “quick”, in an attempt to simulate drained or undrained loading, respectively.

2.2.1. Hughes and Withers (1974)

Hughes and Withers (1974) conducted one of the earlier experimental studies on soft Kaolin clay reinforced with single Leighton Buzzard sand columns. Kaolin specimens with a length of 22.5 cm and a width of 16 cm were first consolidated in a one-dimensional loading apparatus under a constant stress of 100 kPa. Single sand columns having a length of 15 cm and a diameter ranging from 12.5 mm to 38 mm were then constructed in the clay and loaded in stages to ensure complete dissipation of excess pore water pressure during loading. Observations of the mode of failure indicated that vertical and lateral distortions occurred at the top of the columns. Moreover, only the clay within a radial distance of 2.5 column diameters was laterally strained by loading. This indicates that stone columns in groups can be assumed to act without interaction if the spacing between the columns was greater than 2.5 diameters. Furthermore, the vertical displacement of the columns did not extend below four diameters. The presence of sand columns accelerated the rate of settlement by four times and reduced the vertical displacement by a factor of about six.

Hughes and Withers (1974) state that as "the column expands, the radial resistance of the soil reaches a limiting value at which indefinite expansion occurs." They conclude that stone columns in soft ground would act like a column in a triaxial chamber where the cell pressure is limited. They propose the following expression to determine the maximum vertical stress that the column can carry as the sand/stones in the top region reach the critical state of stress:

$$\sigma'_v = \frac{(1+\sin\phi')}{(1-\sin\phi')}(\sigma_{ro} + 4c - u) \qquad (1)$$

Where c and u are the undrained strength and the pore water pressure, respectively while ϕ' is the angle of internal friction of the column material, σ'_v is the vertical capacity of the columns,

and σ_{ro} is the initial radial total stress in the soil prior to column construction. Hughes and Withers (1974) showed that any increase in the column length beyond a column depth to diameter ratio of 6.3 will not increase the load carrying capacity of the column. Finally, the authors state that in practical application, the loads are generally applied on both the column and the surrounding clay. Although the applied load will lead to consolidation of the clayey soil and to increases in the radial stiffness, this increase will not add considerable strength to the load carrying capacity of the column.

2.2.2. Narasimha Rao et al. (1992)

Narasimha Rao et al. (1992) conducted load tests on stone columns having diameters of 25 mm, 50 mm, and 75 mm, with column height to diameter ratios of 5, 8, and 12. The tests were conducted in clay beds prepared at different consistencies in a rectangular tank of dimensions 100 cm x 80 cm and a height of 100 cm. The load was directly applied to the column through a circular steel plate of 1.5 times the diameter of the column. A PVC pipe with outer diameter corresponding to the column diameter was inserted in the middle of the tank, then the tank was filled with clay up to the required column height. The PVC pipe was then slowly removed, and the gap was gradually filled in layers with granite chips ranges from 25mm to 30mm in size through tamping the material with a rod. The angle of friction for the granite chips was 38º.

Results indicated that stone columns transfer the load to the clay through bulging action which helps in mobilizing the passive resistance of the surrounding clay. The area replacement ratio for the different columns was 44.44%. The rate of increase in the ultimate load carrying capacity of the columns decreased for column lengths greater than 8 times the diameter. Thus the optimum length for effective load transfer is between 5 and 8 times the diameter of the column.

2.2.3. Muir Wood et al. (2000)

Muir Wood et al. (2000) performed load tests on stone column groups under a footing by varying the spacing, diameter, and length of columns. The model tests were performed in a loading tank having a diameter of 300 mm using Kaolin clay which was consolidated under a maximum vertical stress of 120 kPa and allowed to swell back under a stress of 30 kPa to a final thickness of 300 mm. The drained angle of the shearing resistance of the Kaolin clay was 23º and the average undrained shear strength was equal to 12 kPa based on vane shear tests. Sand columns with diameters equal to 11 mm and 17.5 mm were constructed from fine quartz sand with a mean particle diameter (D_{50}=0.21mm) and installed into the clay tank by means of a replacement (auguring) method. The sand columns were distributed on a square grid with a spacing that ranges from 17.6 mm to 31.5 mm. This range of column spacing yields area ratios (A_s) that are between 10 % and 30%.

The reinforced clay beds were loaded at a penetration rate of 0.061mm/min through a rigid circular footing with a diameter of 100 mm, and loading was terminated when the displacement reached a value of 30 mm. The load was applied in increments with sufficient time to allow the completion of primary consolidation t_{95} after every load increment. The duration of the test was around 24 t_{95}. Consequently, this time was enough to ensure drained conditions during loading stages. An investigation of the different modes of failure for the sand columns was conducted leading to the following observations:

1. If the column is loaded and not prohibited from expanding radially by near columns, then the average stress in the column increases and the column bulges.
2. If the column is subjected to high stress ratios with small lateral restraint, then a diagonal shear failure plane may form through the column.

3. If the column is adequately short, then the column will punch and penetrate the underlying clay material. As the length of the column increases the penetration of the column into the clay is reduced since a smaller load will reach the base of the column.

The variation of average footing pressure, normalized with initial undrained strength, with footing settlement, normalized with footing diameter was analyzed for the different tests. Results indicated that as the area ratio increases, both stiffness and strength increase; moreover, the column length is significant up to a certain point beyond which increasing the column length will not lead to an increase in strength. Muir Wood et al. (2000) indicate that this critical length increases as the area ratio increases, since the failure mechanism is pushed deeper below the footing.

2.2.4. Malarvizhi and Ilamparuthi (2004)

Malarvizhi and Ilamparuthi (2004) studied the performance of soft clay beds that were improved with encased and ordinary single stone columns (diameter 30mm) of different column height to diameter ratios (L/D varied from 5 to 9.33) using encasement material of varying stiffnesses. The clay bed consisted of marine clay that was prepared at a water content of 52%, resulting in an undrained shear strength of 6 kPa. A PVC pipe was installed in the middle of the tank (30cm in diameter and 28cm in height) prior to preparing the clay bed. Granite stone chips of sizes ranging from 5 to 10 mm were charged into the PVC tube and compacted in three layers to achieve a density of 15 kN/m^3. For the encased stone columns, a stitched geo-grid was installed around the inner side of the tube. Stress controlled tests were then conducted where the stone column and the surrounding clay were loaded in hourly intervals with a circular plate having a diameter of 72 mm.

Test results indicated that the load carrying capacity of the composite column clay bed increases when the stone columns are encased with nets. Moreover, as the stiffness of the encasing material increases the load carrying capacity of the composite column increases proportionally. Load settlement curves indicate that the yield loads obtained were 116N, 113N and 97N for column height to diameter ratios of 9.33, 7.5, and 5, respectively. The yield resistance of the untreated clay was 68N. Furthermore, the ultimate bearing capacity of reinforced columns with geo-grids was double that of the clay bed that was improved with ordinary columns, and triple that of the untreated clay bed. Also the presence of geo-grids was found to increase the stiffness of the columns.

2.2.5. McKelvey et al. (2004)

McKelvey et al. (2004) investigated the load deformation behavior of a small group of sand columns under strip, pad, and circular footings. The material used in the experimental work was Kaolin clay and transparent clay-like material that had almost the same properties as Kaolin clay. Kaolin slurry was consolidated under a vertical pressure of 140 kPa for 8 days. The internal diameter of the loading chamber was 413 mm and its length was 1200 mm, while the length of the sample after 1-dimensional consolidation was around 500 mm and the undrained shear strength was estimated at 32 kPa. At the end of consolidation, the pressure was removed and columns having a diameter of 25 mm were augured into the clay bed and filled with sand poured through a wire mesh. After constructing the columns, a loading plate was installed at the top of the columns. For the Kaolin specimens, 4 sand columns with a square pattern were installed under the pad footing with column length to diameter ratios of 6 (length of column = 150mm) and 10 (length of column = 250mm) and an area replacement ratio of 24%. The model footing

was subjected to a strain controlled loading at a rate 0.0064mm/min using a 9x9cm footing. The loading was terminated when the vertical displacement of the footing reached 40 mm. The consolidation pressure of 142 kPa was removed prior to loading the footing.

The insertion of sand columns with a length of 150 mm and an area ratio of 24% increased the maximum load carrying capacity by 130 % increase. Increasing the length of the column to 250mm increased the improvement by 5%. The authors concluded that increasing the column length to diameter ratio to a value above 6 does not lead to any significant improvement in the load carrying capacity. However, the undrained stiffness for column lengths of 150 mm and 250 mm was 4 times and 5.7 times higher than that of unreinforced clay, respectively.

Observations of the specimens after failure indicated that failure was characterized by bulging, bending or shearing. In long columns, deformations were concentrated in the upper zones of the column while for shorter columns, the columns tended to bulge and bend outward away from the neighboring columns and punched a distance of 10 mm into the soft clay bed. The stress concentration ratio (n) was found to be less than 2 for short columns and greater than 4 for long columns, immediately after the load application on the footing. At higher loading stages, the stress concentration ratio approached a value of 3 regardless of the column length.

2.2.6. Ayadat and Hanna (2005)

Ayadat and Hanna (2005) studied the effect of encapsulating sand columns with four geofabric material on the load carrying capacity of a collapsible soil (78% concrete sand, 10% Leighton Buzzard sand, and 12% Kaolin clay) that was tested in a loading chamber with a diameter of 39cm and a height of 52cm. Single sand columns with diameters equal to 2.3 cm and lengths equal to 25, 30, and 41 cm were constructed at a relative density of 80% ($\phi'=44^o$) in the

middle of a soil specimen with a diameter of 39 cm and a height of 41 cm. Axial loads were applied to the column through a rigid circular plate with a diameter of 4 cm. Results of stress controlled tests indicated that the load carrying capacity of the composite material increased with increases in the stiffness of the geofabric. The increase in the axial capacity of the sand column due to the reinforcement was due to the higher lateral restraint provided by the reinforcement. In addition, the capacity also increased due to the increase in the length of the column.

Ayadat and Hanna (2005) developed an equation to calculate the ultimate carrying capacity of encased stone columns inserted in soft cohesive soils. The vertical stress that could be supported by an encased stone column is given by:

$$\sigma'_{v\lim} = \tan^2\left(\frac{\Pi}{4} + \frac{\phi'}{2}\right)\left(\sigma'_{ho} + kc' + \alpha\frac{\tau_a t}{r_o}\right) \quad (2)$$

Where $\sigma'_{v\lim}$ is the maximum effective vertical stress acting on the column, ϕ' is the angle of shearing resistance of the column material, $\sigma'_{ho} = K_o(q + \frac{\gamma L}{2})$ is the effective lateral stress of the soil before installing the column, k is a constant that is equal to 4, c' is the drained cohesion of the collapsible soil, K_o is the coefficient of earth pressure at rest, q is the surcharge applied on the ground surface, γ is the unit weight of the surrounding soil, L is the length of the stone column, τ_a is the tensile strength of the geofabric material, t is the thickness of the geofabric material, and r_o is the initial radius of the column. The factor (α) is a reduction factor that should be applied to the additional lateral stress provided by the geofabric material, on the premise that the columns may bulge (and thus fail) before the stress in the fabric reaches the ultimate stress. α could be evaluated as a function of the modulus of deformation of the stone column E_p as: $\alpha = 3.2\text{x}10^5 E_p^{-1.37}$, where the modulus E_p of the stone column should be obtained from triaxial tests conducted on the sand column alone.

2.2.7. Ambily and Gandhi (2007)

Ambily and Gandhi (2007) developed a design procedure for stone columns considering the load sharing between the stone and the surrounding soft clay. The authors used the results of an experimental program coupled with FEM numerical analyses to develop the proposed design method. The experimental program involved tests that were conducted on single and group 10cm-diameter stone columns in triangular pattern that were installed to full depth in a 450 mm thick soft clay specimen. The clay was prepared in a cylindrical tank with a height of 50 cm and a diameter ranging from 21 cm to 83.5 cm. Clays with undrained shear strengths of 7, 14, and 30 kPa were used in the experiments. For single stone columns, the diameter of the clay tank ranged from 21 to 42 cm, while for sand columns in groups of 7, the diameter of the tank was 83.5cm. The height of the columns was 45cm.

The clay sample was prepared by compaction. The columns were constructed using crushed stones of size 2 to 10 mm using the replacement method, prepared at a density of 16.62 kN/m^3 and resulting in a friction angle of 43°. Entire area loading and column loading were adopted. The load was applied at a displacement rate of 0.0625mm/min and monitored at equal time intervals till a settlement of 10 mm was exceeded. When the entire area was loaded, columns didn't show signs of bulging, while for loaded column, bulging was observed at a distance of 0.5D from the top of the column. Based on the experimental test results and FEM analysis, the ratio of the limiting axial stress to the corresponding shear strength of surrounding clay was found to be independent of the shear strength of soil and is a constant for a given (s/d) ratio and a given angle of internal friction of column material.

Using FEM analyses, the authors developed the design chart shown in Fig. 2.1. The authors argue that part of the stresses that are applied to the column will be shared by the

surrounding clay. This will add a "surcharge" (q) to the clay which in turn improves the limiting axial capacity σ_{su} of the column. Based on FE analyses involving surcharge, an expression for the limiting axial capacity including surcharge was developed as:

$$\sigma_{suq} = \sigma_{su} + (0.0088\phi^2 - 0.5067\phi + 10.86)q \tag{3}$$

Where σ_{suq} is the limiting axial stress with a surcharge (q) on the surrounding clay and ϕ is the friction angle of column.

In tests where the entire area was loaded, failure of the column didn't occur due to the confinement effect of the boundary of the unit cell. However, the stiffness of the reinforced composite was improved significantly. The authors define the stiffness improvement factor (β) which is the ratio of the stiffness of the reinforced ground to the stiffness of the unreinforced ground. Curves showing the variation of (β) with (s/d) for different values of ϕ were derived using the FE analysis. The stiffness factor (β) was found to be independent of the strength of the surrounding soil. For triangular column groups pattern, the behavior of the reinforced samples was found to be similar to the specimens reinforced with a single column. This indicates that the single column behavior with a unit cell concept can simulate the behavior of an interior column when a large number of columns are simultaneously loaded. As the shear strength of the clay decreases, more load will be taken by the stone column (stress concentration factor between 4 and 6) as indicated in Fig. 2.2. Finally, the authors proposed a design method for stone columns in soft clays.

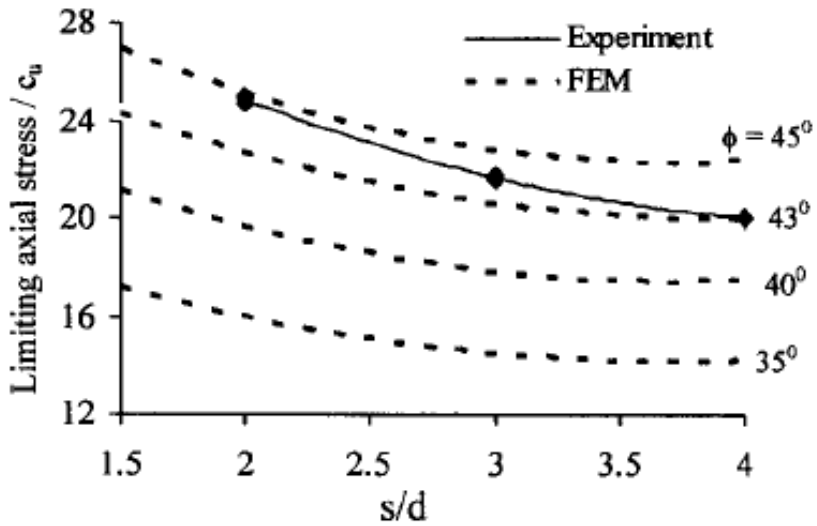

Fig. 2.1 Effect of s/d and Ø on axial capacity of stone column (Ambily and Ghandi 2007)

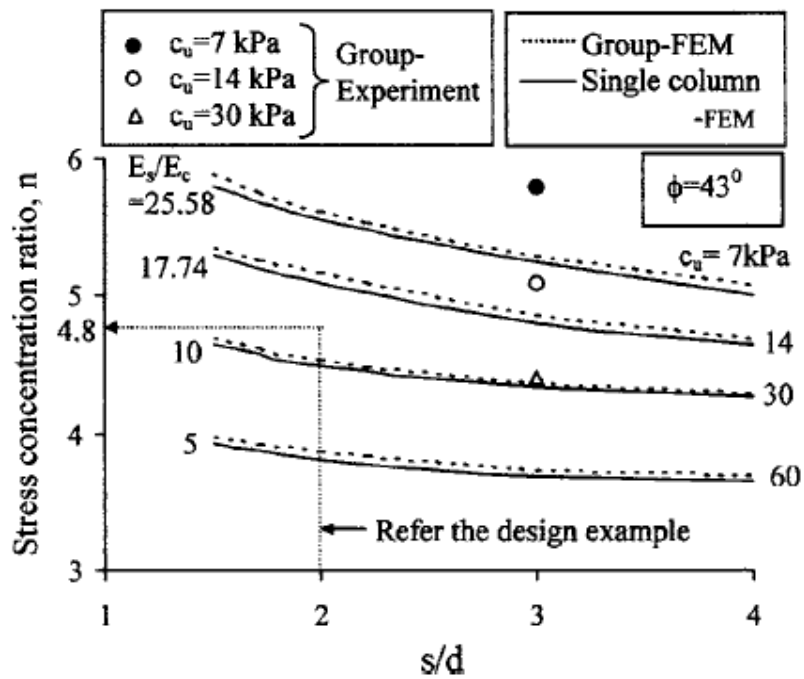

Fig. 2.2 Effect of s/d and cu on stress concentration ratio (n) (Ambily and Ghandi 2007)

2.2.8. Murugesan and Rajagopal (2008)

Murugesan and Rajagopal (2008) investigated the performance of encased stone columns

through 1-g laboratory tests consisting of column loading of granite chips (unit weight =15.7 kN/m^3, ϕ'=41.5^o) that were installed in lucastrine clay in a tank with a diameter of 21cm and a height of 50cm. The parameters that were varied were the diameter of the columns (D=5cm, 7.5cm, and 10cm) and the type of encasement (4 different types). The column was loaded at a rate of 1.2mm per minute to simulate undrained loading. The ordinary stone columns showed a catastrophic failure, whereas the encased columns showed an elastic behavior. The load carrying capacity of individual stone columns for a settlement of 10 mm was increased by 3 to 5 folds. Ordinary columns underwent large settlements because of the excessive bulging, whereas bulging was minimized for encased columns. Results indicated that for ordinary columns, the load capacity is almost the same for all diameters, whereas for the encased columns as the diameter increases, the load capacity of encased stone column decreases. Similar trends were reported by Murugesan and Rajagopal (2006) based on the numerical analysis. Based on the results guidelines were developed for the design of geosynthetic encased stone columns. The bearing support from the soft soil was conservatively ignored in the proposed methodology.

2.2.9. Gniel and Bouazza (2009)

Gniel and Bouazza (2009) conducted laboratory 1-g tests on a unit cell that is comprised of kaolin clay reinforced with encased and ordinary single sand columns with a diameter of 5.1cm. Kaolin was consolidated from a slurry (pressure of about 50 kPa) in two custom-made tall cylinders with a diameter of 15.5cm and a height of 55cm to model the boundary conditions of a column group by a unit cell. A third cylinder was manufactured to allow for testing the behavior of an isolated column. The area replacement ratio of the unit cell was 11% and the height of the clay bed after consolidation was 31cm, resulting in column length to diameter ratio

of about 6. For unit cell tests, all the area was loaded while for single column tests, the load was applied through a 5.1m footing resting on the sand column. In both cases, samples were allowed to undergo full consolidation under loading steps of 10kPa to 75kPa, representing drained loading to a maximum pressure of 350 kPa. Miniature pressure sensors were used in some tests to measure the stress in the sand column, which was prepared at a relative density of 90% using freezing. Two encasements (window mesh) with different stiffnesses were used in the testing program. Encasement lengths corresponding to 25%, 50%, 75%, and 100% of the sample height were used.

For tests conducted in the constrained unit cell, the stress-strain curves indicated a concave upward behavior with the rate of pressure increase becoming higher at larger strains. This behavior is expected for an odometer (1-D consolidation) behavior in a constrained ring. A 25% average reduction in the axial strain was observed for reinforced clay specimens compared to the control clay. The reduction was smaller for larger pressures indicating that the clay was getting stronger due to consolidation. For encased columns, the average strain reductions were 30%, 40%, 50%, and 80% for the different levels of encasement. Radial expansion of non-encased columns was even along column length (about 5%). For partially encased columns, the non-encased length bulged with the largest lateral strain of about 33%. Results from miniature pressure sensors indicated stress concentration factors of about 10 for the fully encased column, reducing to about 2 to 3 for the ordinary columns.

For tests conducted on isolated columns, the capacity of the ordinary column was about 3 times that of the control clay. This capacity increased for encased columns (4 times for 25% fiberglass, 5.5 times for 50% fiberglass, 10 times for 75% fiberglass) with the pressure reaching 676 kPa for the 100% fiberglass without signs of failure (the failure stress for control specimen is

25 kPa). The water content of the clay before and after the test indicated that drained, or at least partially drained loading occurred in the clay immediately surrounding the bulge zone of the column. However, failure comprised rapid radial bulging of the column below the encasement and was thus governed by the undrained strength of the clay.

2.2.10. Murugesan and Rajagopal (2010)

Murugesan and Rajagopal (2010) investigated the performance of encased stone columns through 1-g laboratory tests consisting of column loading of granite chips that were installed in lucastrine clay that was consolidated under a pressure of 10 kPa in a large tank with dimensions of 1.2x1.2x0.85m to a final height of 0.6m. The displacement method was used to install single and group columns having diameters of 5.0, 7.5, and 10cm, at a density of 16 kN/m^3. For single columns, the load was applied with a plate having a diameter that is twice the diameter of the columns at a rate of 1.2mm/min to simulate undrained loading. The column group was comprised of 12 columns with a diameter of 7.5cm placed in a triangular grid at a spacing of 15cm. The group was loaded through a loading plate that inscribed three central columns (diameter of plate is 24.82cm). Four different types of encasements were used in the testing program.

Results of tests with ordinary columns exhibited a clear failure while encased columns did not show signs of failure. The pressure on the encased column at a settlement of 10mm was found to be three to five times greater than the non-encased column. It is interesting to note that the pressures developed in the encased columns were found to decrease as the diameter of the columns increased, since the additional confinement provided by the encasement is inversely proportional to the diameter of the columns. Results of the load tests on the groups indicated that

encased columns showed a linear increase in pressure even at high settlements, while the group of ordinary columns showed clear signs of failure. The load carrying capacity increases 3 to 5 times due to the encasement. The stress concentration factor on the encased columns was found to be about 5. The clay carried only 0.1 to 0.6 of the total pressure on the loading plate, with the clay in the encased group carrying less stress than that in the ordinary group. The stress concentration factor is only 2 for the ordinary columns at failure. Design charts are presented at the end of the paper as a guideline for the design of encased columns in clays.

2.2.11 Cimentada et al. (2011)

Cimentada et al. (2011) conducted 1-g consolidation tests on a unit cell that is comprised of kaolin reinforced with single ordinary gravel columns with diameters of 8.47 and 6.35cm. The kaolin was consolidated from a slurry in a Rowe-Barden cell with a diameter of 25.4cm and a depth of 14.6cm, resulting in area replacement ratios of 11.11% and 6.25% for the two diameters. The gravel columns were prepared using freezing at a dry density of 16.5 kN/m^3. The clay/gravel system was loaded in 100 kPa stress increments. Pore pressures were monitored immediately after loading (undrained condition) and then radial consolidation was allowed through the column for 24 hours. The effective Young's modulus of the clay was estimated at 700 to 2500 kPa, while Young's modulus of the gravel was estimated at 10000 to 33000 kPa. The critical state friction angle of the columns was 35°.

Results show that after consolidation is achieved, the ratio of the stress in the clay to the stress in the column ranged from 0.68 to 0.75 for the two area replacement ratios. The stress concentration ratio at the end of each load step was found to be in the range of 2.52 to 9.25, decreasing with the applied vertical stress. This trend was attributed to the decrease in the

stiffness ratio between the column and the soil as the pressure is increased (clay stiffness increased with pressure). The concentration factors are lower than those predicted assuming that the stress concentration ratio is equal to the ratio of the oedometric moduli and lower than the ratio predicted by elastic solutions, indicating that the columns reached yielding conditions. The vertical strain results indicate that compressibility in the reinforced clay reduced to 70-80% and to 65% for the two area ratios used.

2.2.12. Shahu and Reddy (2011)

Shahu and Reddy (2011) presented results of fully drained 1-g model tests that were conducted in Perspex cylinder tanks of 30-cm diameter and 60cm depth on groups of stone columns installed in a bed of kaolin (30cm thick) consolidated from a slurry using a pressure of 30, 60, or 90 kPa. The undrained shear strength of the clay bed was found to be between 7 and 9 kPa. The columns were formed of Barbadur sand at a typical diameter of 1.3cm with some tests conducted with columns of 2.5cm diameter. A footing with a diameter of 10cm was used to load the groups, with the number of columns in the group ranging from 5 to 21, resulting in area ratios of 10%, 20%, and 30%. All columns were installed in a square grid using the replacement method with heights of 10cm or 15cm and were formed either dry or wet at relative densities of 50% and 80%. The load was applied in 10 to 14 equal increments of 15 kPa maintained until the settlement rate became less than 1mm/day.

Results of stress versus settlement were presented with the stress normalized by the initial effective geostatic stress and the settlement normalized by the column length. Results indicate a relatively linear behavior up to a given displacement at which non-linear behavior is observed. The authors defined this boundary as failure. Results indicate that the higher the area ratio the

higher the failure stress and stiffness of the group. For a given area ratio, increasing the L/D ratio of the columns resulted in an increased in the failure stress and stiffness. Results also indicated that increasing the density of the columns from 50% to 80% decreases the settlement of the group at a given normalized pressure. A 3-D finite element model was created using ABAQUS to analyze the laboratory test results. The clayey soil was modeled using the Cam-clay model and the sand columns using the Mohr-Coulomb elastic-perfectly plastic model. The FE mesh was calibrated with results of triaxial tests. Interesting 3D images of the failure of the column group are presented and indicate that as one moves away from the center of the column group, outward bending of the columns increase, with central columns not showing signs of bending.

2.2.13. Fattah et al. (2011)

Fattah et al. (2011) conducted laboratory 1-g tests on CL soil (10% sand, 42% silt, and 48% clay) that was compacted at a water content of 24% to 35% in a 1.1mx1.0mx0.8m steel tank and reinforced with single and group (2, 3, or 4) crushed stone columns (density=16.3 kN/m^3) having a diameter of 5.0cm and lengths of 40cm (fully penetrating with L/D=8) and 30 cm (partially penetrating with L/D=6). In column groups the spacing was taken as twice the diameter. The loading was stress controlled with a 22-cm diameter with each loading step applied at 2.5 minutes until the settlement was 5cm. A failure criterion was adopted whereby the settlement reaches 50 % of the diameter of the column or 11% of the diameter of the footing. Results indicated that the stress concentration ratio *n* reached a peak value at a point located approximately at a stress of q/c_u=2. After that, the value of *n* either reduced gradually (for c_u = 6 kPa) or suddenly (for c_u = 9 or 12 kPa) with increasing the bearing ratio *q*/cu. The *n* values are 1.2, 2.2, 2.5, and 2.8 in soils having a shear strength of 6 kPa, treated with single, two, three, and

four stone columns at L/D=6, respectively. The n values at failure are 1.4, 2.4, 2.7, and 3.1 in soil having a shear strength of 6 kPa, treated with single, two, three, and four stone columns at L/D=8. The bearing improvement ratio $q$treated /$q$untreated ranges from 1.20 to 2.18 for clays treated with single to four column groups with L/D=6, respectively at S/B=11%.

2.3. "Undrained" Triaxial Tests

Sivakumar et al. (2004), Black et al. (2007), and Najjar et al. (2010) performed conventional consolidated undrained triaxial tests on Kaolin specimens that were reinforced with partially and fully penetrating sand columns.

2.3.1. Sivakumar et al. (2004)

Sivakumar et al. (2004) performed consolidated undrained triaxial tests on model sand columns with a diameter of 3.2 cm and height penetration ratios (ratio of column height to height of specimen) of 0.4, 0.6, 0.8, and 1 in soft Kaolin specimens having a diameter of 10 cm and a length 20 cm. The Kaolin specimens were subjected to two types of axial loading. In the first type, the entire area of the Kaolin specimen was loaded while in the other type, the specimen was subjected to "foundation loading" where the Kaolin specimen was loaded at its middle through a rigid circular footing having a diameter of 4 cm. Furthermore, the effect of increasing the lateral confinement of the sand column by encasing the column with geo-grid reinforcement was studied as a part of the experimental work.

Kaolin specimens were prepared from a slurry at a water content of 105% (1.5 times its liquid limit of 70%) and initially consolidated under a vertical pressure of 200 kPa in a one dimensional consolidometer. After 3 days, the consolidation stage was completed, air pressure

was removed and a sand column with a diameter of 3.2 mm was augured in the middle of the Kaolin specimen. The void ratio of the clay was 1.43±0.05. The lengths of the columns were 8, 12, 16 and 20 cm. Prior to shearing the specimen in the triaxial cell at a strain rate of 4 % per day, the specimens were isotropically consolidated at an effective confining pressure of 100 kPa, and then a back pressure of 300 kPa was applied to guarantee saturation of the specimens.

Sand columns were prepared using two methods: a wet compaction method and a frozen method. In the wet method, sand at a water content of 18% was used to construct the sand columns in layers, whereby each layer was compacted through tamping of the wet sand material. The wet compaction method yielded sand columns with a bulk density ranging from 2300 to 2450 Kg/m^3. In the frozen method, wet sand at a water content of 18% was compacted in layers into a plastic tube and frozen. After freezing, the tube was cut along its length and the frozen column was inserted into the predrilled augured hole. For the encased sand column, geo-grid fabric enclosed the wet sand material prior to installing the plastic tube. The bulk density of the frozen column was about 1930±30 Kg/m^3. The authors state that although freezing of sand columns is not adopted in the field, the method is used in the laboratory because it results in a consistent sand column diameter, leading to little variations in the density of the column.

After failure, samples that were sheared with uniform loading were cut vertically to investigate the failure mechanism. Short columns bulged below the reinforced portion of the clay, while fully penetrating columns bulged relatively uniformly along their length. Analysis of stress strain curves for the different types of loading and different method of column insertion indicated that the generation of excess pore water pressure was smaller in the case of Kaolin specimens with sand columns. Furthermore, the percentage of reduction of the excess pore water pressure was higher for fully penetrating columns compared with partial penetrating columns.

For fully penetrating columns that were installed using the wet compaction method and which were subjected to uniform loading, the deviatoric stress increased by 40 % compared with untreated Kaolin specimen. For partially penetrating columns, the deviatoric stress was reduced in comparison to unreinforced specimens. The authors attributed this behavior to the wet method of column preparation. On the other hand, frozen column that were fully penetrating into the clay resulted in 30% increase in the deviatoric stress. Similarly pore water pressures were reduced due to possible dilatation of the compacted sand column during undrained shearing. Only kaolin specimens reinforced with frozen sand column of height penetration ratios above 0.6 showed an increase in the load carrying capacity of the sand-clay composite (Fig. 2.3).

For foundation loading, the unreinforced specimen carried 280N which is equivalent to a bearing pressure of 220 kPa. Fully penetrating wet and frozen sand columns carried 450 kPa and 400 kPa respectively. The authors used the method by Hughes and Withers (1974) to predict the ultimate capacity of the tested sand columns. For $\phi' = 35$, σ_{ro}=100 kPa, c =28 kPa, and u = 44 kPa, the predicted σ'_v turned out to be equal to 613 kPa. As a result, the estimated pressure on the footing was calculated to be equal to $\sigma'_v - (\sigma'_3 - \Delta u)$=613-(100-44) =557 kPa. The measured value for the bearing capacity of wet fully penetrating sand columns was equal to 450 kPa. The authors state that this indicates good agreement with the values predicted using the model by Hughes and Withers (1974).

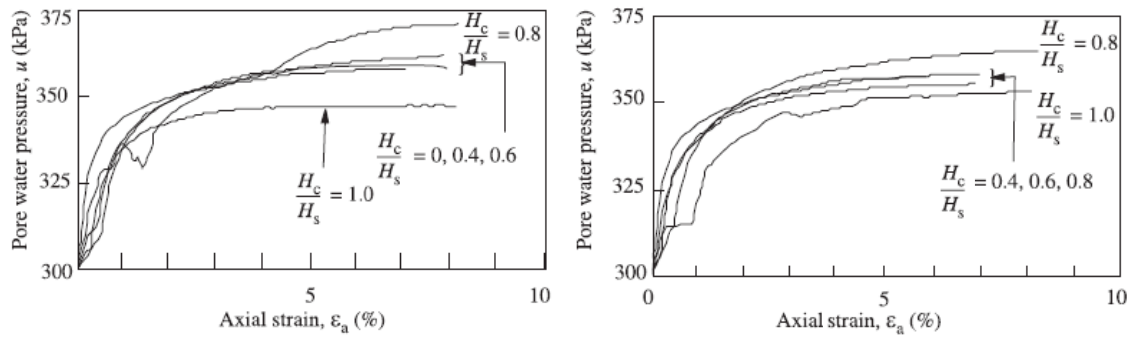

(a) (b)

Fig. 2.3 Stress-strain relationship for uniform loading: (a) wet compaction; (b) previously frozen sand column.

In the case of uniform and foundation loading, the presence of a geo-grid sleeve around the sand column increased the load carrying capacity of the composite sand-column system by 70% and 60% respectively, in comparison to the unreinforced frozen sand columns. Moreover, settlement was reduced significantly in the case of reinforced stone columns. These findings are clearly shown in Fig. 2.4. Similarly, excess pore water pressures were reduced for reinforced sand columns.

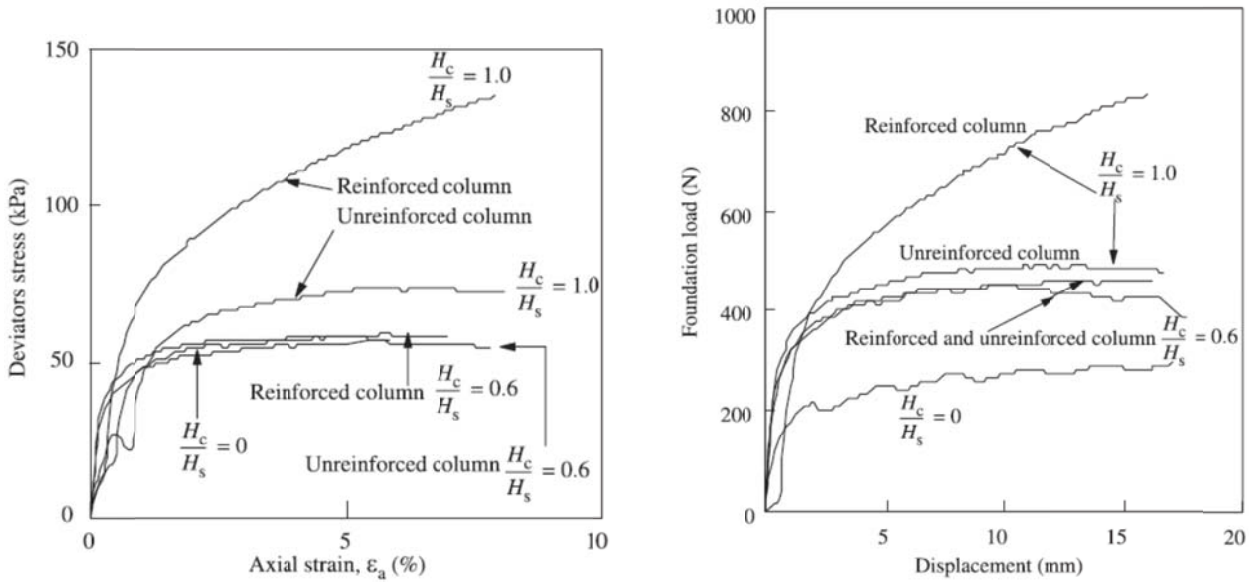

(a) (b)

Fig.2.4 Stress-strain and load-settlement behavior, comparison between reinforced and unreinforced columns (a) uniform loading, (b) foundation loading

2.3.2. Black et al. (2007)

Black et al. (2007) prepared Kaolin specimens with a length of 20cm and a diameter of 10cm from slurry that was consolidated under 1-dimensional conditions. Specimens were reinforced either with a single frozen sand column with a diameter of 3.2cm or with three frozen sand columns with a diameter 20cm. The length of the columns was taken as 12cm and 20 cm corresponding to column height penetration ratios of 0.6 and 1 respectively.

Prior to undrained shearing at a strain rate of 0.167% per hour, the Kaolin specimen was isotropically consolidated under a pressure 100 kPa. The results shown on Fig. 2.5 indicate that the deviatoric stress for the unreinforced specimen was 56 kPa increasing to 75 kPa for fully penetrating columns (increase of 33% for A_s=10%). In partially penetrating columns, the increase in the deviatoric stress was marginal. For column groups, the deviatoric stress increased from 56 kPa to 70 kPa for partially penetrating columns, and to 87 kPa for fully penetrating columns (increase of 55 % for A_s=12%). Thus a 20% increase in area replacement ratio caused 20% increase in capacity. The authors conclude that for undrained loading, the relative increase in the strength of the columns is independent of the column configuration, signifying that what governs the strength of the column is not the column geometry and arrangement, but the area replacement ratio.

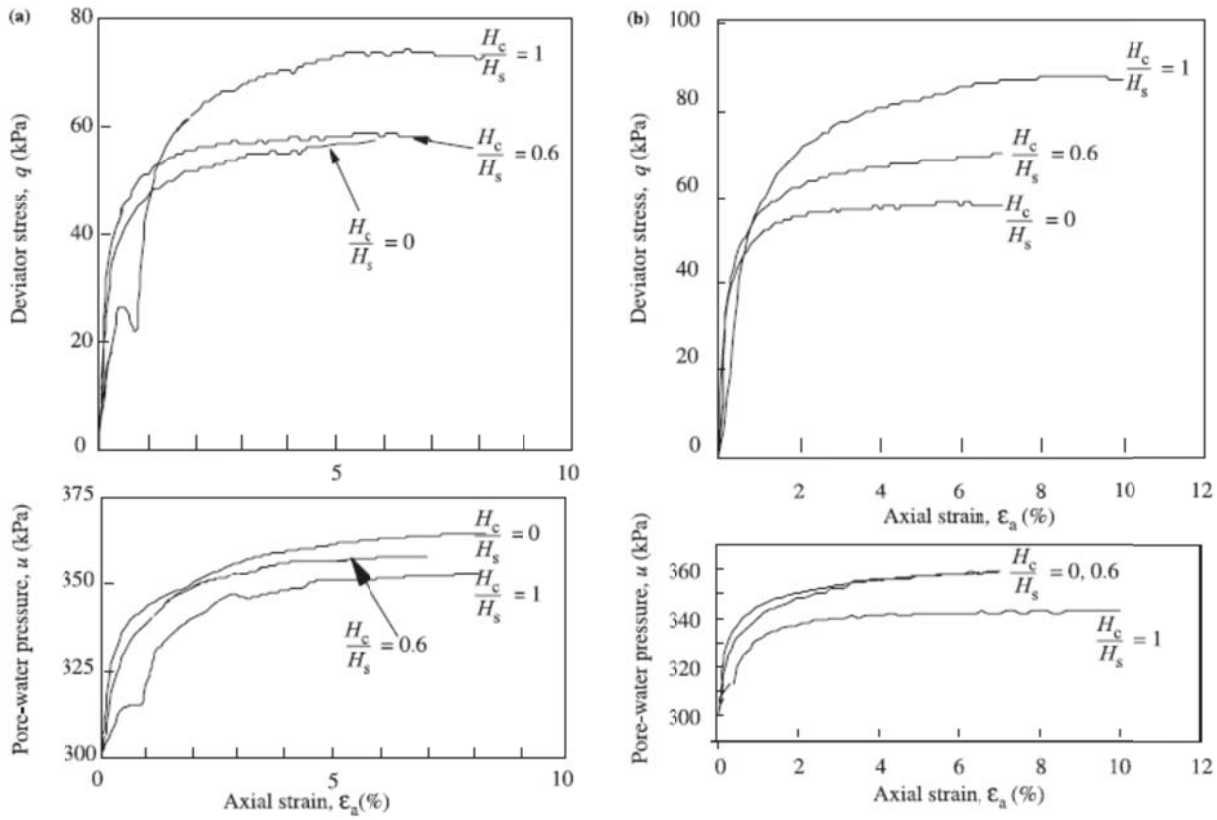

Fig. 2.5 Stress-strain response under uniform undrained loading for (a) single column and (b) group of columns

In some tests, Kaolin specimens were sheared under drained conditions. In these tests, the deviatoric stress of the clay specimen at 2% strain increased from 92 kPa for the unreinforced sample to 104 kPa for column groups (3 columns with a diameter of 2 cm) to 112 kPa for the specimen that was reinforced with a single column (diameter of 3.2 cm). The authors state that more research needs to be done to explain the results obtained in the drained tests.

2.2.6. Najjar et al. (2010)

This paper consists of a comprehensive testing program to assess the impact of sand columns on the undrained load response of soft clays in practical application involving the use of sand drains or sand columns in clayey soils. The experimental program involves performing 32

isotropically consolidated undrained triaxial tests on one-dimensionally consolidated kaolin specimens having a diameter of 7.1cm and a length of 14.2cm with pore pressure measurement on soft clay specimens that were reinforced with sand columns. The parameters that were varied in the program were:

1) The area replacement ratio, A_c/A_s, defined as the ratio of the cross sectional area of the sand column A_c to the cross-sectional area of the specimen A_s (7.9% and 17.8% for the 2cm and 3cms sand column diameter respectively)
2) The column penetration ratio, H_c/H_s, defined as the ratio of the height of the sand column H_c to the height of the specimen H_s (0.5, 0.75 and 1)
3) The confinement of the sand column with a geosynthetic fabric.

The tests were conducted at three effective confining pressures (100kPa, 150kPa and 200kPa) to isolate the effect of confinement on the degree of improvement in the mechanical properties of the sand column-clay system including undrained strength and Young's modulus, but more importantly to characterize and compare the effective Mohr-Coulomb failure envelopes for control clay specimens and specimens that were reinforced with sand columns. The program of testing is summarized in Table 2.1.

Table 2.1: Laboratory Testing Program and Results (Najjar et al. 2010)

Test number	Effective confining pressure $(\sigma'_3)_o$ (kPa)	Diameter of sand column (cm)	Area replacement ratio A_c/A_s (%)	Height of sand column (cm)	Column penetration ratio (H_c/H_s)	Column height to diameter ratio (H_c/D_c)	Undrained shear strength (kPa)	Excess pore-water pressure (kPa)	$(E_{sec})_{1\%}$ at 1% axial strain (kPa)	Increase in undrained shear strength (%)	Reductio in exces pore pressure (%)
1	100	0	0	0	0	—	32.3	61.3	4,150	—	—
2		2	7.9	7.1	0.50	3.55	32.5	59.9	4,166	0.6	2.9
3		2	7.9	10.65	0.75	5.32	35.2	57.3	4,220	9.0	6.5
4		2	7.9	14.2	1	7.10	36.6	51.2	4,390	13.3	16.5
5		2 (ESC)	7.9	7.1	0.5	3.55	32.8	58.8	4,187	1.5	4.1
6		2 (ESC)	7.9	10.65	0.75	5.32	37.2	58.0	4,762	15.1	5.4
7		2 (ESC)	7.9	14.2	1	7.10	52.0	58.9	5,132	61.0	3.9
8		3	17.8	10.65	0.75	3.55	38.9	48.9	4,597	20.4	20.2
9		3	17.8	14.2	1	4.73	56.7	42.7	5,853	75.5	30.3
10		3 (ESC)	17.8	7.1	0.5	2.36	36.0	59.2	4,280	11.5	3.5
11		3 (ESC)	17.8	14.2	1	4.73	64.8	42.8	7,150	100.6	30.2
12	150	0	0	0	0	—	42.1	95.1	6,092	—	—
13		2	7.9	10.65	0.75	5.32	48.2	88.9	6,100	14.5	6.5
14		2	7.9	14.2	1	7.10	50.3	87.8	6,368	19.5	7.7
15		2 (ESC)	7.9	7.1	0.5	3.55	42.3	89.4	4,920	0.5	6.0
16		2 (ESC)	7.9	10.65	0.75	5.32	50.9	85.4	6,402	20.8	10.2
17		2 (ESC)	7.9	14.2	1	7.10	58.5	76.8	6,093	39.0	19.2
18		3	17.8	7.1	0.5	2.36	46.0	87.2	6,101	9.3	8.3
19		3	17.8	10.65	0.75	3.55	56.8	78.1	6,697	34.9	17.9
20		3	17.8	14.2	1	4.73	73.9	65.2	8,624	75.5	31.4
21		3 (ESC)	17.8	7.1	0.5	2.36	46.8	92.7	6,574	11.1	2.5
22		3 (ESC)	17.8	14.2	1	4.73	79.4	67.8	8,045	88.7	28.7
23	200	0	0	0	0	—	55.1	130.9	7,637	—	—
24		2	7.9	10.65	0.75	5.32	60.1	120.3	7,904	9.1	8.1
25		2	7.9	14.2	1	7.10	65.8	112.1	7,996	19.4	14.4
26		2 (ESC)	7.9	7.1	0.5	3.55	58.4	119.2	7,788	6.0	8.9
27		2 (ESC)	7.9	10.65	0.75	5.32	61.9	121.1	8,144	12.4	7.5
28		2 (ESC)	7.9	14.2	1	7.10	70.9	115.7	8,228	28.6	11.6
29		3	17.8	10.65	0.75	3.55	71.2	107.8	8,983	29.2	17.6
30		3	17.8	14.2	1	4.73	92.3	89.4	10,103	67.5	31.7
31		3 (ESC)	17.8	7.1	0.5	2.36	58.2	119.7	8,121	5.6	8.5
32		3 (ESC)	17.8	14.2	1	4.73	103.3	86.5	11,407	87.4	33.9

The mode of failure of the specimens with fully penetrating sand columns shows minimal and uniform bulging throughout the height of the sand column as indicated in Fig. 2.6 (a). Whereas for partially penetrating sand columns, bulging was significant and concentrated at the lower portion of the column which indicates that the stresses at the base of the column generally exceed the bearing capacity of the soil leading to premature bearing capacity failure in the unreinforced lower portion of the specimen (Fig. 2.6 (b) and (c)). The use of encasement reduces the degree of bulging comparing it to control specimen and specimens that were reinforced with

non-encased columns (Fig. 2.7).

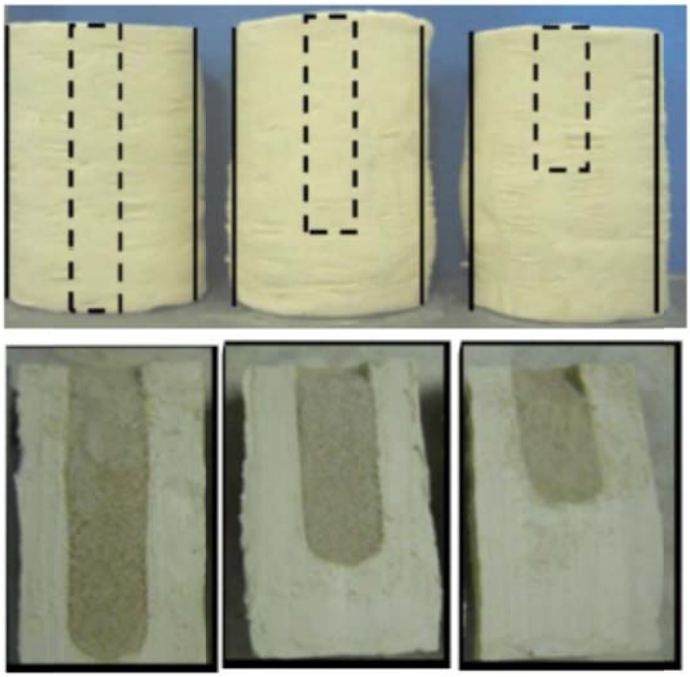

Fig. 2.6 Modes of failure of clay specimens (upper part) and sand columns (lower part) reinforced with (a) fully penetrating column; (b) column with penetration ratio of 0.75; and (c) column with penetration ratio of 0.5

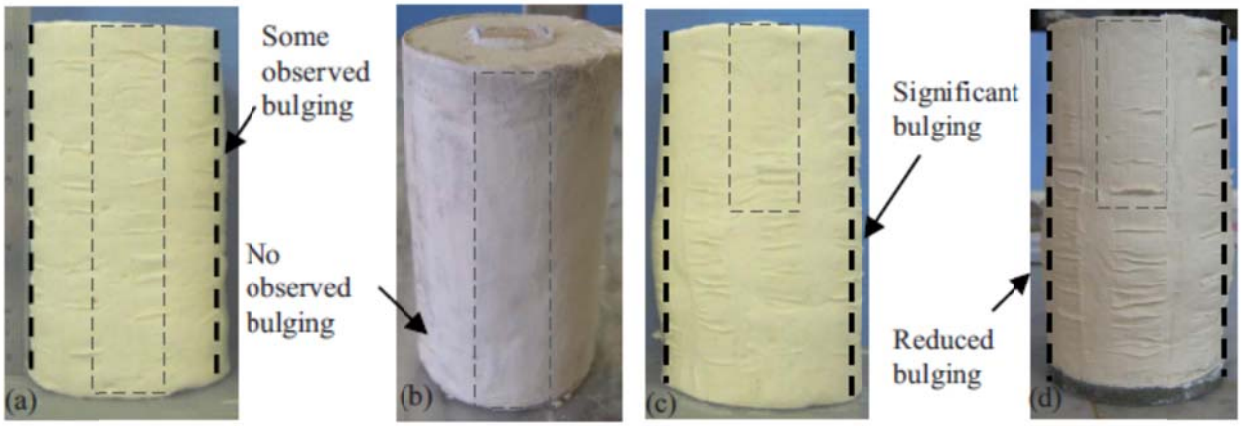

Fig. 2.7Modes of failure of clay specimens with (a) fully penetrating unreinforced column; (b) fully penetrating reinforced column; (c) unreinforced column with penetration ratio of 0.5; and (d) reinforced column with penetration ratio of 0.5

The stress-strain curves and the pore pressure versus strain curves are presented in Fig. 2.8 and 2.9 for ordinary and encased sand columns, respectively. The sand columns improved the undrained shear strength on average by a factor of 17.4% and 72.8% for an area replacement ratio of 7.9% and 17.8% respectively. The encasement of the sand columns shows an increase in the average improvement on the undrained shear strength by a factor of 2.5 and 1.3 for an area replacement ratio of 7.9% and 17.8% respectively. Table 2.1 indicates that for samples that were reinforced with fully penetrating non-encased sand columns with area replacement ratios of 7.9 and 17.8%, the average reduction in the excess pore-water pressure at different effective confining pressures was 12.9 and 31.3%, respectively. The reduction in the generation of excess pore-water pressure during undrained loading is likely due to the dilatational tendency and the higher stiffness of the sand columns. For partially penetrating columns with H_c/H_s=0.75, the average reductions of excess pore-water pressure at different effective confining pressures were reduced to about 7 and 17% for area replacement ratios of 7.9 and 17.8%, respectively. Hence, the insertion of sand columns reduces the excess pore-water pressure generation during undrained loading, and their effectiveness in reducing the water pressure increases with increasing the column height and area replacement ratio. The insertion of fully penetrating encased sand column with area replacement ratios of 7.9 and 17.8% leads to an average reduction of 11.6 and 30.9% in the excess pore-water pressure, respectively.

With regards to the effective shear strength envelops (Fig. 2.10), the effective friction angle (ϕ ') and the apparent cohesion (c') of clay specimens that were reinforced with non-encased sand columns were not significantly affected by the presence of the sand column. However, for samples that were reinforced with fully penetrating sand columns with an area ratio

of 17.8%, c' increased from 0 kPa (for unreinforced specimen) to 12 kPa.

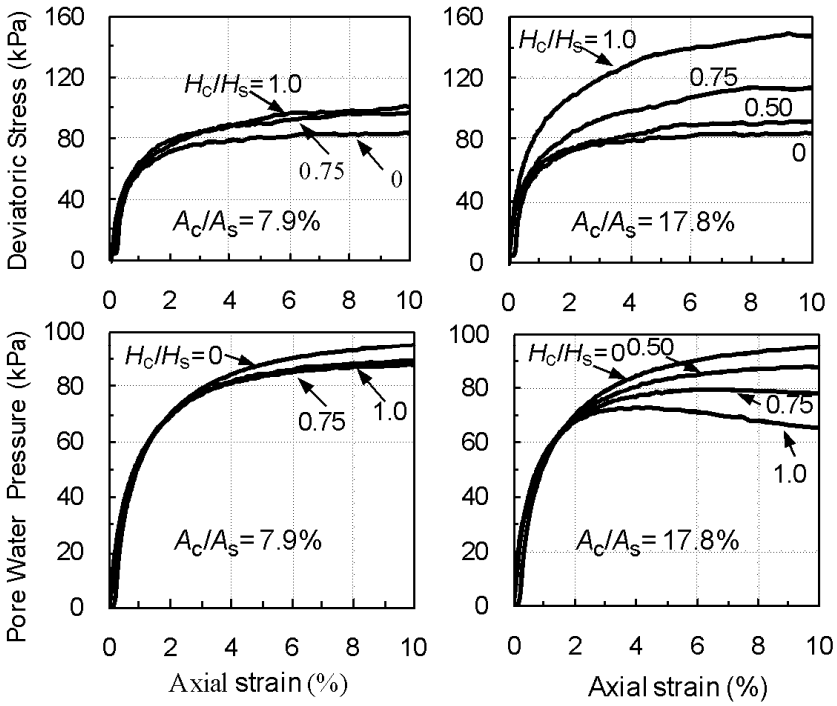

Fig. 2.8 Deviatoric stress and excess pore water pressure versus axial strain for kaolin specimens reinforced with non encased sand columns ((σ'3)o=150 kPa)

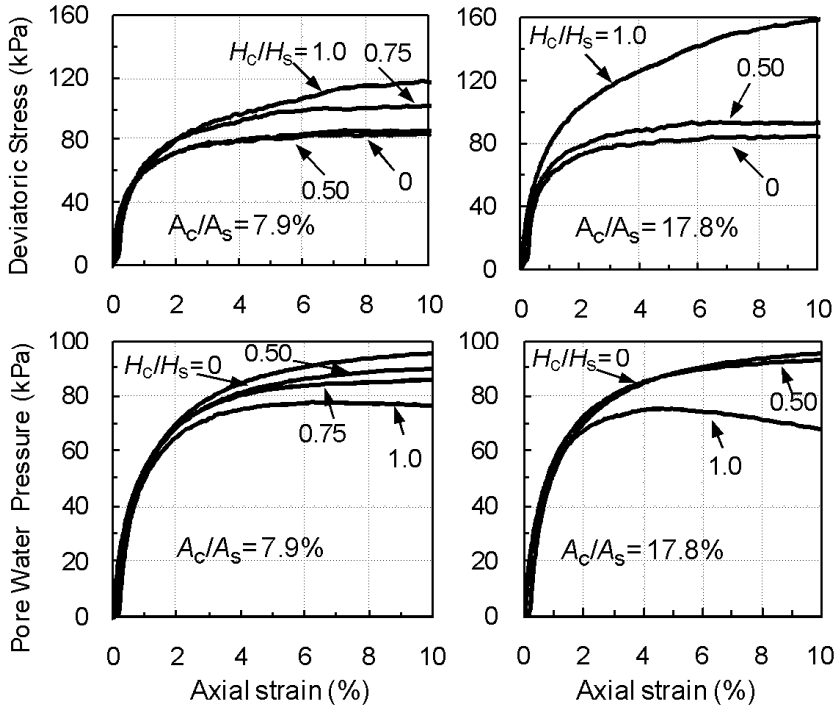

Fig. 2.9 Deviatoric stress and excess pore water pressure versus axial strain for kaolin specimens reinforced with encased sand columns ((σ'3)o=150 kPa)

As a result, it can be concluded based on the data that was collected in this study that reinforcing soft normally consolidated clays with sand columns with a friction angle of about 33 degrees, will not have a significant impact on the effective shear strength parameters of the reinforced clay, except if fully penetrating columns with relatively high area ratios (greater than 17%) were used to reinforce the clay. The encasement of sand columns with a geotextile fabric improved the apparent cohesion of the composite, particularly for small area replacement ratios (Ac/As=7.9%) and fully penetrating columns. However, the increase in c' was accompanied by a reduction in the effective angle of friction. For an area replacement ratio of 17.8%, the increase in c' was not as significant.

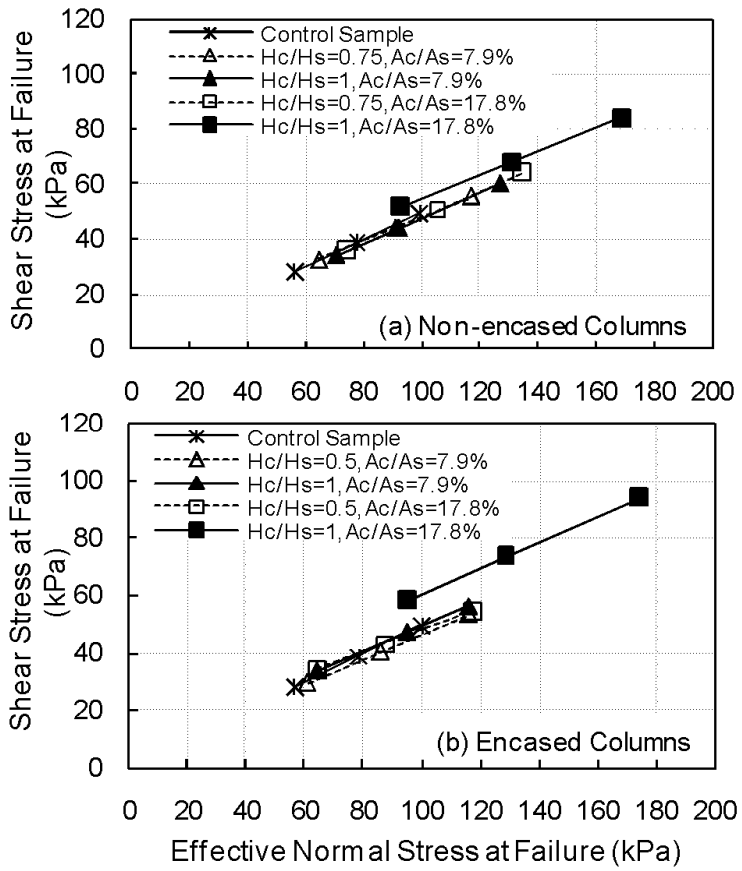

Fig. 2.10 Effective failure envelops for unreinforced and reinforced kaolin specimens

2.4. "Drained" Triaxial Tests

Black et al. (2006), Black et al. (2011), and Sivakumar et al. (2011) conducted tests that involved drained foundation loading of isotropically and K_o-consolidated kaolin samples at rates of 0.8 to 1.0 kPa/hour. The tests were conducted in a large triaxial cell on clay specimens with a diameter of 30 cm and a height of 40 cm, but the loads were independently applied to the sample via a circular plate with a diameter of 6 cm.

2.4.1. Black et al. (2006)

Black et al. (2006) manufactured a triaxial testing apparatus that has the capability of testing Ko-consolidated samples having a diameter of 30 cm and a height of 40 cm. In the proposed test setup, the load is independently applied to the sample via a circular plate with a diameter of 60 mm.

Kaolin specimens were prepared from a slurry and consolidated under a 1-dimensional vertical stress of 75 kPa. Sand columns with a diameter of 25mm were prepared using the wet compaction method using the procedure described in Sivakumar et al. (2004). The specimen was then placed into the triaxial test chamber and initially subjected to an isotropic effective confining pressure of 75 kPa. This was then followed by Ko loading where the vertical stress (σ_1') and horizontal stress (σ_3') where raised slowly to reach values of 125 kPa and 100 kPa respectively. A back pressure of 200 kPa was maintained all the time. Foundation loading was applied to the specimen at a rate of 0.8 kPa/hr to achieve fully drained loading conditions. The test took 2-3 week to reach a settlement of 15 to 20 mm.

For a footing displacement of 10 mm, the capacity of the unreinforced column was 1.25 kN. The capacity increased by 12% and 28% due to the insertion of sand columns of height to diameter ratio of 6 and 10 respectively (see Fig. 2.11). The area replacement ratio was 17%. Readings from pressure cells that were installed in the sand column and in the surrounding clay indicated that for sample reinforced with the long column, the pressure in the column at a settlement of 10 mm was equal to 1100 kPa, while the pressure in the clay was equal to 600 kPa. This indicates a stress concentration factor of about 1.83. This relatively small value of the stress concentration was attributed to the small area replacement ratio and to the drained loading conditions, since n values are usually higher in the case of undrained loading conditions.

Observations of the modes of failure revealed that short columns had no distinct variation in column diameter, while long columns showed crucial deformation in the top regions. These findings are in line with the observations of Hughes and Withers (1974) who stated that long columns fail by bulging while short columns penetrate in the underlying clay. The authors conclude that the optimum column length to diameter ratio is somewhere between 6 and 10.

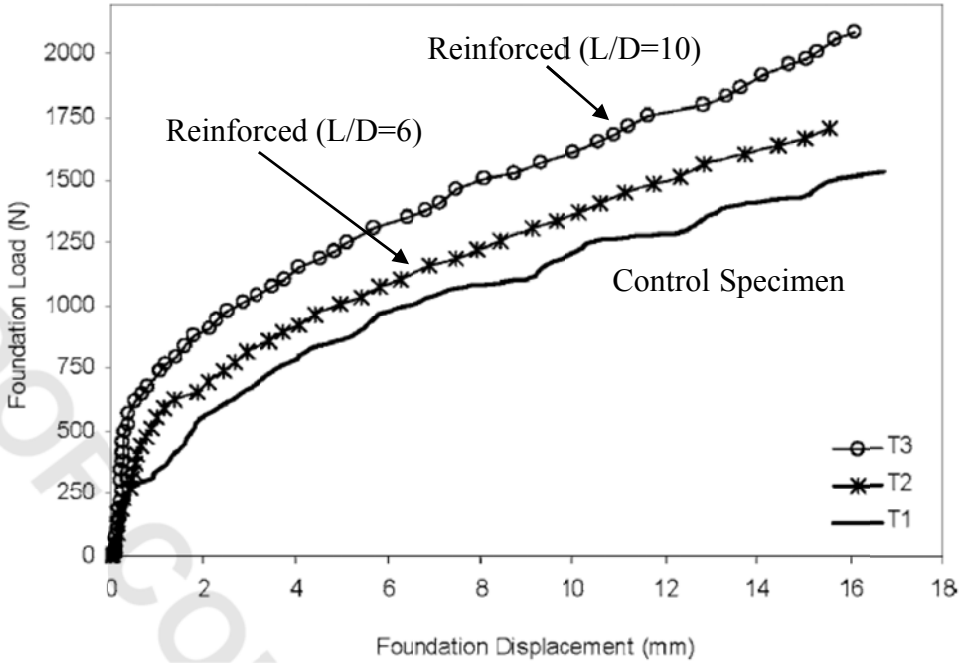

Fig. 2.11 Load-settlement behavior for control and reinforced specimens (L/D = 6 and 10)

2.4.2. Black et al. (2011)

Black et al. used a large triaxial cell to test clay samples with diameters of 30cm and depths of 40cm, that were consolidated under Ko conditions. Kaolin slurry was initially consolidated to a vertical pressure of 150 kPa resulting in clay specimens with an undrained shear strength of 35 kPa. The clay was then moved to the triaxial cell after being trimmed to a height of 40cm. Gravel columns with diameters of 2.5cm, 3.2cm, and 3.8cm (area ratios of 17, 28, and 40% when loaded with a 6cm wide footing) were installed using the replacement method

and compacted in layers using 10 blows of a 1.0 kg rod that was raised a distance of 5cm to form columns with a density of about 15.5 kN/m^3. The authors state that 6% increase in cavity volume occurred during the installation of the columns. For group loading, three columns of 1.8cm and 2.2cm diameters were adopted to produce area ratios of 28% and 40%, respectively. Three column lengths were considered (12.5cm, 25cm, and 40cm) to represent column penetration ratios of 0.31, 0.62, and 1.0 respectively. Following the column installation, the sample was consolidated under an effective cell pressure of 75 kPa followed by Ko consolidation with a Ko of 0.71. The Ko consolidation was assumed to represent the unit cell concept where zero lateral displacement is maintained at the boundaries. The final step included applying foundation loading under drained conditions at a rate of 1 kPa/hour.

Monitoring of settlement versus stress during Ko consolidation indicated that the strains measured for the reinforced samples were 0.77%, 0.72%, and 0.54%, for area ratios of 0.7%, 1.1%, and 1.6%, respectively (total area reinforced with single columns), compared with a strain of 1.5% for the unreinforced clay. Comparison of settlements for partially penetrating columns indicated that settlements reduce as the depth of treatment increases as indicated in Fig. 2.12. Foundation loading indicated that the settlement improvement factors increase as 11 the L/D ratio increases for a given area ratio, although the improvement seems to level off at L/d between 8 and 10. The settlement improvement factor also increased with increase in the area replacement ratio, but the improvement seems to decrease at a threshold of about 30% to 40% area replacement. For foundations supported on column groups, the pressure-settlement response was found to be similar to the individual columns at the same area replacement ratio.

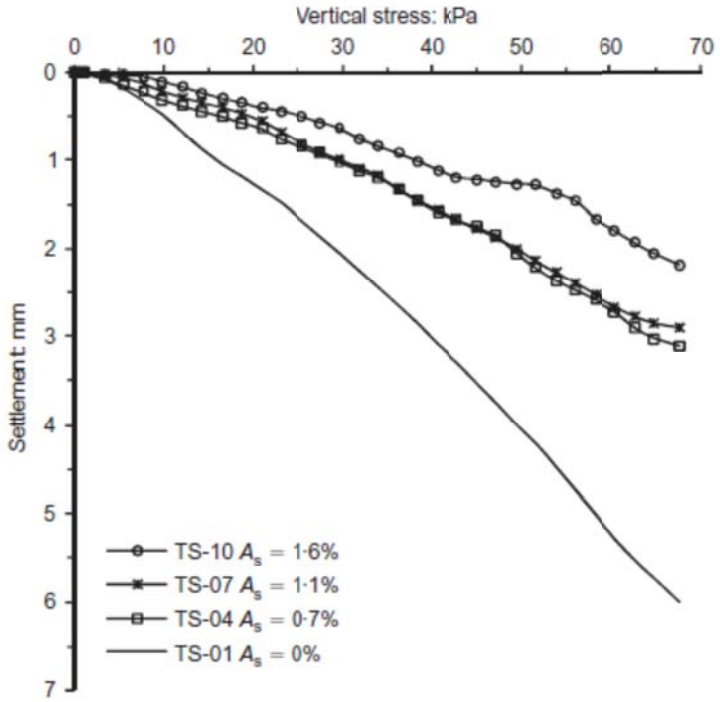

Fig. 2.12 Settlement under unit cell consideration with increasing area replacement ratio

Settlement improvement factors for the area replacement of 28% and 40% were 3.2 and 3.8 respectively. The settlement improvement factors for the corresponding single columns were about 6.5 to 7.5 indicating that the performance of the group is not as good as that of the single columns. Limited results for pressures recorded in the column and in the clay in the group indicate a stress concentration factor in the order of 1.5.

2.4.3. Sivakumar et al. (2011)

Sivakumar et al. used a large triaxial cell to test clay samples with diameters of 30cm and depths of 40cm, reinforced with columns of compacted crushed basalt. Samples were saturated and consolidated under a confining pressure of 50 kPa followed by foundation loading at a rate of 1

kPa/hour. The column diameters were 4, 5, and 6cm and the loading plate had a diameter of 6cm. During consolidation, the stone columns settled with time due to consolidation of the surrounding clay. Since the clay consolidated more than the columns, negative skin friction was generated on the columns. In the control clay test, the footing settled 15 mm at a pressure of 300 kPa. For the 6cm columns, the pressure under the footing increased by 500 kPa. The critical length of the columns was estimated to be about 5 column diameters. For a pressure of 150 kPa, a comparison of the settlements indicated improvement factors of 1.7, 1.7, and 4.8 for the 4, 5, and 6cm columns respectively as presented in Fig. 2.13. These factors are smaller than those predicted by Priebe (1995) who assumed a unit cell whereby zero lateral strains are imposed and Black et al. (2011) who had rigid boundary conditions which increased the confinement.

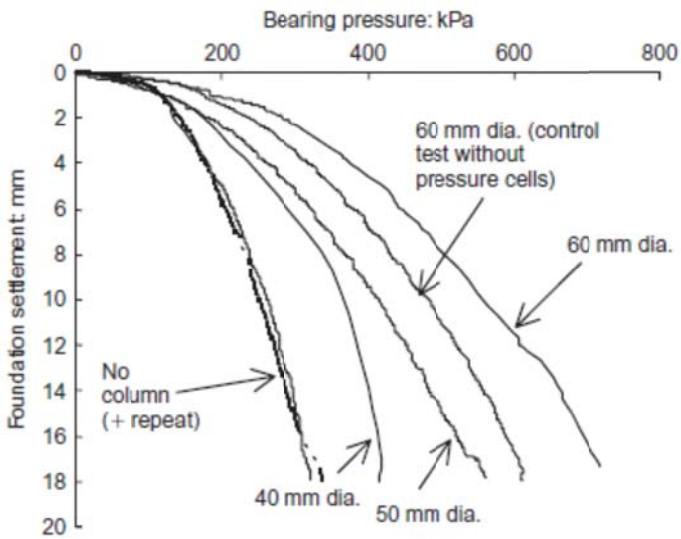

Fig. 2.13 Bearing Pressure-settlement characteristics

2.5. "Partially Drained" Triaxial Tests

Juran and Guermazi (1987) and Andreou et al. (2008) studied the effects of partial drainage and rate of loading on the improvement brought by the addition of sand columns to soft soils in a

triaxial framework.

2.5.1. Juran and Guermazi (1988)

Juran and Guermazi used a modified triaxial cell to investigate the effect of partial drainage of a soft silty soil (D=10cm) that was reinforced by compacted river-sand columns (RD=80%, φ'=38°) at area replacement ratios of 4 and 16% (D=20 and 40mm). They conducted tests at a rate of 0.05mm/min while allowing drainage of the sand columns (partially drained tests) and tests where both the sand column and the surrounding soil were not allowed to drain (undrained test). Results presented in Fig. 2.14 indicated that the drained column significantly improved the resistance of the reinforced soil to the applied strain. Moreover, results indicated that the maximum load carried by the "drained" column was about twice that carried by the undrained column. The stress concentration ratio was equal to about 6 for samples that were reinforced with the drained column compared to 3 for samples reinforced with undrained columns.

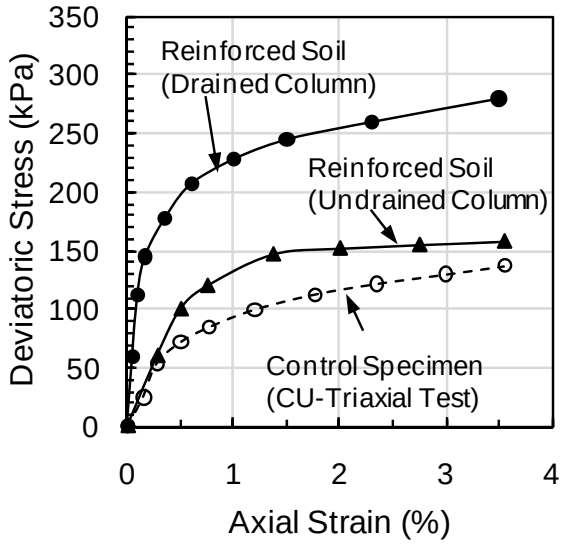

Fig. 2.14 Effect of drainage on response of reinforced soil specimens to triaxial compression

2.5.2. Andreou et al. (2008)

Andreou et al. conducted triaxial compression tests on kaolin clay reinforced with single columns consisting of Hostun (HF) sand and gravel. Drained, undrained, and partially drained tests were conducted to highlight the influence of the drainage condition and rate of loading. Columns with a diameter of 2cm and a height of 20cm were used to reinforce specimens with a diameter of 10cm (area ratio of 4%). The samples were consolidated under confining pressures of 50 to 200kPa. Results in Fig. 2.15 indicated that the strength increase in the reinforced specimens depended on the drainage condition and the loading rate. The maximum deviatoric stress carried by the reinforced sample under drained conditions is twice that of the undrained condition. An increase in the rate of shearing (from 0.003 to 0.3mm/min) while allowing drainage leads to a reduction in the strength of the reinforced sample compared to the fully drained case; however, the measured strength remained higher than that of the reinforced undrained sample. Results of the undrained tests indicated that the improvement in undrained strength decreased from 45 to 20% as the confining pressure increased from 50 to 200 kPa and that the effective friction angle increased slightly compared to unreinforced samples (23° to 24°).

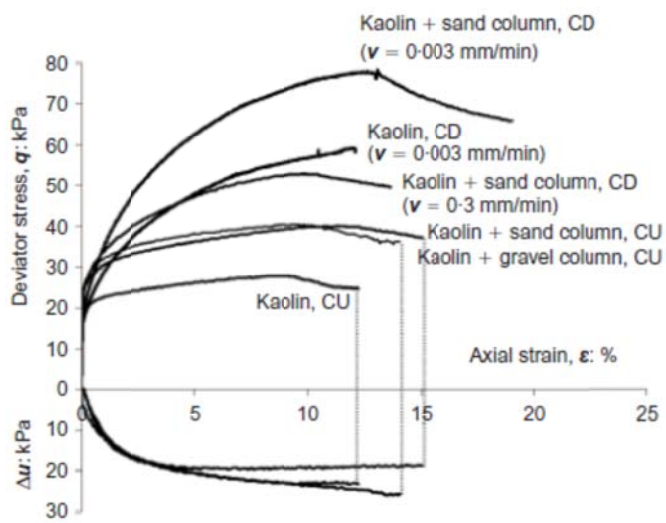

Fig. 2.15 Variation of deviator stress and excess pore pressure with axial strain

2.6. Summary

Based on the above literature review, it is clearly shown that the insertion of stone columns in soft to medium stiff clay enhances the load carrying capacity of the soft clayey material, reduces the settlement under the foundations, and reduces the generation of excess pore water pressure during loading stages. The axial capacity of the column depends on the angle of internal friction of the column granular material, the geometric properties of the column such as column diameter, area replacement ratio, height penetration ratio, column spacing, ratio of column height to the column diameter, and on the undrained shear strength of the surrounding soft material, and the lateral/radial restraint provided by the surrounding weak soil. Moreover, the presence of geotextile fabric around the periphery of the column can enhance significantly the lateral support provided by the soft soil to the column material, and as a result, the extent of improvement in the load carrying capacity and reduction of settlement will be amplified due to the increase in the lateral confinement which will prevent the column bulging during loading stages and will increase the stiffness of the composite column clay material.

CHAPTER 3

TEST MATERIALS AND SAMPLE PREPARATION

3.1. Introduction

This chapter describes the properties of the materials used in the testing program. These materials include Kaolin clay, Ottawa sand, and the geotextile fabric. Atterberg limits, specific gravity, hydrometer analysis, and 1-dimensional consolidation tests were performed using Kaolin clay. The results of the consolidation tests were used to determine the coefficient of consolidation of the clay using the log time method and the square root of time method. For Ottawa sand, sieve analysis, triaxial, and relative density tests were performed. The geotextile fabric was subjected to pull out tests for the purpose of determining the tensile strength and the stiffness of the material, with the fabric oriented in both the lateral and the vertical directions.

Furthermore, a detailed description of the process of sample preparation is presented. The process includes the preparation of Kaolin specimens form a slurry, 1-dimensional consolidation of the slurry in custom-fabricated consolidometers, and installation of encased and ordinary sand columns in pre-augured holes in the specimens.

3.2. Test Materials

3.2.1. Kaolin Clay

Kaolin clay was brought to the laboratory in sealed bags with a weight of 25kg from Uniceramic, a local tile manufacturer. A large percentage of the clay was composed of round clodded particles with an approximate length of 2cm and a diameter of about 0.4cm. The clay

clods were crushed with a rubber tipped hammer and stored in a tightly closed plastic drum in order to preserve their water content. Index properties for the Kaolin clay were determined in the laboratory and are presented in Table 3.1.

Table 3.1 Index properties of Kaolin clay

Liquid limit (%)	Plastic limit (%)	Plasticity index	Specific gravity	Percent finer than 10 μm (%)	Percent finer than 2 μm (%)
55.7	33.3	22.4	2.52	85	53

The consolidation properties of the Kaolin slurry were obtained from a one-dimensional consolidation test that was conducted on a clay sample with a diameter of 5.08cm and a height 1.91cm. The test specimen was trimmed from a larger specimen which was consolidated from a slurry in a 1-dimensional prefabricated consolidometer under a vertical effective stress of 100 kPa as will be explained in section 3.3.2. The specific gravity, initial water content, and initial void ratio of the slurry-consolidated specimen are presented in Table 3.2.

The consolidation test was performed in accordance with the requirements of ASTM 2435. The results pertaining to the loading and unloading stages are presented in Table 3.3. Fig. 3.1 shows the variation of the void ratio versus the logarithm of the effective vertical stress, where the void ratio is defined at the end of each load increment (24 hours from the onset of loading). Based on the e-Log p curve presented in Fig. 3.1, the virgin compression (C_c), reloading (C_r), and swelling (C_s) slopes are computed as 0.413, 0.146, and 0.157, respectively. Based on Casagrande's approach, the pre-consolidation pressure was determined from the e-log p curve as 96 kPa.

Table 3.2. Initial properties of 1-dimensional consolidation test specimen of Kaolin clay

Specific gravity	2.52
Initial water content (%)	61
Initial void ratio	1.53
Initial saturation (%)	100 (assumed)

Table 3.3. One-Dimensional consolidation pressure test results

Cosolidation pressure (kPa)	Final dial reading (cm)	Change in specimen height (cm)	Final specimen height (cm)	Height of void (cm)	Final void ratio	Average height during consolidation (cm)
0	0		1.905	1.153	1.534	
		0.144				1.833
10	0.144		1.761	1.009	1.342	
		0.033				1.7445
20	0.177		1.728	0.976	1.298	
		0.05				1.703
49	0.227		1.678	0.926	1.232	
		0.068				1.644
98	0.295		1.61	0.858	1.141	
		0.08				1.57
196	0.375		1.53	0.778	1.035	
		0.09				1.485
383	0.465		1.44	0.688	0.915	
		0.097				1.3915
775	0.562		1.343	0.591	0.786	
		0.103				1.2915
1550	0.665		1.24	0.488	0.649	
		-0.044				1.262
383	0.621		1.284	0.532	0.708	
		-0.07				1.319
98	0.551		1.354	0.602	0.801	
		-0.062				1.385
20	0.489		1.416	0.664	0.883	

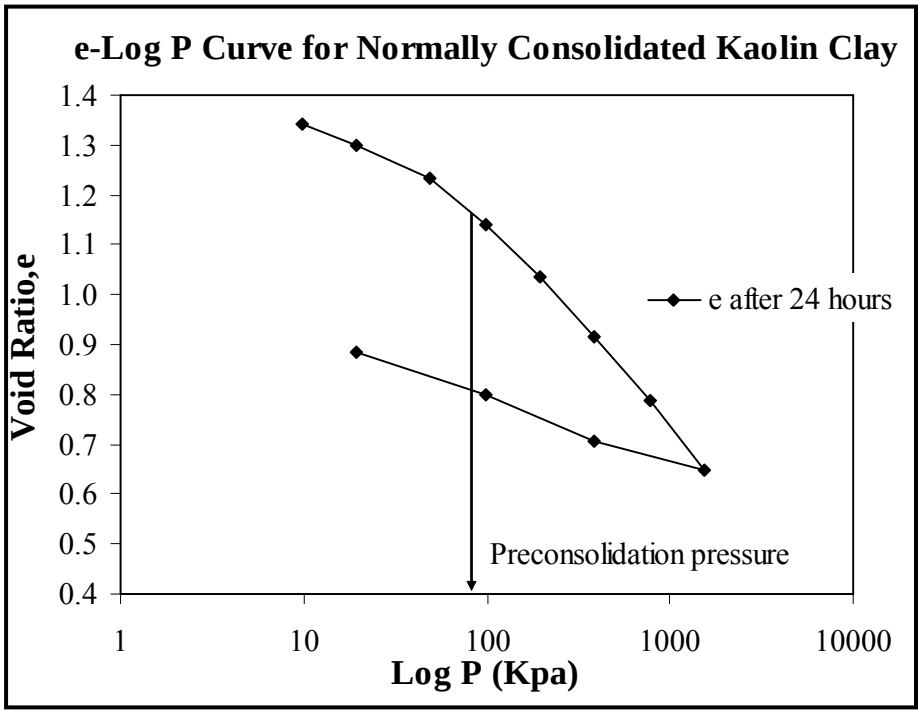

Fig.3.1 e-log P for normally consolidated Kaolin clay

The values of the coefficient of consolidation were calculated based on the times (t_{50}) and (t_{90}) which correspond to average degrees of consolidation of 50% and 90%, respectively. Casagrande's method was used to determine t_{50} while Taylor's method was used to determine t_{90}. To determine t_{50}, the vertical settlement of the specimen is plotted against the log of time for a given consolidation pressure and the time that corresponds to 50% consolidation is determined. The coefficient of consolidation (C_v) can then be obtained as a function of t_{50} such that $C_v = T_{50} H^2 / t_{50}$, where T_{50} is the time factor corresponding to an average degree of consolidation of 50% (equals to 0.197), and H is the drainage path which is half the height of the specimen. In Taylor's method, the settlement is plotted as a function of the square root of time and t_{90} is determined as the time corresponding to an average degree of consolidation of 90%. C_v

is then calculated as $C_v = T_{90} H^2 / t_{90}$, where T_{90}=0.848.

Calculated values for the coefficient of consolidation (C_v) are presented as a function of the vertical effective stress in Table 3.4, and are plotted as a function of the logarithm of the vertical effective stress on Fig. 3.2. Measured time-settlement curves for typical pressures of 10 kPa to 383 kPa are also shown in Figs. 3.3 through 3.6 for both log-time and square root of time methods.

Table 3.4. Coefficient of consolidation obtained from t_{50} and t_{90}

Consolidation pressure (kPa)	Coefficient of consolidation, C_v (cm^2/min)	
	From t_{90}	From t_{50}
10	0.055	0.103
20	0.101	0.156
49	0.104	0.156
98	0.112	0.175
196	0.136	0.182
383	0.147	0.231
775	0.152	0.214
1550	0.030	0.013

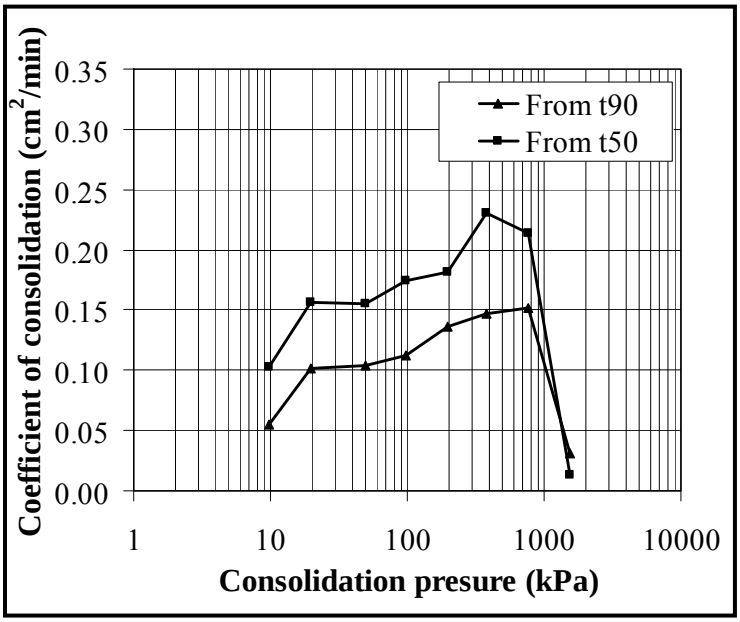

Fig. 3.2 Variation of Cv with consolidation pressure for Kaolin clay

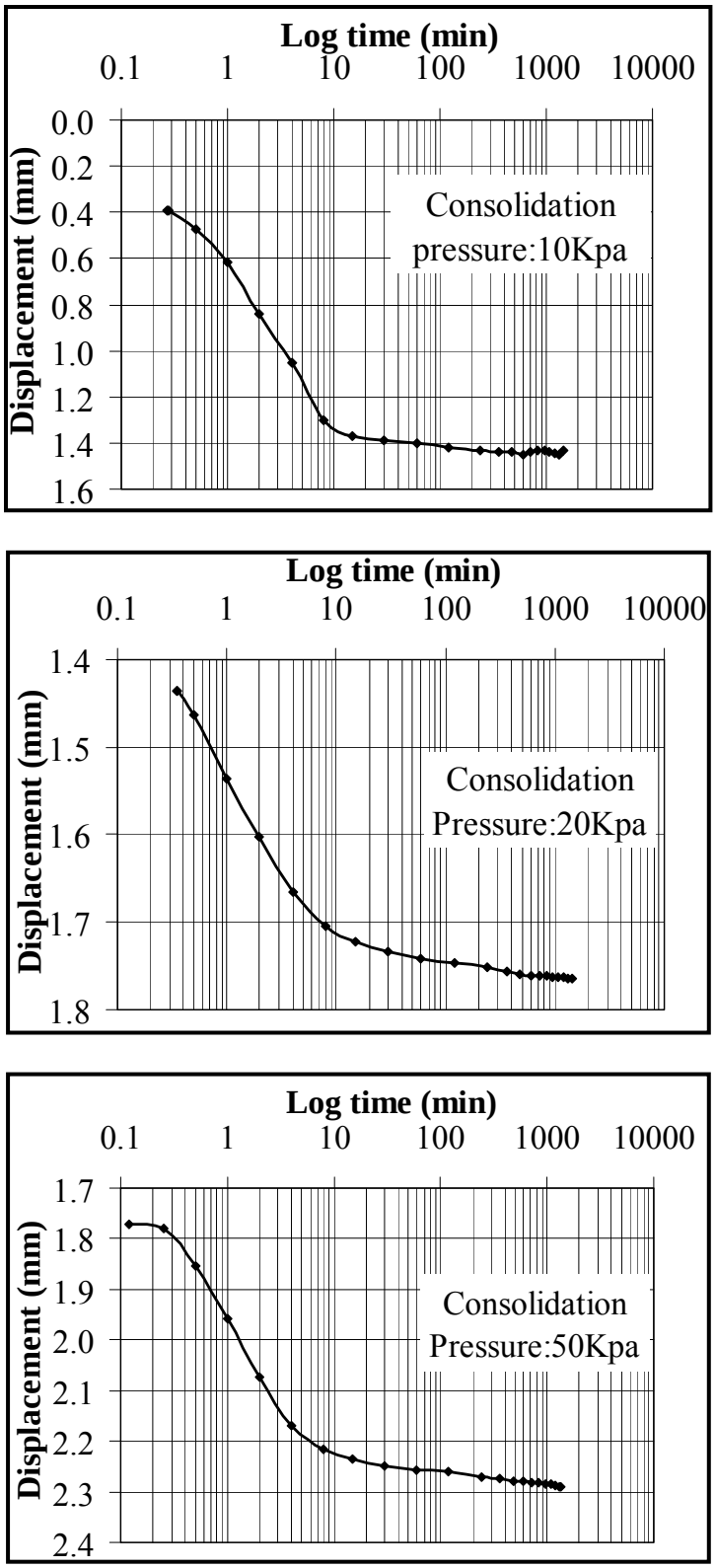

Fig. 3.3 Displacement vs. Log time for consolidation pressure of 10, 20 and 50 kPa

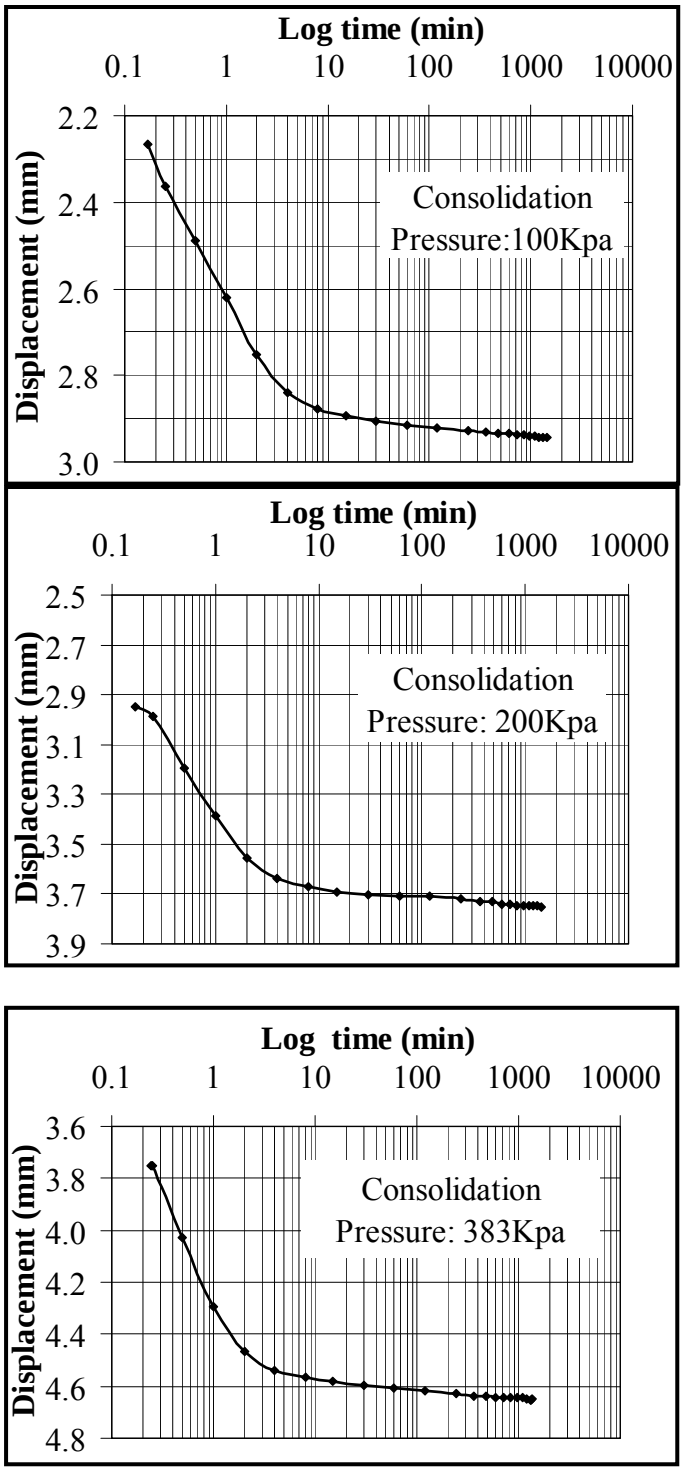

Fig. 3.4 Displacement vs. Log time for consolidation pressure of 100, 200, and 383 kPa

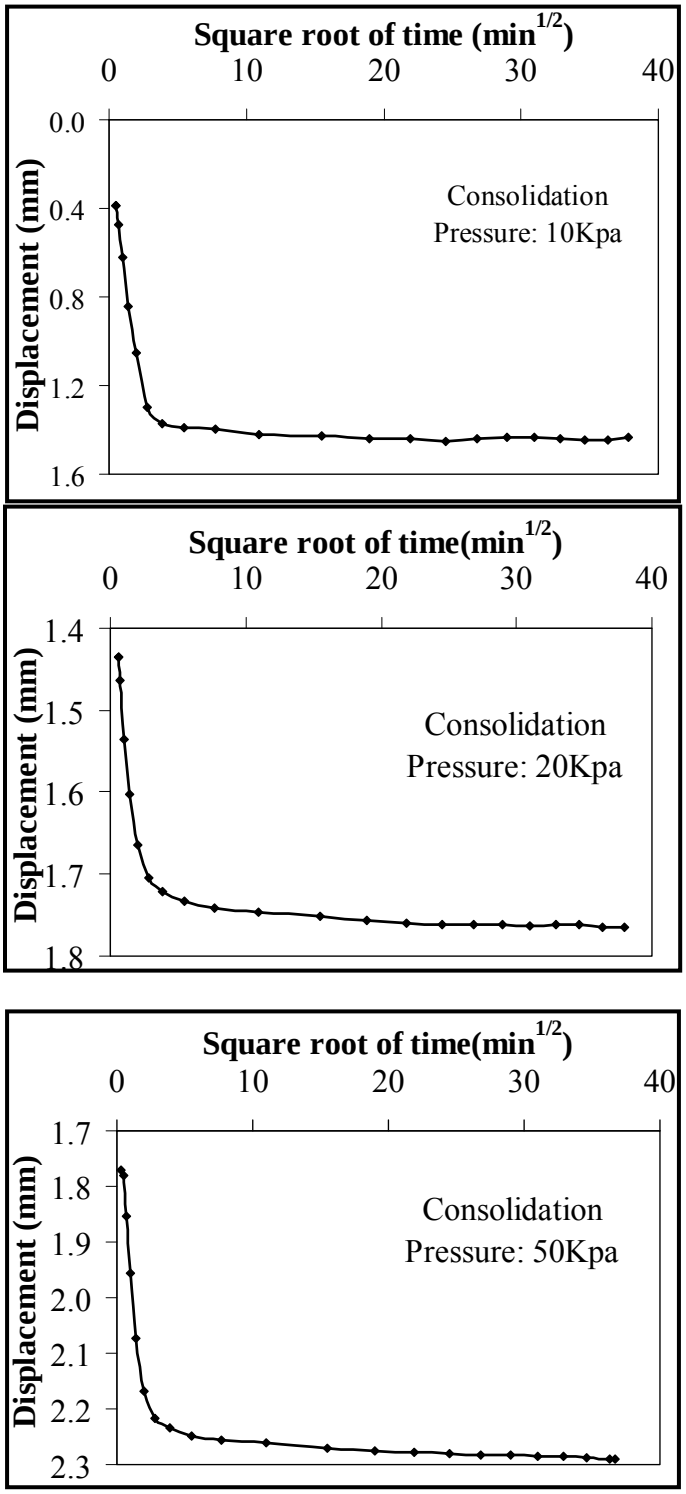

Fig. 3.5 Displacement vs. square root of time for consolidation pressure of 10 kPa, 20 kPa, and 50 kPa

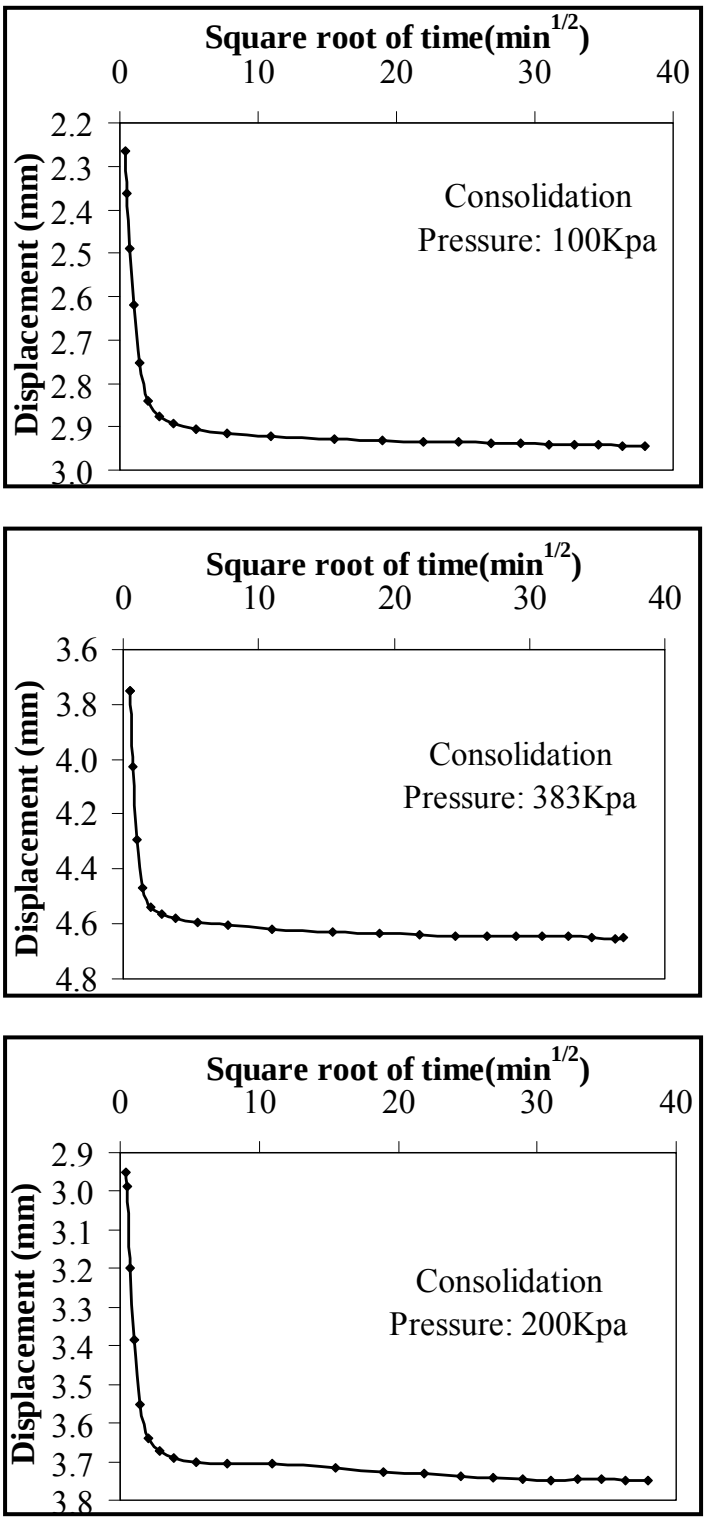

Fig. 3.6 Displacement vs. square Root of time for consolidation pressure of 100 kPa, 200 kPa, and 383 kPa

3.2.2. Ottawa Sand

The soil used in the reinforced columns was Ottawa sand which is a well-known laboratory tested material. Grain size distribution analyses conducted on Ottawa sand indicate that the particles have a mean diameter, D_{50} of 0.34mm, a uniformity coefficient, U_c of 2.3, and a coefficient of curvature, C_c of 0.82. The sand classifies as poorly graded sand (SP) according to the Unified Soil Classification System (USCS). The index properties for Ottawa sand and the sieve analysis results are shown in Table 3.5. and 3.6, respectively, while the particle size distribution curve is shown in Fig. 3.7.

Table 3.5. Index properties of Ottawa sand

D_{10} (mm)	0.22
D_{30} (mm)	0.3
D_{60} (mm)	0.5
Coefficient of uniformity (D_{60}/D_{10})	2.3
Coefficient of curvature $(D_{30})^2/(D_{60}*D_{10})$	0.82
Soil classification (USCS)	SP
Maximum void ratio (e_{max})	0.49
Minimum void ratio (e_{min})	0.75
Specific gravity	2.65
Drained angle of internal friction (Ø')°	33

Table 3.6. Sieve analysis results for Ottawa sand

Sieve No.	Diameter (mm)	Weight of retained soil (gm)	Cumulative percent retained (%)	Cumulative percent finer (%)
20	0.84	0	0.0	100.0
40	0.42	223.8	28.0	72.0
60	0.25	464.4	86.2	13.8
100	0.15	87.2	97.1	2.9
140	0.105	18.5	99.5	0.5
200	0.075	1.5	99.6	0.4
pan		2.8	100.0	0.0

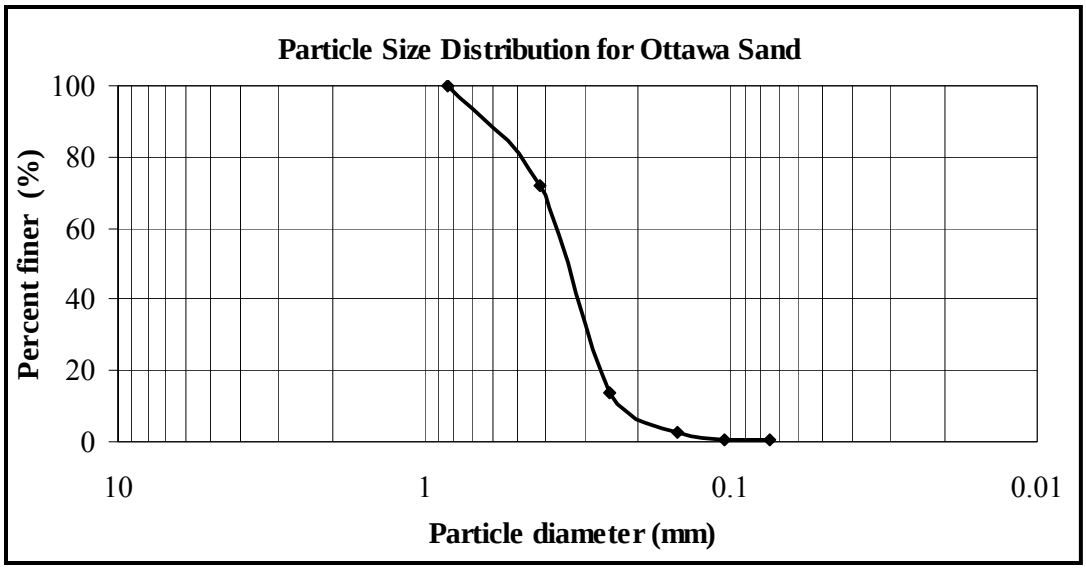

Fig. 3.7 Sieve analysis curve for Ottawa sand

Consolidated drained (CD) triaxial tests were conducted on Ottawa sand at confining pressures of 100, 150, and 200 kPa. Ottawa sand triaxial specimens with a height of 14.2cm and a diameter of 7.1cm were prepared at a dry density of 16.2 kN/m^3 (corresponding to a relative density of 44%, and a void ratio of 0.604). This density corresponds to the dry density of the sand column that was used to reinforce the Kaolin clay specimens in the testing program. Variation of deviatoric stress and volumetric strain with axial strain for the Ottawa sand during CD testing at the different confining pressures is shown on Fig. 3.8. As indicated by the Mohr Coulomb effective stress failure envelop for the Ottawa sand (Fig. 3.9.), the drained angle of friction (Ø') corresponds to a value of about 35º and a cohesion of zero.

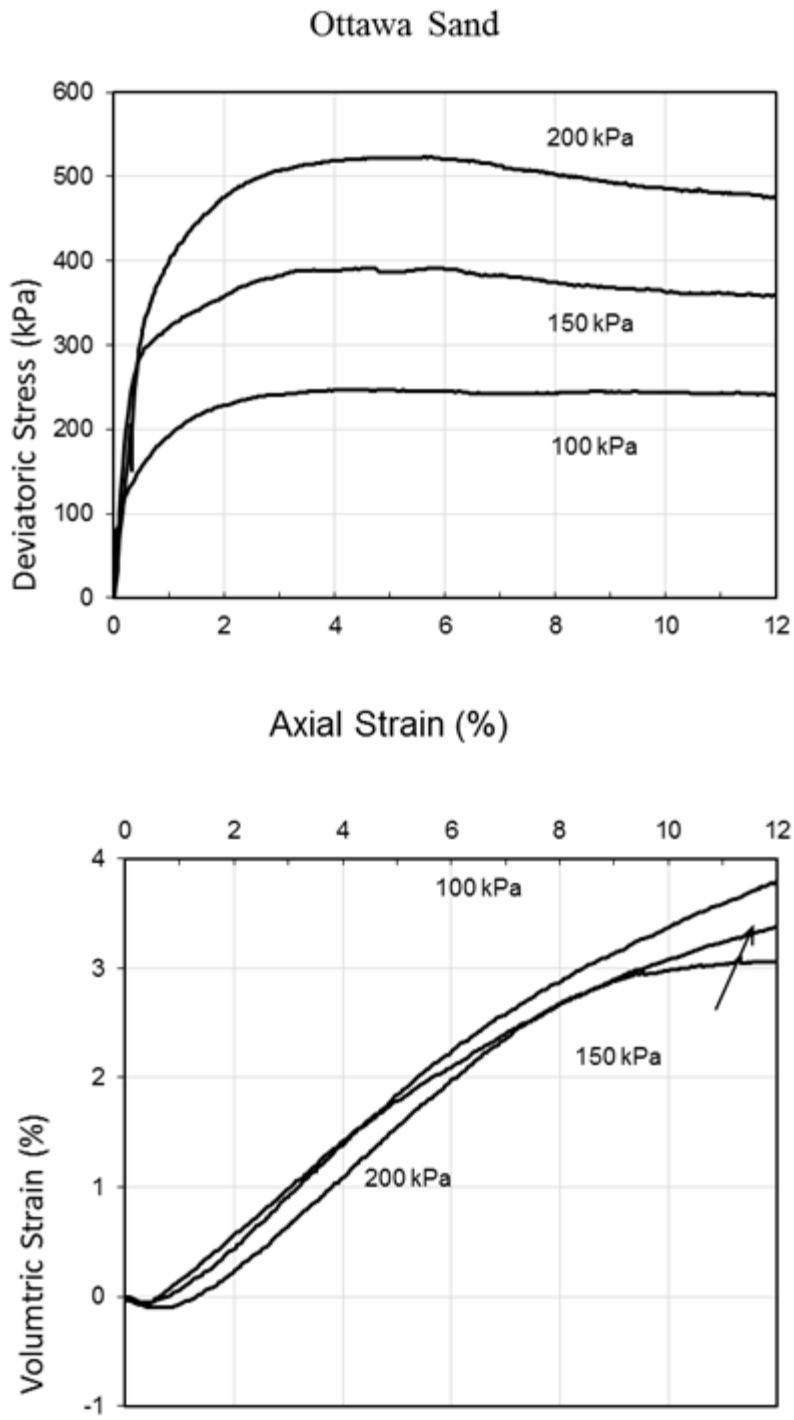

Fig. 3.8 Deviatoric stress and volumetric strain versus axial strain for Ottawa sand

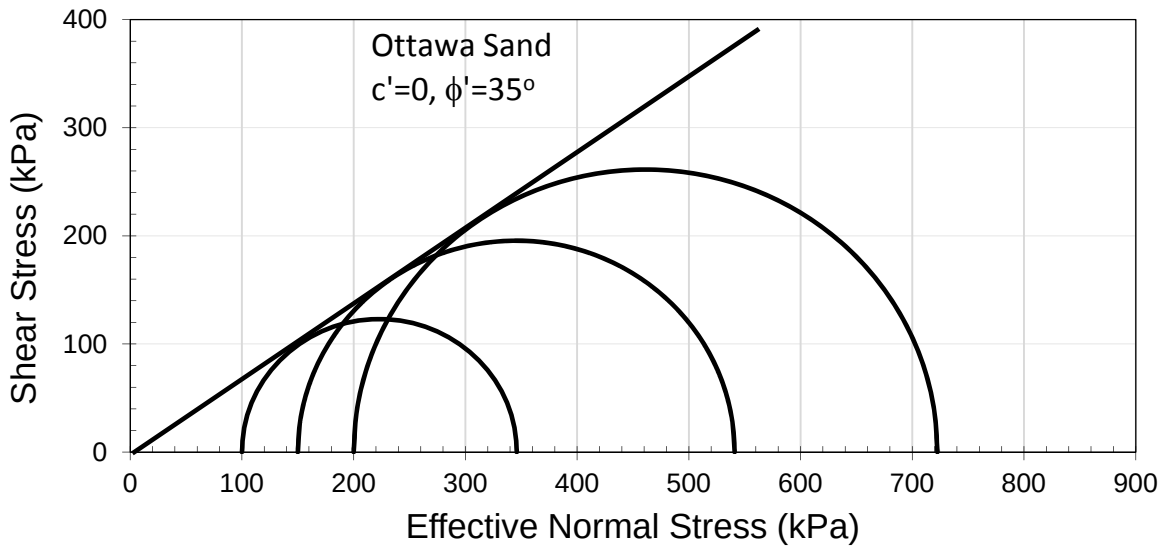

Fig.3.9 Mohr Coulomb effective stress failure envelop for Ottawa sand

3.2.3. Geotextile Fabric

The selection of the type of the geotextile fabric was made based on several criteria. First, the fabric had to ensure a moderate lateral support for the encased Kaolin specimen during loading. Second, the geotextile fabric had to provide proper drainage of pore water during isotropic consolidation. Finally, the fabric had to prevent the mixing of the sand column material with the surrounding clay during insertion of the column into the Kaolin specimen. Based on these criteria, the geotextile fabric was selected and brought from a tailor supplier. The width of the geotextile fabric roll was 0.8m and its length was 5m. At the tailor shop, the geotextile fabrics were cut and sewed to provide a cylindrical shape having a length of 19cm and diameters of 2cm and 3cm as shown in Fig. 3.10. The fabrics were sewed along the weak longitudinal direction, which represents the orientation of the weak fabric for the geotextile material. The orientation of the strong fabric was in the lateral direction.

The tensile strength of the geotextile fabric was determined in the laboratory using a digital force gauge. A piece of fabric with a length of 30cm, a width of 10cm, and a thickness of 0.11mm was subjected to a pullout force by fixing one end of the geotextile and applying a tensile force to the other end. In the test, the fabric was fixed at each end to two steel plates by wrapping the fabric into multiple layers between the plates, which were attached to each other using two bolts (Fig. 3.11). From one end, the steel plates were connected to a fixed plate through a steel ring, while from the other end the plates were connected to the digital force gauge through a hook as shown in Fig. 3.11. The peak rupture force was recorded on the screen of the digital force gauge.

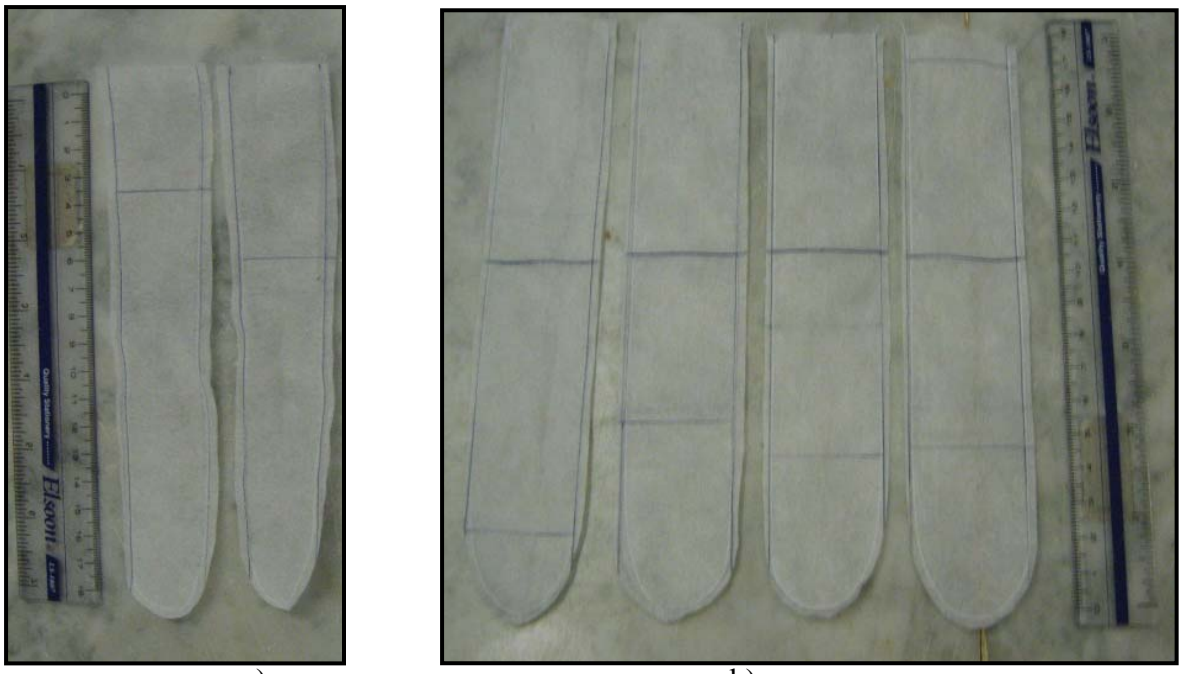

a) b)

Fig. 3.10 Preparation of cylindrical geotextile fabric of diameter (a)2cm and (b)3cm

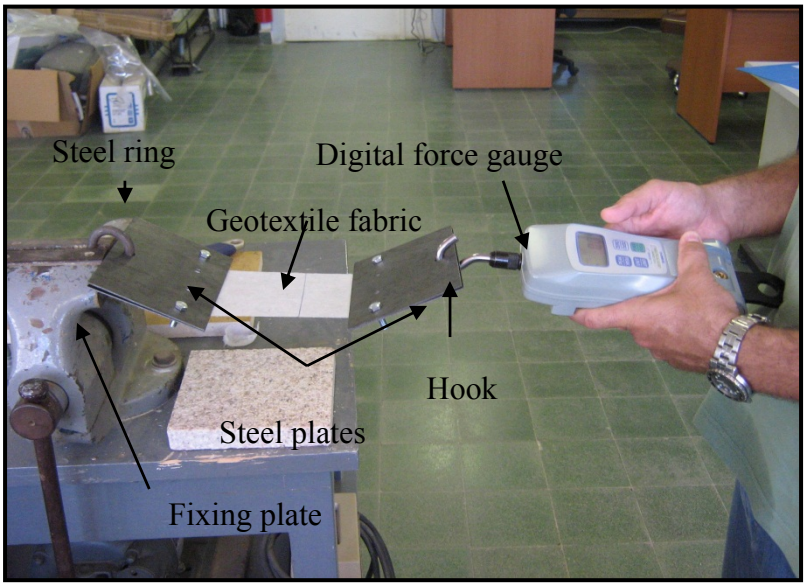

Fig. 3.11 Performing pull out test on geotextile fabric

The fabric was tested in dry and soaked conditions and along the strong and weak fabric orientations. Each test was repeated twice to confirm the results and to obtain average values for the tensile force. The average values for the tensile strength of both dry and soaked geotextiles are presented in Table 3.7. Soaking the fabric with water led to a 25% decrease in the value of the tensile strength, which was determined to be about 5.8 MPa and 3 MPa for strong and weak fabric orientations, respectively. Moreover, the secant modulus of elasticity for the dry and the soaked geotextile fabrics was determined at a strain of 1% as shown in Table 3.7.

Table. 3.7. Results of pullout tests on geotextile fabrics

Test#	Fabric orientation	Geotextile condition		Tensile force (N)	Average tensile strength (KPa)	Secant modulus of elasticity at 1% strain (KPa)
		Dry	Soaked			
1	Along strong fabric orientation	X		61	5770	35400
2		X		66		
3			X	47	4410	22600
4			X	50		
5	Along weak fabric orientation	X		31	3000	14300
6		X		35		
7			X	22	2300	10000
8			X	28		

3.3. Preparation of Normally Consolidated Kaolin Samples

3.3.1. Preparation of Kaolin Slurry

Kaolin clay powder was mixed with water at a water content of 100% (i.e. 1.8 times its liquid limit). A mass of 0.5kg of Kaolin material was initially mixed with 0.5 liters of water by means of an electric mixer with a capacity of 1.5 liters (Fig. 3.12). To ensure proper mixing and homogeneity of the slurry material, the slurry was mixed at a constant rate of 200 rounds per minute for a period of one minute.

Fig. 3.12 Electric Mixer for preparing Kaolin slurry

3.3.2. One-Dimensional Consolidometers

Four 1-D consolidometers were fabricated for the purpose of consolidating the Kaolin slurry (Fig. 3.13). Each consolidometer consisted of a PVC pipe segment with a height of 35cm, an external and internal diameter of 7.3cm and 7.1cm respectively, and a wall thickness of 0.1cm. The PVC pipe segment was cut longitudinally in the vertical direction into two halves to function as a split mold (Fig 3.14. a), thus eliminating the need for extruding the soil sample after consolidation. The two PVC sections were held in place using high-strength duct tape (Fig. 3.14. b) which was wrapped around the two cylindrical PVC sections to prevent leakage of slurry and to ensure that lateral strains are negligible during 1-D consolidation under the desired axial load. The advantage behind using a split PVC pipe was to ensure that an undisturbed, relatively soft, normally consolidated clay specimen can be obtained and removed with minimal disturbance after consolidation was achieved.

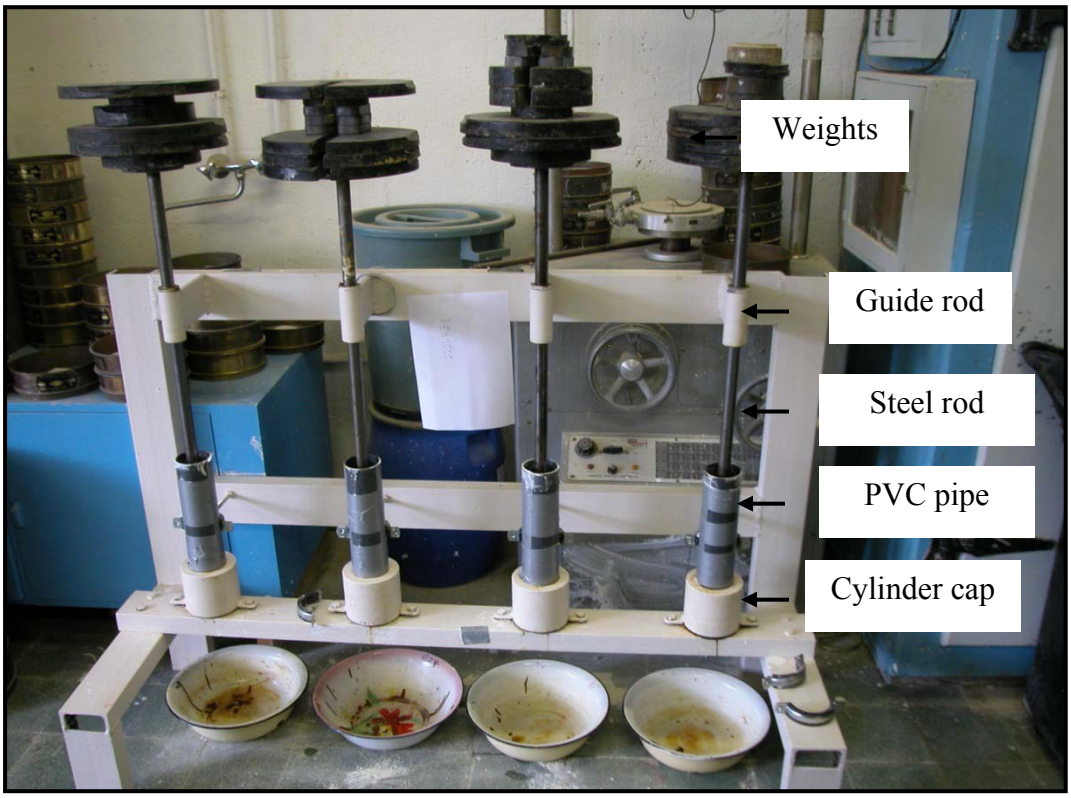

Fig. 3.13 Picture for custom fabricated 1-dimensional consolidometers

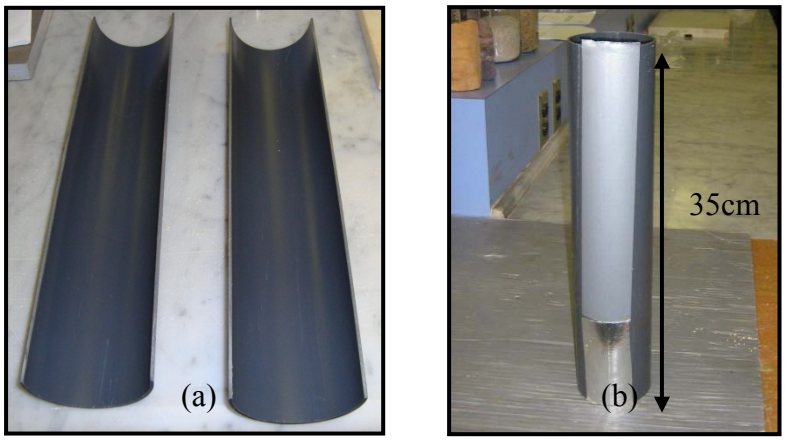

Fig. 3.14 Photo for (a) Split PVC pipe and (b) Wrapped PVC pipe with duct tape

At its lower end, the PVC pipe segment was fixed in place by means of a hollow steel cylinder with a height of 9cm as shown in Figs. 3.13. and 3.15. The stiff and heavy cylinder wraps tightly around the bottom of the PVC segment to provide additional lateral confinement and support to the PVC segment during slurry consolidation. The inner walls of the steel cylinder were coated with a thin layer of oil to facilitate the removal of the PVC segment once consolidation was achieved. Moreover, the circumference of the steel rod was coated with a thin layer of grease at the location of the steel rod guide to reduce friction between the steel rod and the guide rod. A porous stone and a filter paper were used to provide a freely draining boundary at the lower end of the soil specimen.

At its upper end, the soil specimen was loaded with a loading system consisting of dead weights similar to those used in 1-D consolidation tests. The dead weights were seated on a circular steel plate that transferred the load to the top of the soil specimen through a circular steel rod having a diameter of 1cm. A perforated circular steel piston with a diameter of 7.1 cm (same as inner diameter of PVC pipe) was fixed to the bottom of the steel rod to act as a loading plate which transmitted the load to the slurry. The soil was separated from the loading plate with a porous stone and a filter paper to provide a freely draining boundary at the top of the soil specimen. To reduce friction between the perforated loading plate and the PVC segment, the outside periphery of the loading plate was also coated with a thin layer of oil.

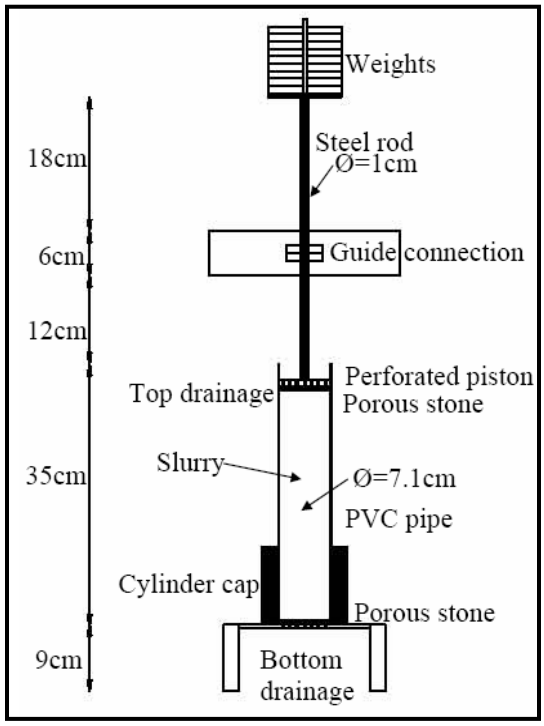

Fig. 3.15 Custom fabricated 1-dimensional consolidometer

3.3.3. One Dimensional Consolidation of Kaolin Slurry

The slurry was poured into the appropriate consolidometer and consolidated under K_o conditions using a vertical effective stress of 100 kPa. With four consolidometers, four clay samples could be prepared simultaneously, three of which were used for testing while the fourth sample was kept on reserve. Each consolidometer could handle a volume of slurry that is equivalent to two mixed batches of kaolin slurry, i.e. one kg of Kaolin with one liter of water. After pouring the slurry in the appropriate consolidometer (initial specimen height was 35cm), the clay was allowed to consolidate under its own weight for a period of 4 hours. During 1-D consolidation, drainage was allowed from both ends of the sample through the top and bottom

porous stones. Dead weights were then added in stages to the top of the sample, with each weight applied for a specified time period according to the loading sequence shown in Table 3.8.

Table 3.8. Loading sequence during 1-D consolidation of Kaolin slurry

Accumulated weights (Kg)	0.5	1	2	4	8	12	20	30	40
Applied pressure (kPa)	1.25	2.5	5	10	20	30	50	75	100
Duration (Hr)	4	4	24	24	24	24	24	24	24

The consolidation time periods that were allocated to each loading increment were estimated based on the results of the 1D consolidation test and were adjusted using trial and error. The objective was to develop a loading sequence which was repeatable, and which resulted in Kaolin specimens that were uniform. A typical time duration that is required to fully consolidate a clay sample under an effective normal stress of 100 kPa is approximately 7.5 days.

The water content after consolidation was found to be relatively uniform (about 53%) throughout the depth of the sample. The variations of the water content and the void ratio with depth were determined by slicing a consolidated clay sample into 7 pieces and determining the void ratio and water content for each slice. The variation of the void ratio and water content with depth for a typical sample is shown in Fig. 3.16. The variations are relatively small indicating a relatively uniform degree of consolidation in the sample. As expected, the void ratio was found to be the smallest at the upper and lower ends of the sample where the sample is completely drained during consolidation.

Additional measures were taken to further reduce disturbance during sample preparation. These measures included spreading a thin layer of oil over the inner surfaces of the

PVC pipes to reduce friction between the kaolin specimen and the inner surface of the pipe. This allowed for dismantling the pipe and removing the soil specimen from the consolidometer with minimal disturbance to the soil specimen.

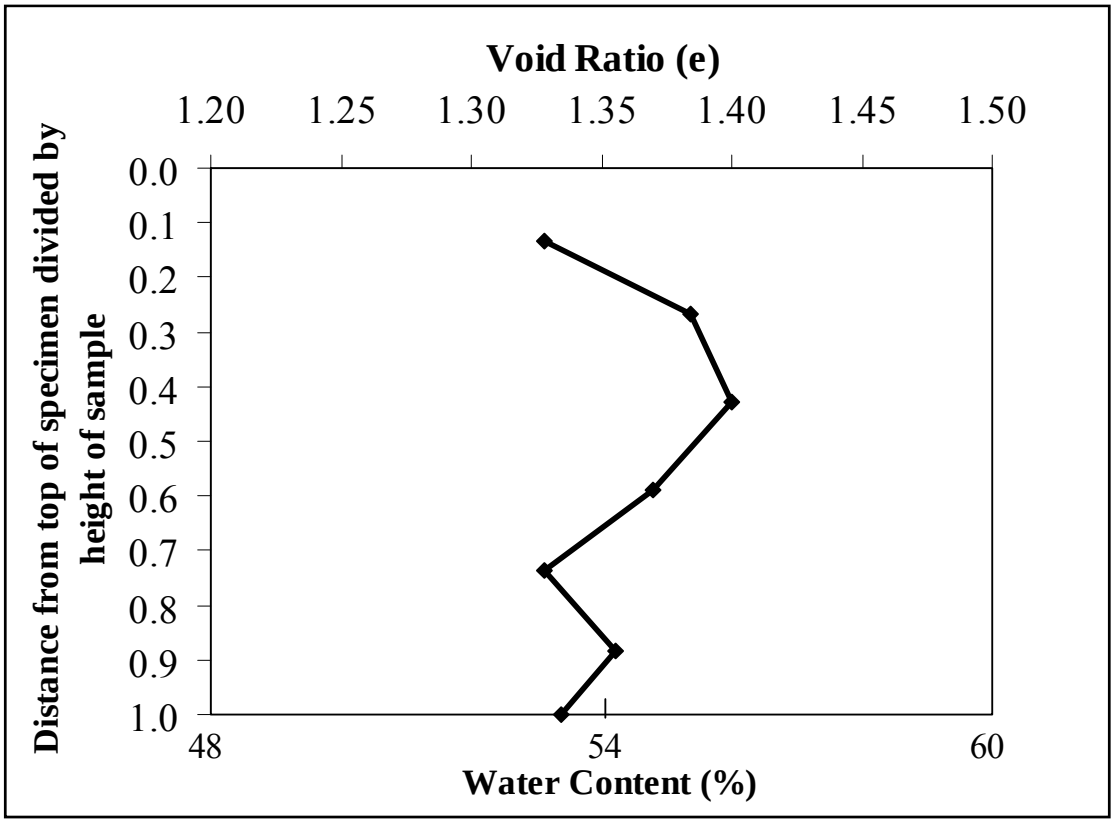

Fig. 3.16Water content and void ratio along the height of the sample after consolidation

3.3.4. Sample Preparation Prior to Placement in the Triaxial Cell

At the end of primary consolidation under a pressure of 100 kPa, the dead weights were removed and the PVC cylinder was slowly pulled out from the cylindrical cap of the consolidometer as shown in Fig. 3.17. (a). The duct tape surrounding the periphery of the PVC cylinder was unwrapped and the two PVC pieces were dismantled as shown in Fig. 3.17. (b). The consolidated Kaolin specimen is shown in Fig. 3.17. (c). The clay specimen was then trimmed to a final height of 14.2cm (initial height is about 18 cm) by means of a sharp spatula as shown in Fig. 3.18.(a). Two presoaked porous stones were then placed on the top and bottom of the Kaolin specimen and the sample was prepared for triaxial testing as shown in Fig. 3.18. (b). Finally, the sample was wrapped with a presoaked filter paper that has longitudinal perforations in order to speed up the process of consolidation in the triaxial cell (Fig. 3.18. c).

Fig. 3.17 (a) Kaolin specimen after removal from custom fabricated consolidometer, (b) dismantling of PVC pipe, and (c) Kaolin specimen after removal form PVC pipe.

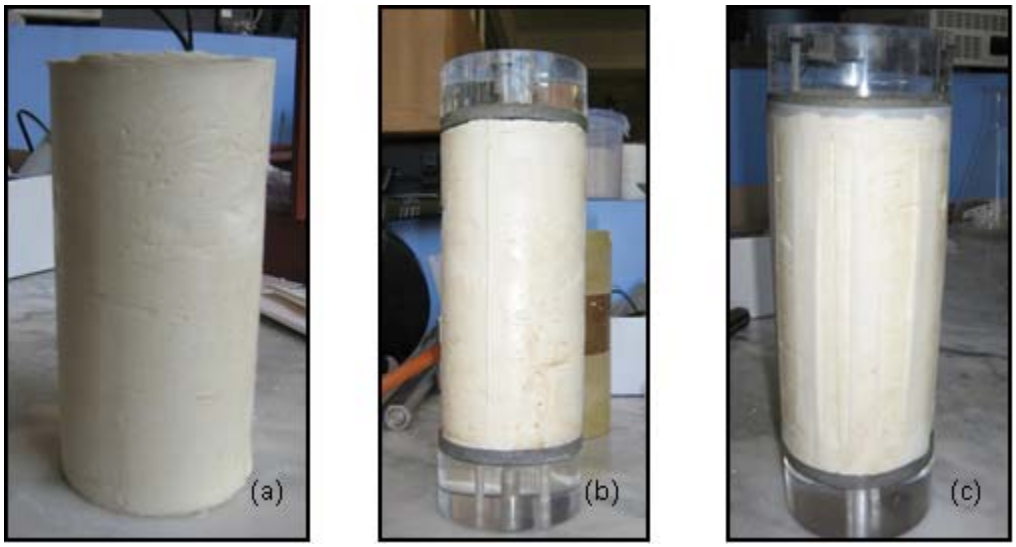

Fig. 3.18 (a) Kaolin specimen after trimming, (b) Installation of porous stones, (c) installation of filter paper around Kaolin specimen.

A thin rubber membrane with a diameter of 7.1cm was then placed on the inside of a cylindrical brass membrane stretcher. To facilitate the placement of the membrane into the stretcher, a thin layer of powder was sprayed over the membrane. Vacuum was then applied to ensure that the membrane adhered well to the inner walls of the stretcher (Fig. 3.19.(a)). The stretcher was then positioned around the soil specimen and the vacuum was released. Rubber bands were used to fasten the membrane tightly around the specimen. The specimen was then attached to the base of the triaxial cell and the top drainage tubes were inserted into the holes of the top cap as shown in Fig. 3.19.(b). The triaxial cell was then assembled and the seating piston positioned over the top cap (Fig. 3.19.(c)). Finally, the triaxial cell was placed in the "TruePath" system in preparation for saturation, consolidation, and shear as will be explained in Chapter#4.

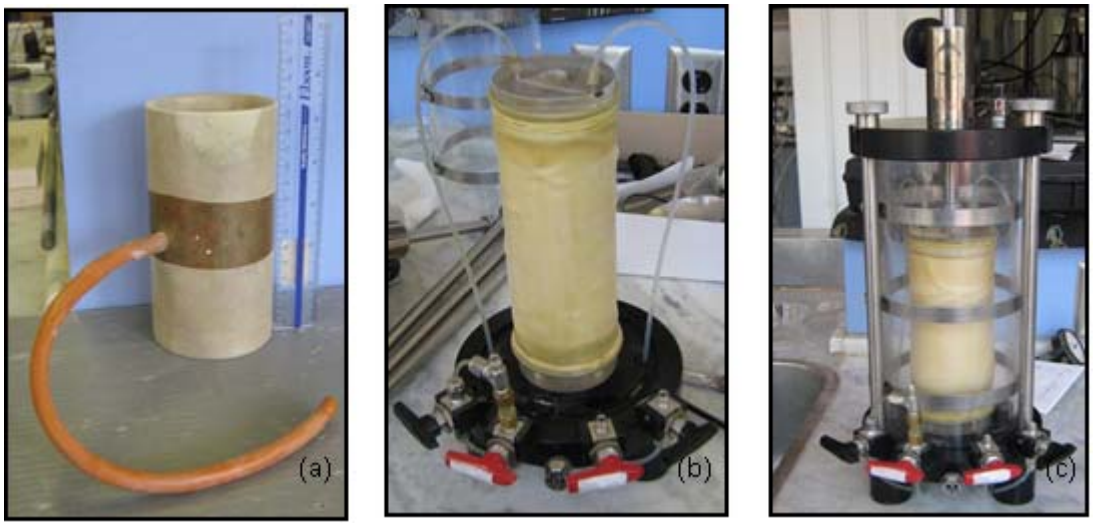

Fig.3.19 (a) Brass tube with the rubber membrane. (b) Installation of Kaolin specimen on the cell chamber, (c) Insertion of glass cover around cell chamber

3.4. Preparation of Sand Columns

The first step in the preparation of clay specimens that were reinforced with single sand columns involved the formation of a hole with a diameter of 2cm or 3cm, in the middle of the clay specimen. For this purpose, a custom-fabricated hand auguring apparatus was manufactured in the machine shop. The auguring apparatus was used to drill holes with different penetration depths in the clay specimen. The procedure followed in drilling holes is presented below.

After dismantling the cylindrical Kaolin specimen from the PVC pipe and trimming it to a final height of 14.2cm, the specimen was wrapped with two lubricated plastic cylindrical PVC tubes which were in turn wrapped with duct tape around their circumference as shown in Fig. 3.20. The wrapped specimen was then placed on the auguring apparatus that is shown in Fig. 3.21.(a). Augurs with diameters of 2cm or 3cm were connected to the auguring machine as shown in Fig. 3.21(b) and (c) respectively. During drilling, the vertical alignment of the rotating

rod is maintained through the presence of plastic guide plates that are connected to the top and bottom of the steel rod. The penetration of the augur into the specimen is continued in stages till the required penetration length is achieved. The augured clay material was collected on the augur as shown in Fig. 3.21. (c).

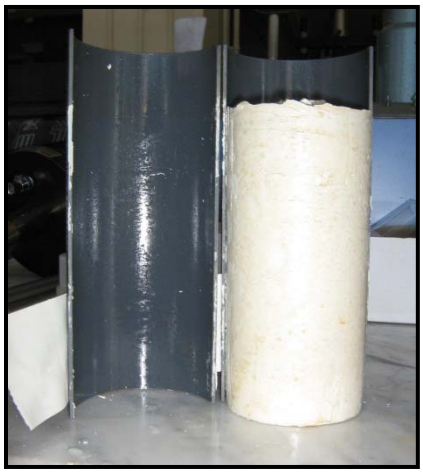

Fig. 3.20 Wrapping the Kaolin specimen with PVC tubes prior to auguring

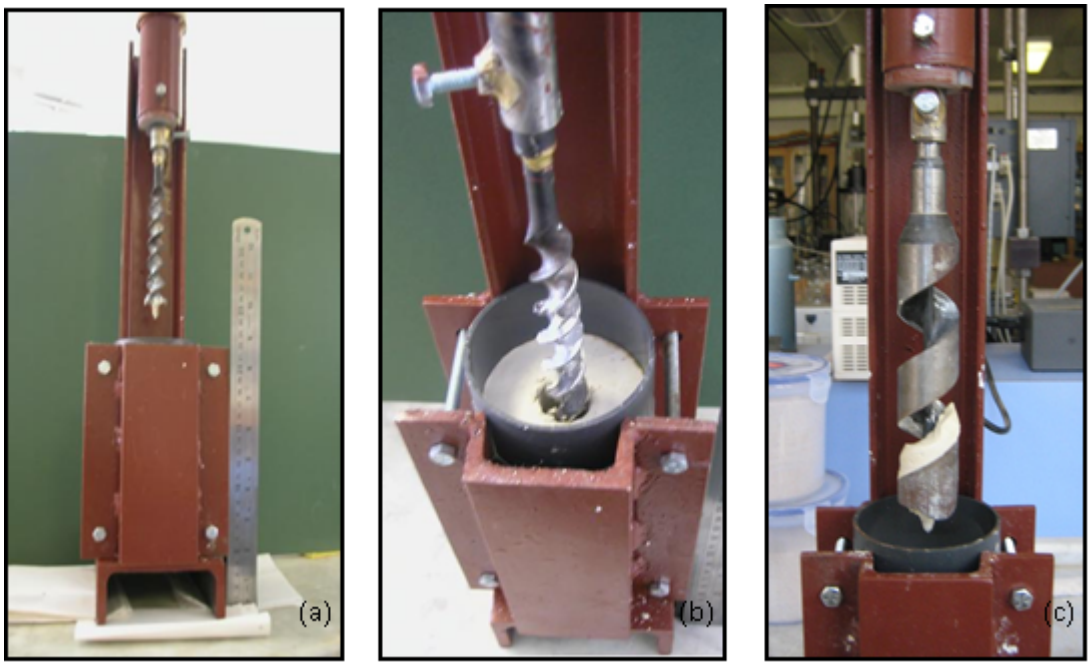

Fig. 3.21Custom fabricated auguring machine (a) 2cm -diameter auger (b) auguring of specimen by 2cm diameter augur, (c) Removal of Kaolin material by 3 cm diameter augur

For sand columns with heights of 10.65cm (partially penetrating column), a mark was made on the steel rod to indicate the required penetration distance of the augur. Auguring was continued in stages until the depth of the augured hole reached the marked length. The maximum penetration distance of the augur into the Kaolin specimen in each stage is 3cm for the purpose of reducing the suction pressure that is generated as the augur is retrieved from the Kaolin specimen.

3.4.1. Encased Sand Columns with Geotextile Fabric

For both encased and ordinary sand columns, geotextile fabrics that were prepared to the desired diameter and length as discussed in Section 3.2.3 were used to construct a column using Ottawa sand. The empty cylindrical geotextile fabric was inserted in a glass tube of the same diameter, which was in turn placed in a plastic tube that was attached to a vibrating motor as shown in Fig. 3.22. Ottawa sand was placed in the geotextile column in three layers, and every layer was vibrated by means of a custom fabricated electric vibrator for a period of 1 minute. Prior to placing sand in the empty geotextile column, the required column heights of 14.2cm, 10.65cm or 7.1cm were marked on the geotextile by means of a pen and the calculated weight of sand that was required to reach the desired density was poured into the column. The eccentric weight at the bottom of the motor caused the attached plastic tube to vibrate thus shaking the glass tube containing the sand. The dry density of the sand columns after vibration for the different column heights was 16.2 $kN/m^3 \pm 0.22$. The same density was maintained for the two column diameters of 2 cm and 3 cm.

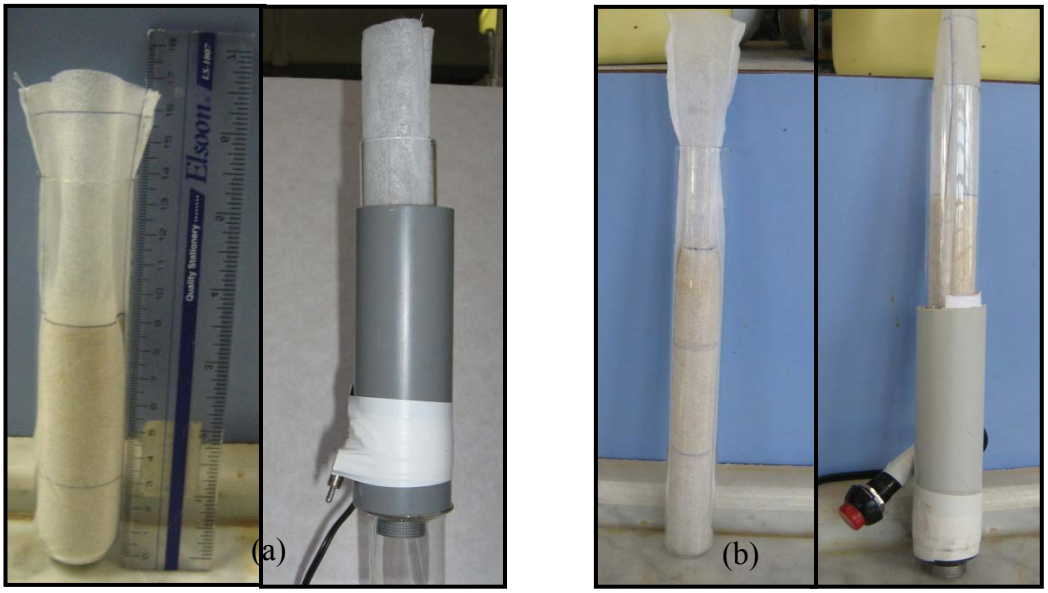

Fig. 3.22 Vibration of encased sand columns with geotextile fabrics, (a) 3cm column diameter and (b) 2 cm column diameter

After ensuring that the target dry density is achieved, the sand column is saturated with water which is permeated slowly from the top of the column to its bottom. It was found that the sand columns generally get saturated at a water content of about 20%. The water content was measured after removing the sand column from the glass tube. Measurement of the total weight and the dimensions of the sand column indicated that the total weight corresponded to the saturated weight at a water content of about 20%. The bulk density of the vibrated sand column after adding 20% water was 19.4 kN/m^3± 0.22.

In clay specimens that were reinforced with encased sand column, the columns were inserted in the pre-drilled holes and any extra height of the geotextile fabric that remained protruding from the soil specimen was cut using a sharp cutter. Fig. 3.23 shows the sequence of installing encased sand column into the Kaolin specimen.

Fig. 3.23 Installation of 3-cm diameter encased sand column with geotextile fabric

3.4.2. Ordinary Sand Columns

Sand columns that were encased with geotextile fabrics were also used to prepare ordinary columns. After saturating the sand column with water, the column was inserted into a flask and placed inside the freezer (Fig. 3.24. a). After freezing, the geotextile fabric was detached from the frozen sand column by cutting the geotextile fabric along its vertical stitching using a sharp cutter. To prevent thawing of the sand column while cutting the geotextile fabric, the cutting operation was performed on a tray filled with frozen water (Fig. 3.24. b). The unreinforced sand column (Fig. 3.24.c) was then inserted in the predrilled hole (Fig. 3.25. a through c) and left to thaw. It is worth noting that while preparing frozen sand columns, the fabric was initially overturned so that stitches of the geotextile were on the outer face. This facilitated the process of removing the fabric prior to installing the columns in the clay specimen. The uniformity and the vertical alignment of the inserted frozen sand column is revealed in Fig. 3.26. where a kaolin specimen was cut vertically along its length directly after inserting the ordinary sand column of diameter 2cm and height of 10.65cm.

Although freezing of sand columns is not usually implemented in the field, the idea behind using frozen sand columns in this research is to be able to construct columns with mechanical properties that are repeatable and uniform across the different samples. The friction angle of Ottawa sand depends on the initial density of the column material, which in turn depends on the column diameter. Thus, any variation in the column diameter form one sample to another will lead to variations in the column density and the friction angle of the column material. By constructing frozen columns in which sand particles are compacted outside the Kaolin specimen, the column diameter and density will be uniform and repeatable.

Fig. 3.24 (a) Freezing the sand columns (b) and (c) removal of geotextile fabric

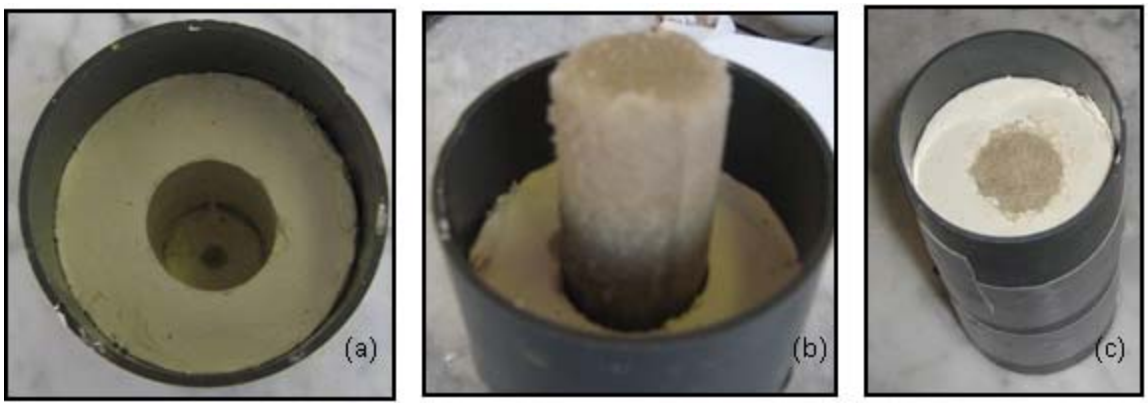

Fig. 3.25 Photographs (a) Predrilled 3-cm diameter hole, (b) Insertion of frozen sand column in clay, and (c) Reinforced Kaolin specimen with frozen sand column.

Fig. 3.36 Photograph of vertical cross section of Kaolin specimen with ordinary sand column of diameter 2cm and height 10.65cm after column insertion.

3.5. Summary

Index and compressibility characteristics for the Kaolin clay were presented in a comprehensive way in this chapter; moreover, the engineering properties, particle size

distribution, and shear strength of Ottawa sand were also presented in this chapter. Through using a digital pullout tensile machine, the tensile strength of the geotextile fabric in both directions, strong and weak fabric orientation, was determined using a digital force gauge. Kaolin was prepared from slurry and consolidated in a prefabricated one dimensional consolidometer after which Kaolin specimen was arranged for CD testing. Step by step methods for preparing encased and ordinar sand columns were discussed in a simple way enriched with pictures and photos for the purpose of clarifying the preparation process and making it plain and easy for tracking the details for the method of sand column preparation.

CHAPTER 4

TRIAXIAL TESTING

4.1. Introduction

This chapter describes the method and steps to be followed in performing consolidated drained tests using the automated triaxial "TruePath" equipment. The step by step approach which describes the process from the initial stage of seating the test specimen to the final stage of shearing the specimen under drained conditions is designed to be a guide for future users of the "TruePath" equipment.

4.2. General Steps in Performing Consolidated Drained (CD) Tests

After preparing the Kaolin specimen as described in section 3.3.4, the triaxial cell (with the sample inside it) is placed in the automated triaxial "TruePath" system. The main components of the system are presented in Fig. 4.1. The "TruePath" system consists of four main parts which are the load frame with pressure transducer and the deformation sensor, the cell pump which provides the confining cell pressure to the cell chamber, the back/pore pump which provides the back pressure for the specimen and measures the pore water pressure through connecting a pressure transducer to valve#3 (as will be explained in a later stage), and the operating system which allows the user to perform the test and monitor its progress through the screen that displays all the stages of the test.

The triaxial test consisted of four stages which include seating, back pressure saturation, consolidation, and shearing. Each stage is characterized by a series of commands that appear on

top of the screen and guide the user throughout the test. The four tabs, which represent each stage, become active after specimen and test data files are created. A specific tab representing a specific stage will become active only after the previous stage is completed. The following steps describe the detailed procedure to be followed in performing consolidated drained tests (CD) on normally consolidated clay samples.

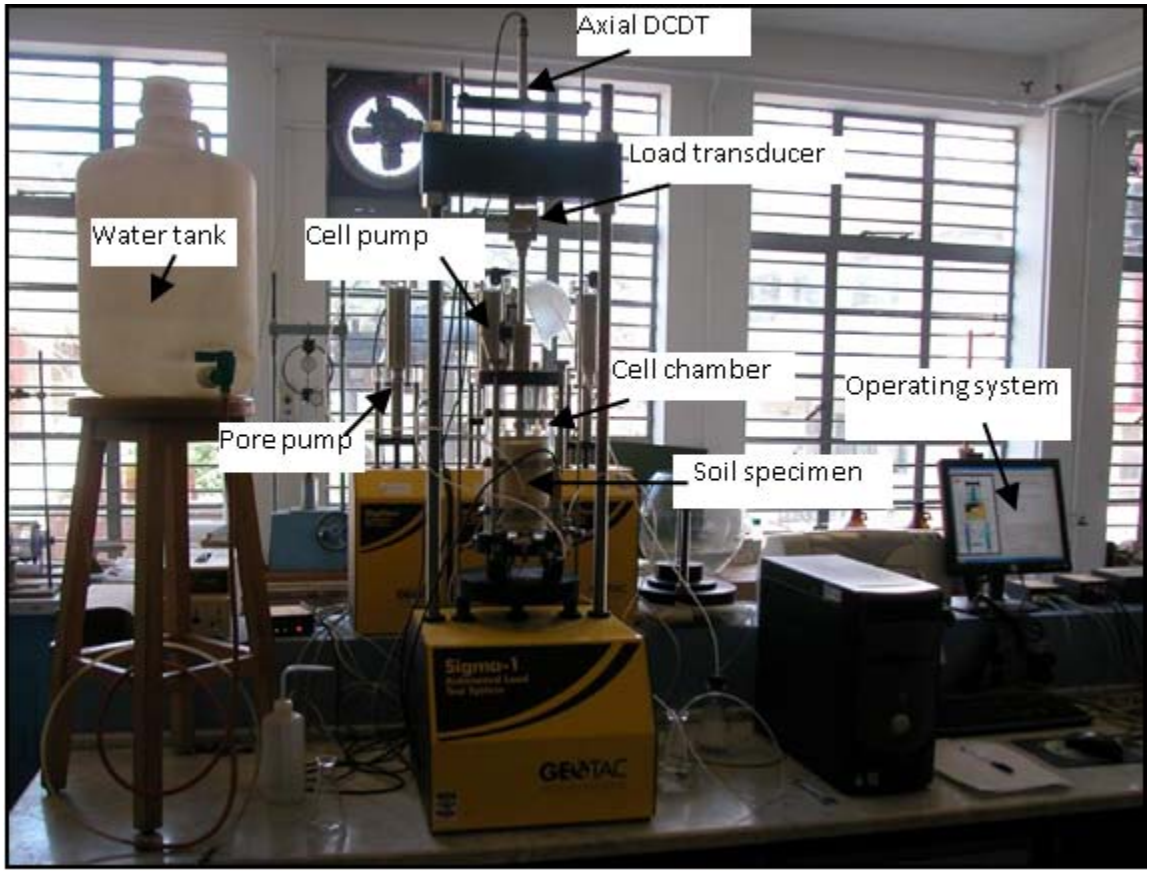

Fig. 4.1 Automated triaxial equipment "TruePath"

4.3. Creating Specimen and Test Data Files

In order to view the test results while performing the test, the file called "graph initiative" should be deleted prior to the start of the test from the "TruePath" folder which is

located under the “program files” folder. The first step in performing the CD test involved setting all the sensors and load transducer readings to zero. This can be achieved by entering the “Set Up” menu and selecting “Sensor”. After highlighting the required sensor or transducer and pressing “Test”, a window will appear for the selected sensor. On this window, the “Take Zero” button should be pressed so that the sensor reading will indicate the average of ten consecutive readings that are almost zero. This process should be repeated for all the sensors, i.e. pore pressure, back pressure, cell pressure sensors, external load cell and axial DCDT. Figs. 4.2 to 4.4 show a step by step procedure for setting the sensors to zero readings.

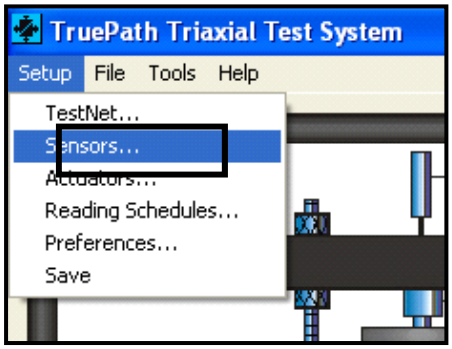

Fig. 4.2. Selection of sensor button

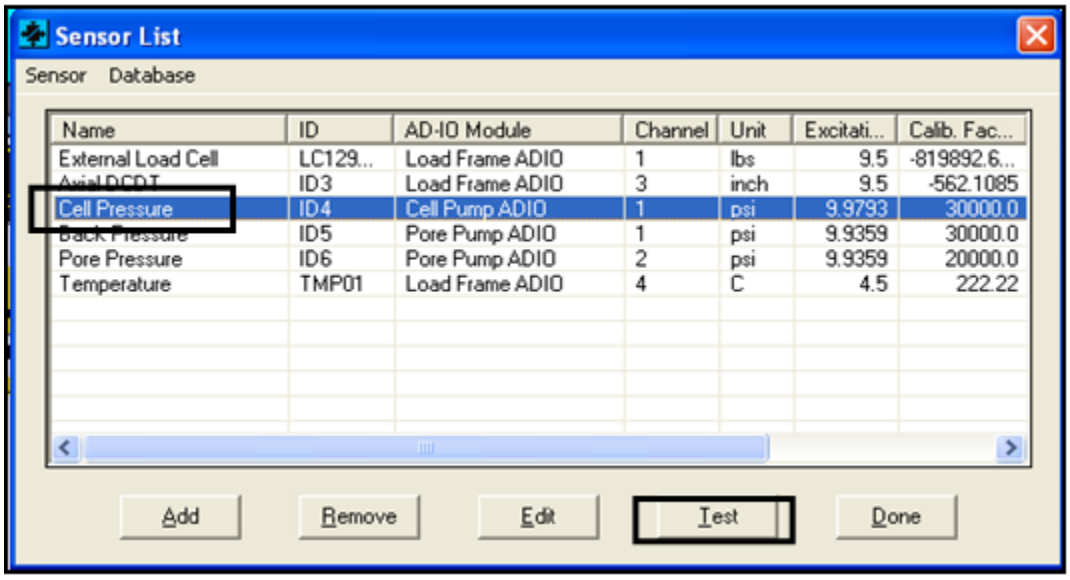

Fig. 4.3. Selection of the cell pressure sensor

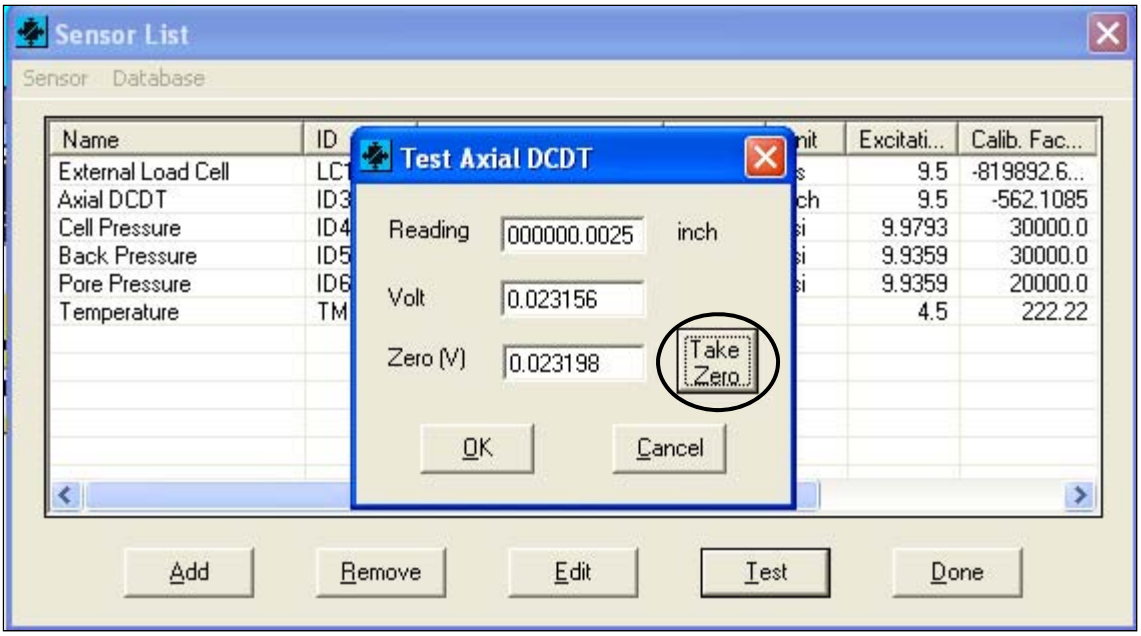

Fig. 4.4 Initializing readings for the selected sensors

The second step involved accessing the "File" menu and choosing "Specimen Data" as shown in Fig. 4.5. Then the "specimen data" window will appear as shown in Fig.4.6 where the user has to click each box to fill the appropriate information which includes the sample height (5.79 inch), sample diameter (2.5 inch), and the sample number and project number. The third step is also initiated from the "File" menu by selecting "Test Data" as shown in Fig. 4.5. A window will appear as shown in Fig. 4.7 where the user has to enter the control test parameters in the empty spaces.

The input data for the test consists of four categories that are included in one window. The user has to enter the following:

- The value of the target seating pressure which is defined as the seating confining pressure needed to keep the membrane pressed against the specimen during the

flushing of the drain lines. A pressure of 5 Psi (35kPa) is used for the samples in the testing program.

- The value of the saturation/back pressure that is needed to saturate the sample. A pressure of 45 Psi (310 kPa) is chosen for the Kaolin sample to ensure proper saturation.
- The type of consolidation (isotropic in this test program) and the value of the target effective stress that is needed to consolidate the sample. Since the test program involved three different confining cell pressures, an initial cell pressure of 14.5 Psi (100 kPa) was applied to the Kaolin sample, and then in the consolidation stage, the confining pressure was raised to the required values of either 21.75 Psi (150 kPa) or 29 Psi (200 kPa). The stress rate for the target effective stress was chosen to be 300 Psi (2073 kPa) per hr to guarantee instantaneous application of the consolidation pressure.
- The drainage conditions which were defined in this testing program to be "consolidated drained" (CD) condition, the loading direction which was chosen to be "compression", the maximum vertical effective stress which was taken as 150 Psi (1036 kPa), the maximum strain which was taken as 15%, and the strain rate was taken as 0.25%/hr. It was also chosen that shearing will be terminated when either the maximum stress or the maximum strain is reached.

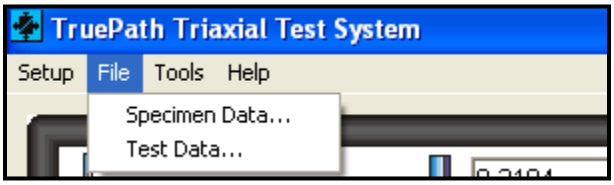

Fig. 4.5 Entering file menu to select Specimen Data

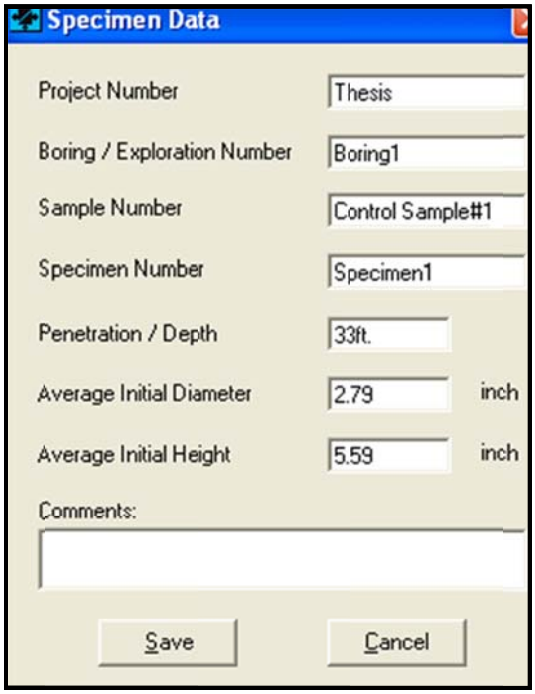

Fig.4.6 Writing the specimen data information

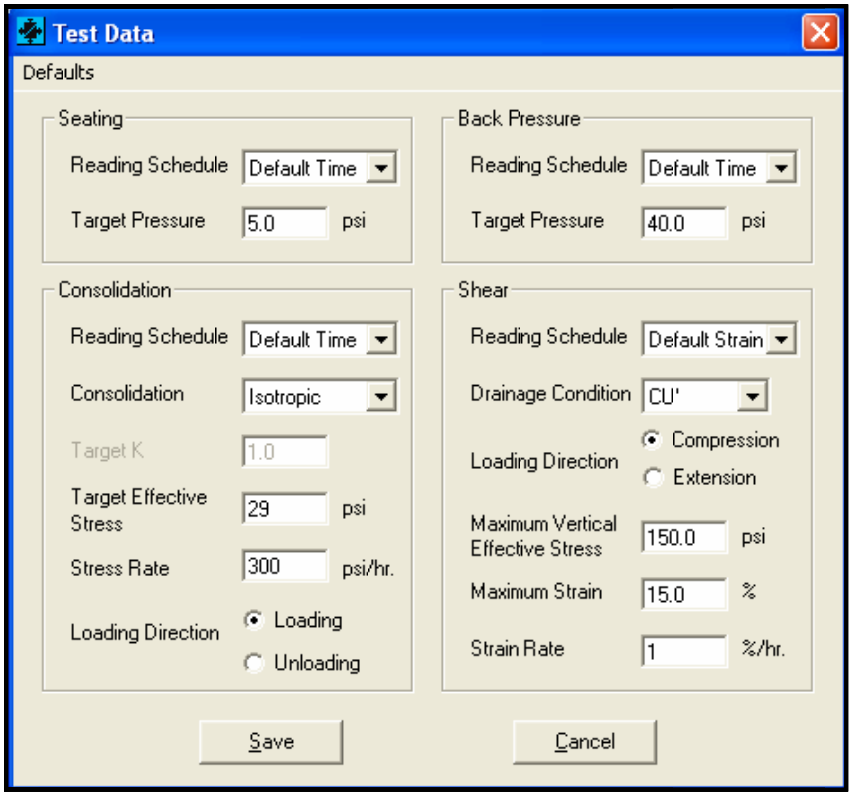

Fig.4.7 Entering the control test parameters

4.4. Seating Stage

After entering the specimen data, the "Seating" tab becomes active. The seating process involves seating the piston, adjusting the external load transducer, filling the cell with water, selecting the cell pressure, flushing the drains, and maintaining the volume of the sample.

4.4.1 Seating the Piston

The process of seating the piston involves locking the piston and minimizing the gap between the piston and the load button using manual control. This is achieved by entering the "Tools" menu, selecting "Manual Mode", pressing on the "Load Frame" and then pressing on the 1st upward button. When the "Start" button is pressed, the platen will move upward till it reaches the load button. Figs. 4.8 through 4.9 show the sequence followed for reducing the gap between the piston and the load button.

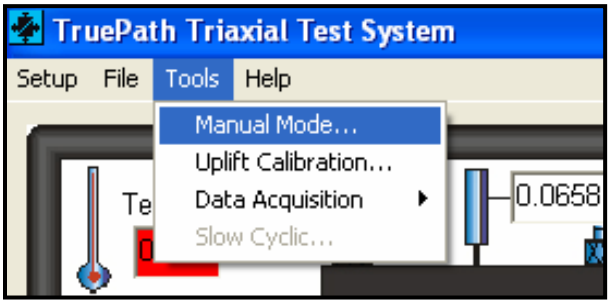

Fig. 4.8. Selection for the manual mode

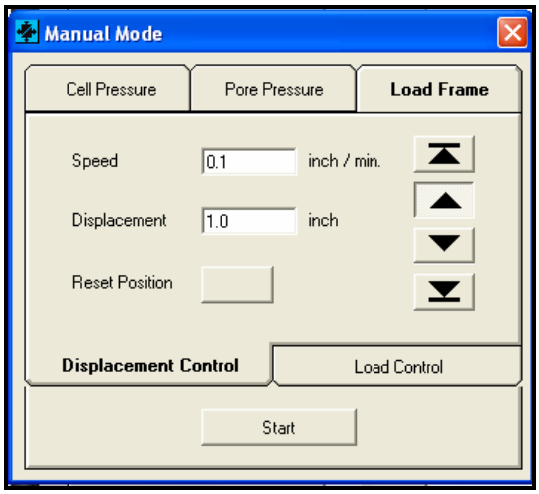

Fig. 4.9 Reduction of gap between the piston and the load button

After reducing the gap, the "start" button is pressed as shown in Fig. 4.10 and another window will appear. In this window, the "Start" button has to be pressed again and the platen will move upward till it reaches the load button and the platen stops automatically when the load button is seated on the piston.

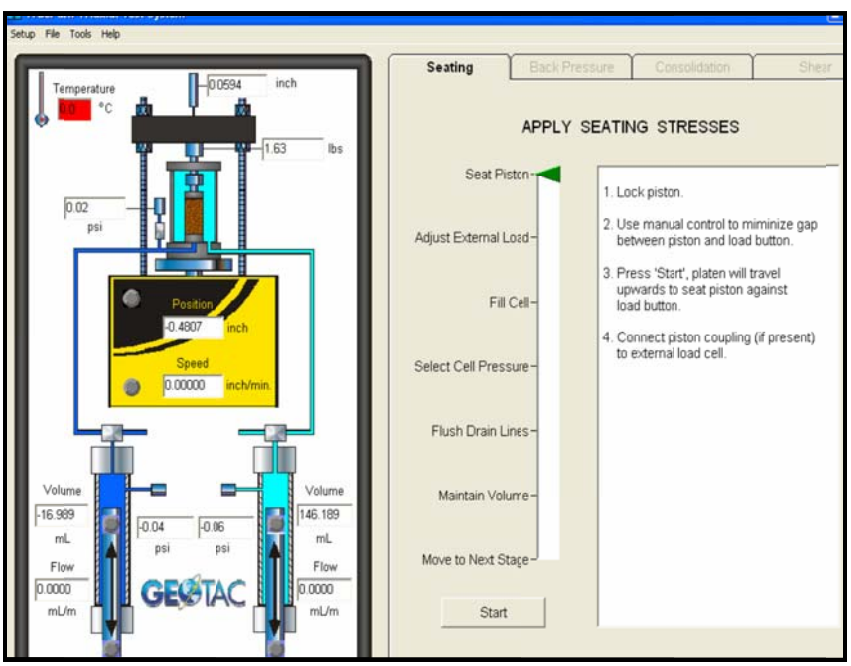

Fig. 4.10 Window for seat piston

4.4.2. Adjust the External Load Sensor

When the “Adjust external load” button is pressed followed by pressing the “Start” button, the reading of the load cell becomes almost zero. The piston should be unlocked when the load cell reading approaches zero. Fig. 4.11 shows the procedure for adjusting the load.

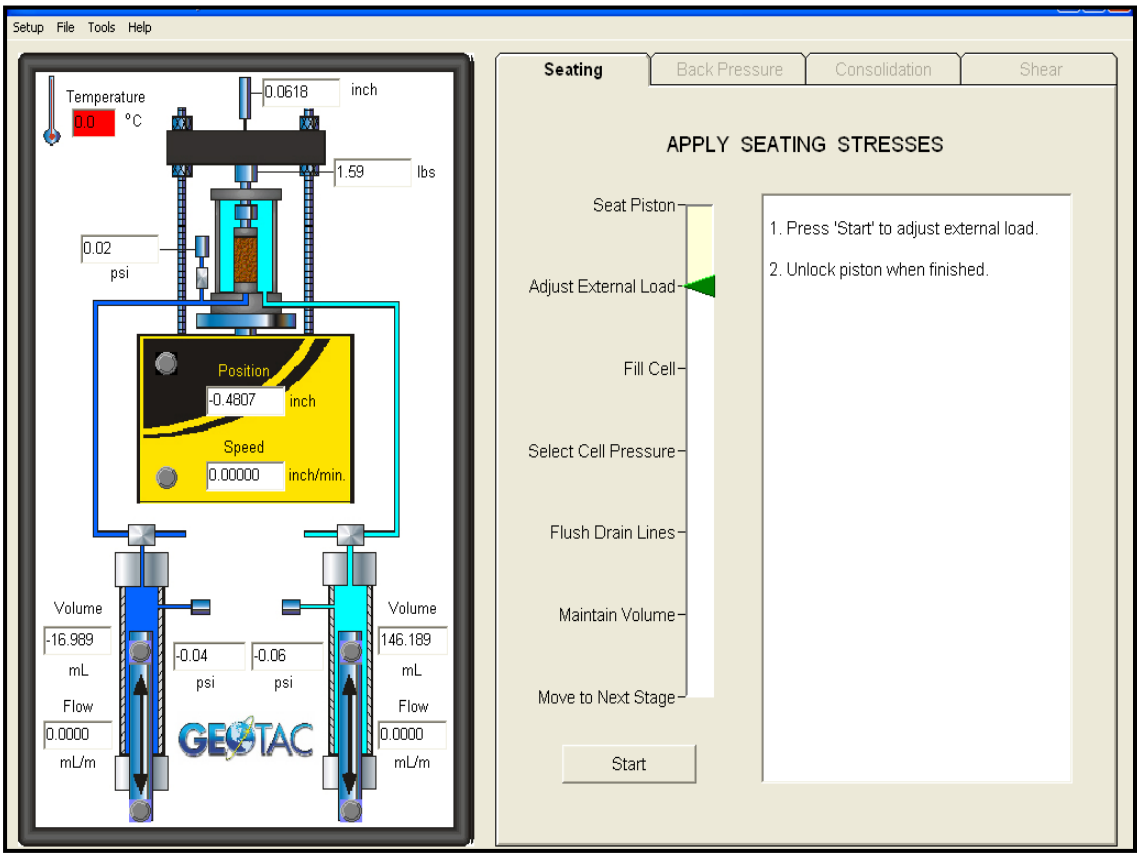

Fig. 4.11 Adjustment for the external load transducer

4.4.3. Fill the Cell Chamber with Water

To fill the cell chamber with water, the “Fill Cell” button needs to be clicked and the ventilation air valve should be inserted into the top of the cell as shown in Fig. 4.12. Then water should be supplied from an elevated water tank to the bottom quick connect of the cell through a plastic hose with a fitting on its top to allow entrance of the hose into the cell. The air in the cell

is displaced by the water and is allowed to escape through the vent port. After filling the cell, water is allowed to flow out from the air vent port to ensure that all the air was driven out of the cell. The elevated water source should then be closed and the water hose is removed together with the air vent valve. The user can follow the step by step instructions that are displayed on the screen for the purpose of filling the cell with water as shown in Fig. 4.13.

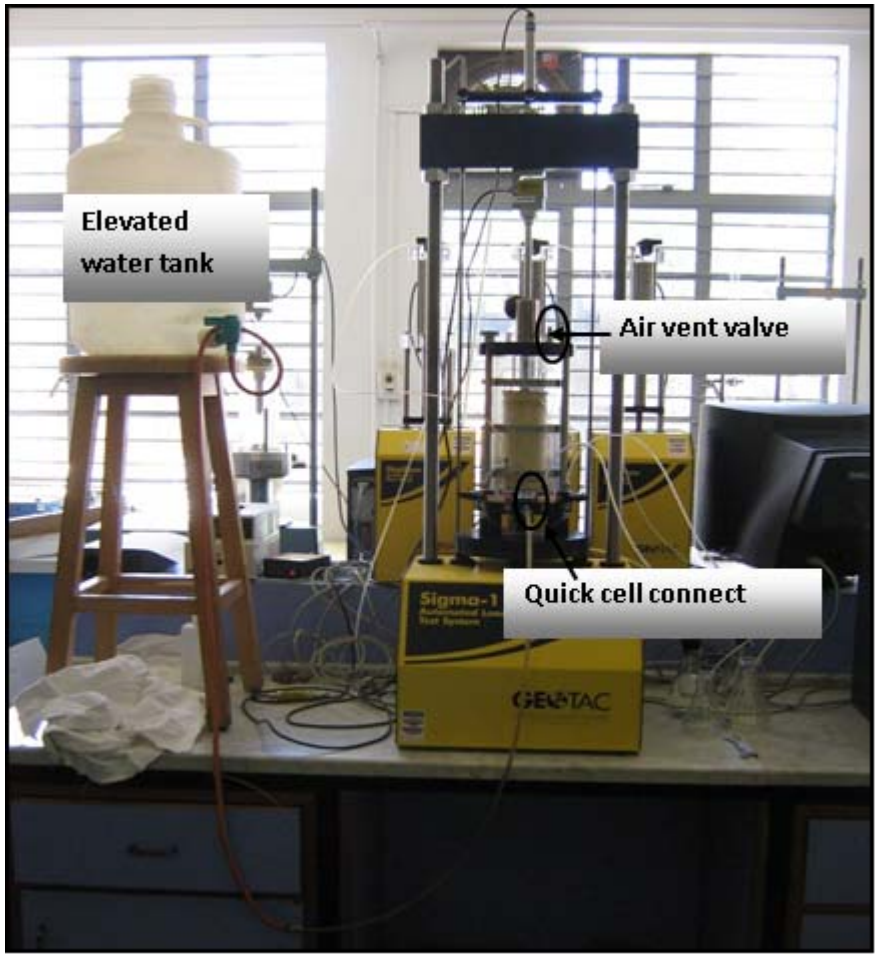

Fig. 4.12 Filling the cell chamber with water

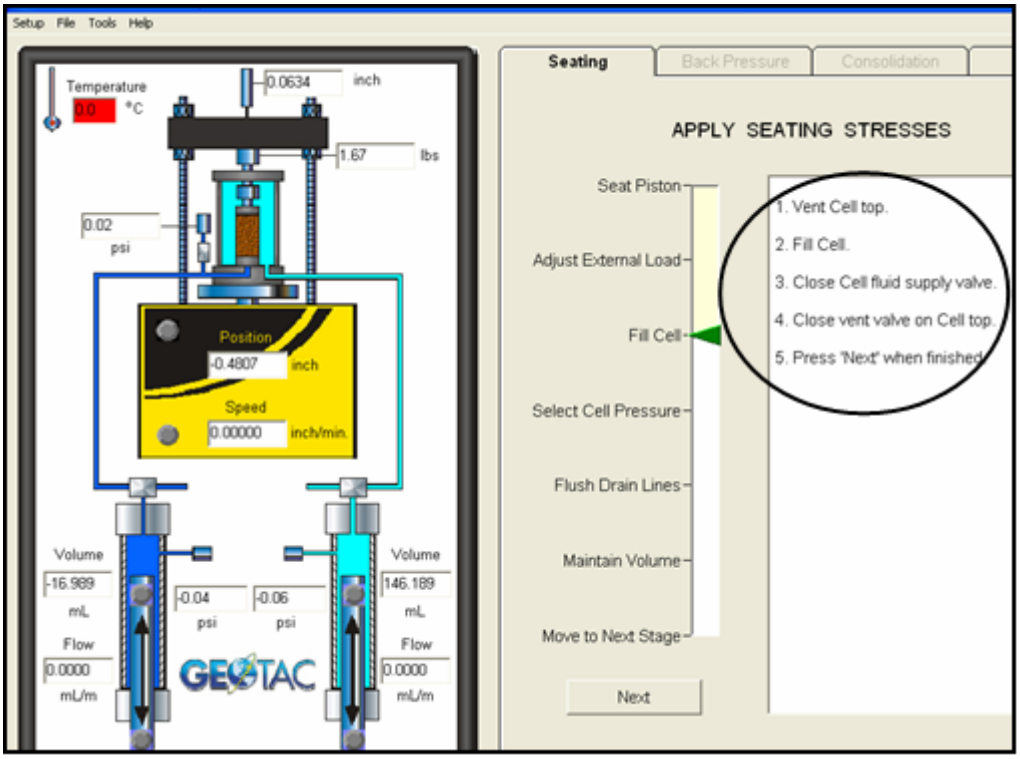

Fig. 4.13 Steps for filling the cell chamber with water

4.4.4. Cell Pressure Selection

For the purpose of keeping the membrane pressed against the Kaolin sample during the drain line flushing, a small confining pressure of 5 Psi (34 kPa) is applied to the specimen. This can be achieved by opening the port valve of the cell pressure and connecting the cell pump pressure line to the cell bottom quick connect as shown in Fig. 4.14. The “Start” button should then be pressed to produce a window in which a pressure of 5 Psi should be entered. After about 2 minutes, the cell pressure will reach the required value and become stable. When this is achieved the user should press the “Done” button to complete the operation.

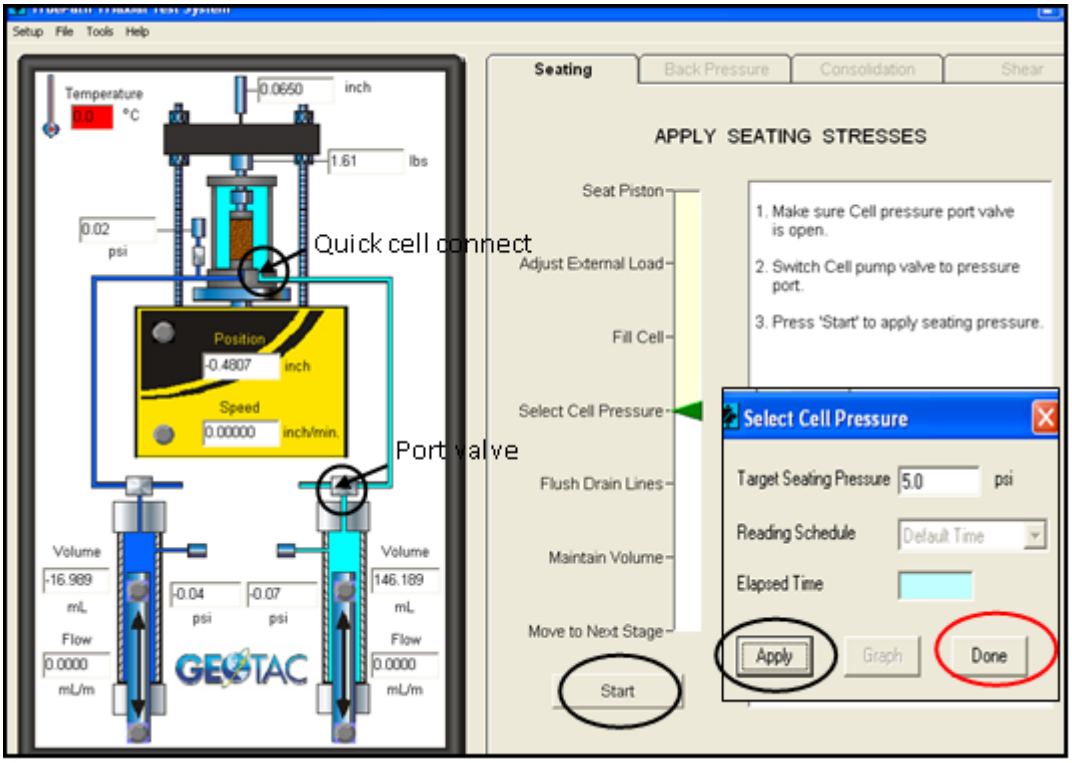

Fig. 4.14 Application of initial confining pressure

4.4.5. Flushing the Drains

This technique is intended to force water to flow through the top and bottom drain lines using the bottom pump in order to expel air from these drain lines. First the bottom pump pressure line should be connected to the T fitting as shown in Fig. 4.15. Then the bottom pump valve is switched to the pressure line and the top drain inlet valve#1 and the top drain vent valve#4 are opened. An overflow tube is then attached to valve#4 and the “Start” button is pressed. Water should flow from the bottom pump into the T fitting through valve#1 and into the container through valve#4. In order to dislodge completely the air bubbles from the drain lines, the flow can be stopped and restarted simultaneously; Moreover, closing the vent valve #4 for one or two seconds and reopening it again while water is flowing from the top drain line valve can help in creating a pump pressure that speeds up the process of dislodging the air bubbles.

After pressing the “Stop” button, valves#1 and 4 are closed and the bottom drain inlet valve #2 and bottom drain vent valve#3 are opened and the same procedure is repeated.

This technique is repeated until no more air bubbles are expelled through the drain lines. It is better to refill the bottom pump before completing the flushing step by switching the bottom pump to the refill container, pressing on “Tools” from the main menu, pressing “Manual Mode”, and selecting “Pore pump” (bottom pump). The “down” arrow is then clicked so that the bottom pump piston will move downward while water from the container will be drawn into the pump. The pore pump valve should then be returned to the pressure line, and flushing is continued if needed. Finally, the flushing stage should be terminated by closing valves#1 though 4 and pressing the “Done” button.

Fig. 4.15 Flushing of the drains

4.4.6. Maintain the Volume

The final step is to apply a confining pressure of 14.5 Psi (100 kPa). First, the "Maintain Volume" tab should be pressed as shown in Fig. 4.16. Next, the "Start" button is pressed and inlet drain valves #1 and 2 are opened. The required confining cell pressure is then typed in the appropriate space and the "Start" button is pressed. The time required for the seating stage for the clays tested in this study is around 2 to 3 hours. A graph can be displayed to show the variation of the confining pressure with time. Furthermore, a curve showing the volume of water that is drained from the specimen as a function of time can also be displayed on the screen. When water stops draining out from the sample under the specified confining pressure, the maintain volume stage can be terminated. This is done by clicking on the "Stop" button and then on the "Done" button to end the maintain volume stage.

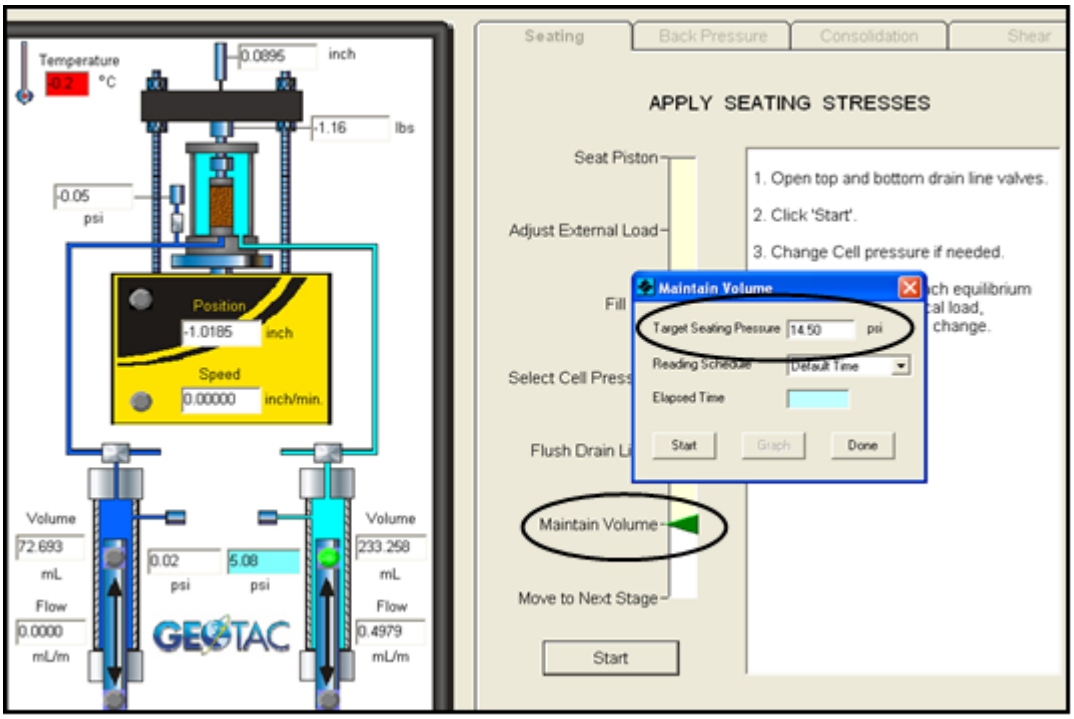

Fig.4.16 Application of confining pressure

4.5. Back Pressure Saturation Stage

To ensure full saturation of the slurry-consolidated Kaolin specimen, a back pressure/saturation pressure of 45 Psi is applied to the specimen using the back pump. The back pressure saturation stage consists of the following steps:

- Keep the bottom drain vent valve#3 closed, remove the drain line from bottom drain valve#3, and install in its place the pore pressure transducer and open drain vent valve#3.
- Check that inlet drain valves #1 and 2 are opened and make sure that the port valve of the bottom pump is opened, while drain valve #4 is closed.
- Input the value of the required saturation pressure (45 Psi), and initiate saturation by click on the "Start" button as shown in Fig. 4.17.
- View the curve that shows the increase of back saturation pressure with time as shown in Fig. 4.18. The value of the back pressure can be checked either by looking at the curve or by looking directly at the bottom pressure transducer that is displayed on the left side of the screen. Usually a period of 3 to 5 hours is needed to reach the back pressure value.
- Once the saturation pressure has reached its value, press on "Stop saturation", and check the B value. To do that, click on "Check B" and enter a small increment of cell pressure (5 Psi) as shown in Fig. 4.19. Then, close drain inlet valves#1 and 2, and press on "Start". The cell pump will instantaneously increase the cell pressure by 5 Psi, and the pore water pressure should indicate a similar increase of pore water pressure if the sample is completely saturated. The software calculates the B-value and

reports its value every 15 seconds on the screen. During this check, a B-value of 0.96 to 1 was generally obtained for tests conducted in this study.

- After an acceptable B-value is ensured, click on “Done” and wait till the window for the B value check disappears by itself. When this happens, re-open drain inlet valves#1 and 2, and press on “Done” to end the back pressure saturation stage. If saturation was not achieved using the initial specified back pressure of value 45 Psi, increase the saturation pressure by a certain increment and repeat the saturation process.

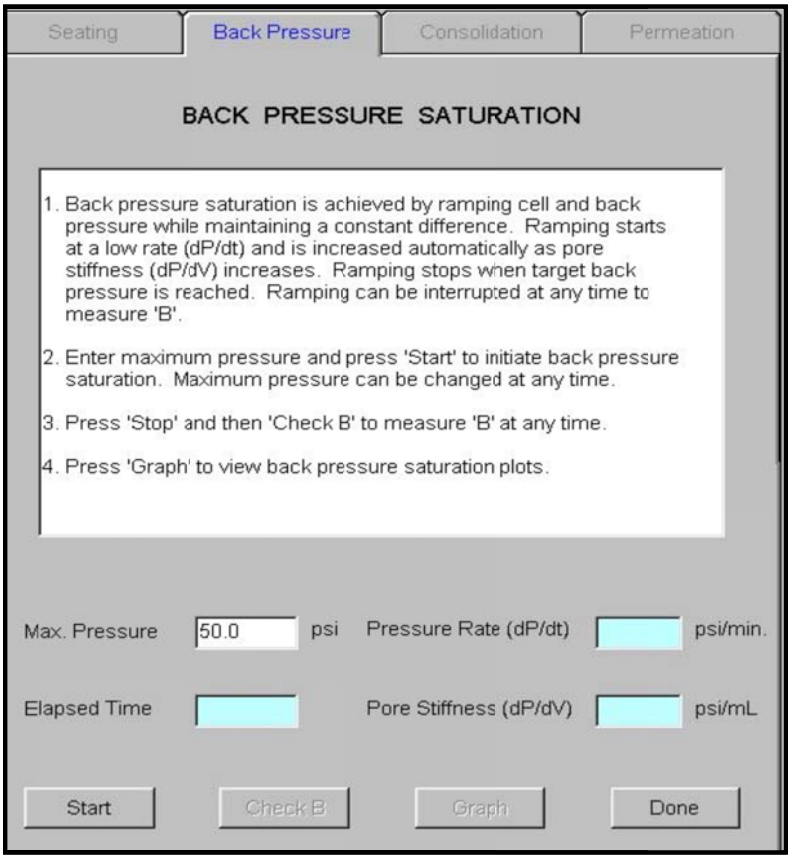

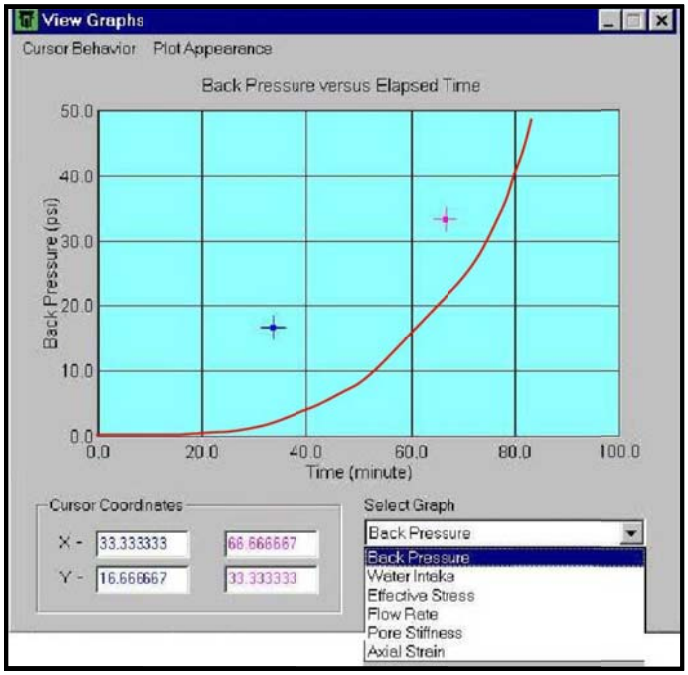

Fig. 4.17. View the curve during the saturation process

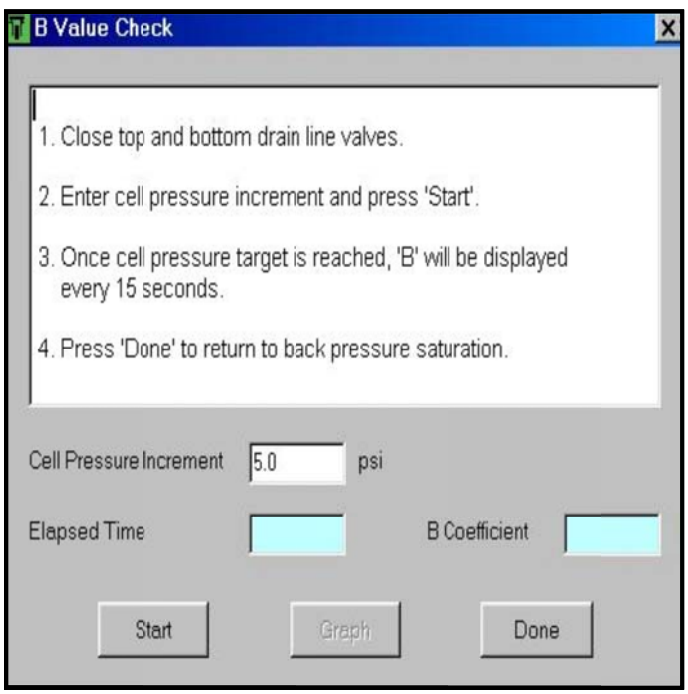

Fig. 4.18 Window for “B” value check

4.6. Isotropic Consolidation Stage

The consolidation stage is initiated by clicking on the “Consolidation” tab. First, the relevant data which includes the effective confining pressures and the stress rate that have been previously entered during the creation of the data test file should be checked. The activated window for isotropic consolidation is shown in Fig. 4.20. In this stage, the user can still change the target effective stress and the vertical stress rate, but cannot change the type of consolidation. Once all the input data is verified and consolidation is initiated, consolidation continues until the reading of the pore water volume intake for the pore pump becomes a constant. At this time, the isotropic consolidation stage can be assumed to be completed. A period of 1 hour, 2 hours, and 6 hours is usually needed to consolidate the Kaolin specimens at confining pressures of 14.5 Psi, 21.75 Psi, and 29 Psi respectively.

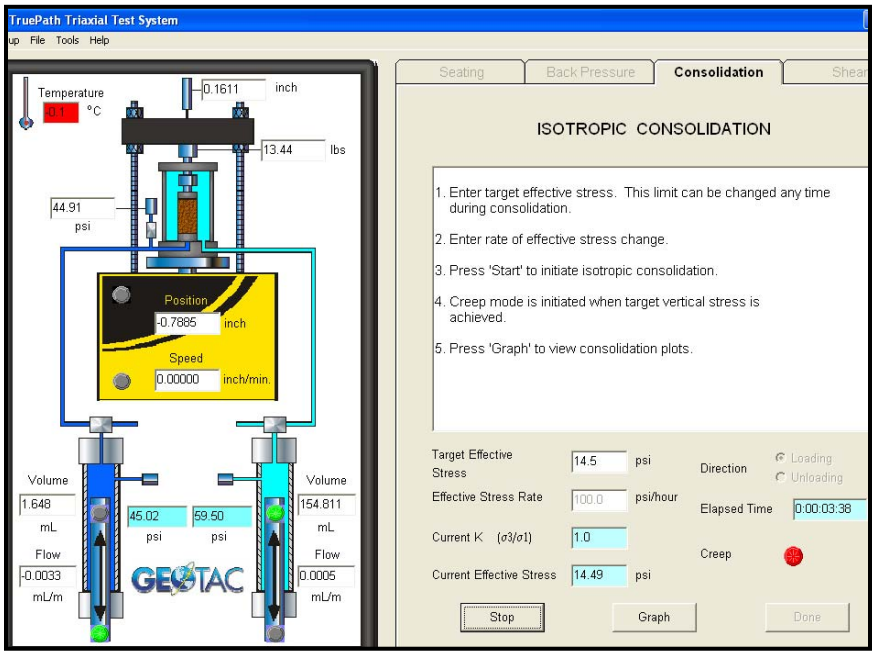

Fig.4.19 Window for isotropic consolidation

4.7. Drained Shearing Stage

At the end of the isotropic consolidation stage, a gap will form between the top cap of the specimen and the bottom of the loading piston. The user has to use the manual controls to close the gap and reestablish contact before starting the shearing stage. Once the window for the "Drained shear" is activated, the user is required to enter the strain rate. In this research, a value of 0.25%/hour is used for the strain rate.

Once the strain rate is chosen, cell valves#1 and 2 that are connected to the pore pump are closed, and valve#3 between the pore pressure sensor and the pore pump should be checked to be open. The "Start" button is then clicked as shown in Fig. 4.21 to initiate drained shearing. Different curves can be viewed while the test is in progress. These include curves that show the variation of the deviatoric stress and excess pore water with axial strain. When the strain reaches a percentage of 10-12%, click on the "End test" tab to terminate the test and to close the software.

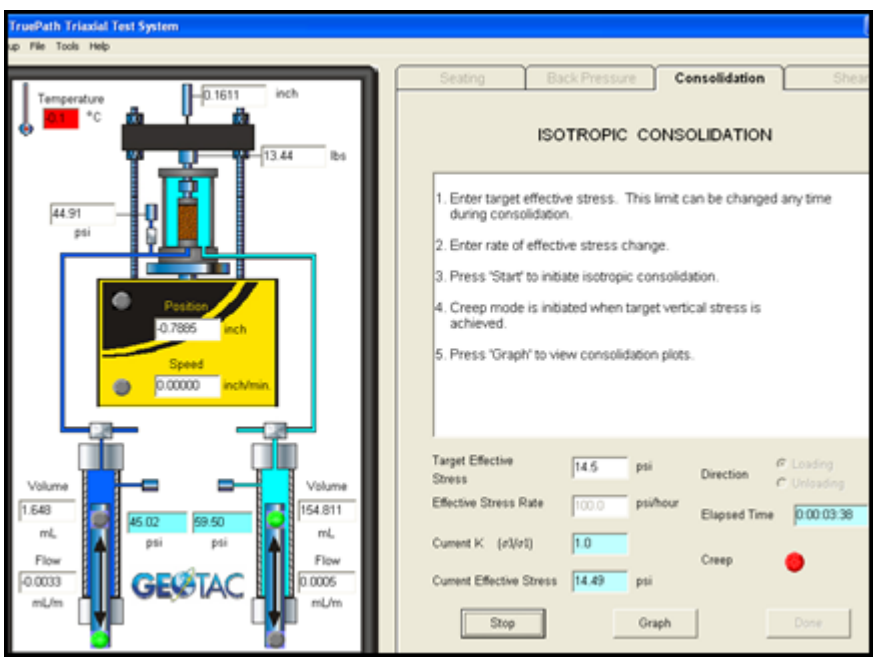

Fig. 4.20 Window for drained shear test

4.8. Test Tear Down

Test tear down process involves removing pressures from the specimen and the triaxial chamber and the load frame. This can be accomplished as follows:

- Enter the True Path software and lock the cell piston.
- Select the manual controls, and choose cell pump. After that, choose "Pressure control" as shown in Fig. 4.22 and record a value of 0 Psi for the cell pressure and press start. Water will drain out from the cell chamber into the cell pump to reduce the cell pressure to zero.
- Use the manual control and reduce the pore pump pressure to zero.
- Use the manual control to lower the loading frame platen.
- Connect the top air vent valve and remove the hose from the bottom cell connect and replace it with a tube that discharges water into a container.
- After the water is drained out from the cell, remove the triaxial chamber from the loading frame, and dismantle the cell parts, wash them, and prepare them for another test.

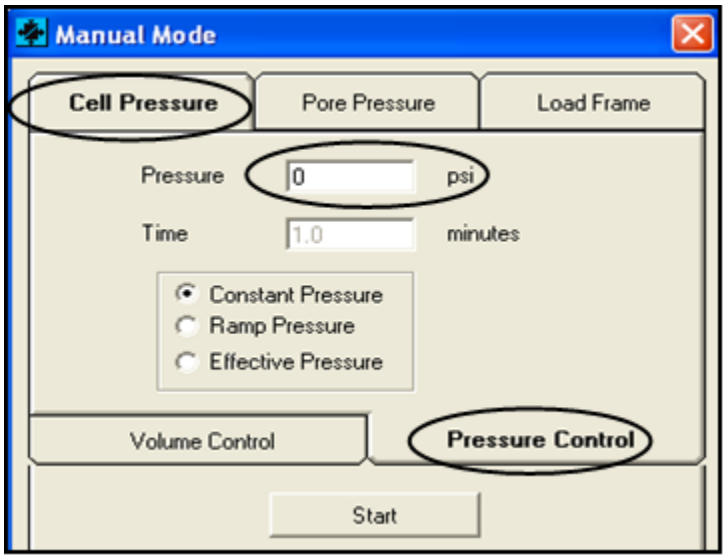

Fig.4.21 Window for unloading stage

4.9. Summary

A comprehensive description for operating the automated triaxial equipment "TruePath" was presented in this chapter in a simple way which includes a step by step procedure with figures and charts that facilitate the understanding of the testing process. The information presented in this chapter will make it easier for any future user to work and operate the "TruePath" equipment. However, reading the manual of the "TruePath" system is crucial and vital in order to complete all the required information that the user should know prior to operating the system.

CHAPTER 5

TEST RESULTS AND ANALYSIS

5.1. Introduction

The automated triaxial test setup "TruePath" by Geotac was used to conduct CD tests on control and reinforced clay specimens saturated with a back pressure of 310 kPa. The samples were then isotropically consolidated under confining pressure of 100, 150 and 200 kPa and sheared drained at a strain rate of 0.25%/hr, while measuring volume change through drain lines connected to the porous stones at the top and bottom of the sample. The measured volume change reflects a global change in the composite sample and do not provide information on local changes in the water content in the sand column and the surrounding clay. Throughout the tests, the total confining pressure was kept constant as the vertical stress was increased in the compression.

The test results of consolidated drained tests conducted on 27 Kaolin specimens are presented in this chapter which includes the results of control or unreinforced specimens, specimens reinforced with ordinary sand columns, and specimens reinforced with encased sand columns. The results include a description of the modes of failure that characterize the behavior of the different test specimens and a detailed analysis of the parameters which are known to affect the load response of clay specimens that are reinforced with sand columns. The effect of these parameters which include the area replacement ratio, column penetration depth, geotextile encasement, and confining pressure on the drained shear strength, stiffness, volume change, and effective shear strength parameters of the Kaolin specimens is investigated and highlighted in this chapter. Furthermore, the test results corresponding to Kaolin

specimens reinforced with ordinary and encased sand columns are compared and analyzed to isolate and investigate the effect of geotextile fabric on the degree of improvement in the mechanical properties of reinforced specimens.

5.2. Test Results

The test results are presented in the form of deviatoric stress versus axial strain curves and volumetric strain versus axial strain curves. Since no peaks were exhibited in the deviatoric stresses (σ_d) in the majority of the tests, failure was defined at an axial strain of 12%, unless a peak was observed at smaller strain levels.

5.2.1. Unreinforced/Control Kaolin Specimens

Curves showing the variation of the deviatoric stress and the volumetric strain versus axial strain at confining pressures of 100 kPa, 150 kPa, and 200 kPa for the control Kaolin specimens are presented in Fig. 5.1. For all confining pressures, the deviatoric stress continued to increase with axial strain, even at strains exceeding 11% to 12%, which were the maximum strains measured in the control tests. However, it could be observed that the rate of increase in deviatoric stress appears to decrease appreciably at strains exceeding 6% to 8%. The same applied to the variation of the volumetric strain with axial strain.

The Mohr Coulomb effective stress failure envelope for the control specimens is shown on Fig. 5.2. The effective cohesion (c') and the effective angle of internal friction (Ø') for the control specimen were determined to be 0 kPa and 21º respectively.

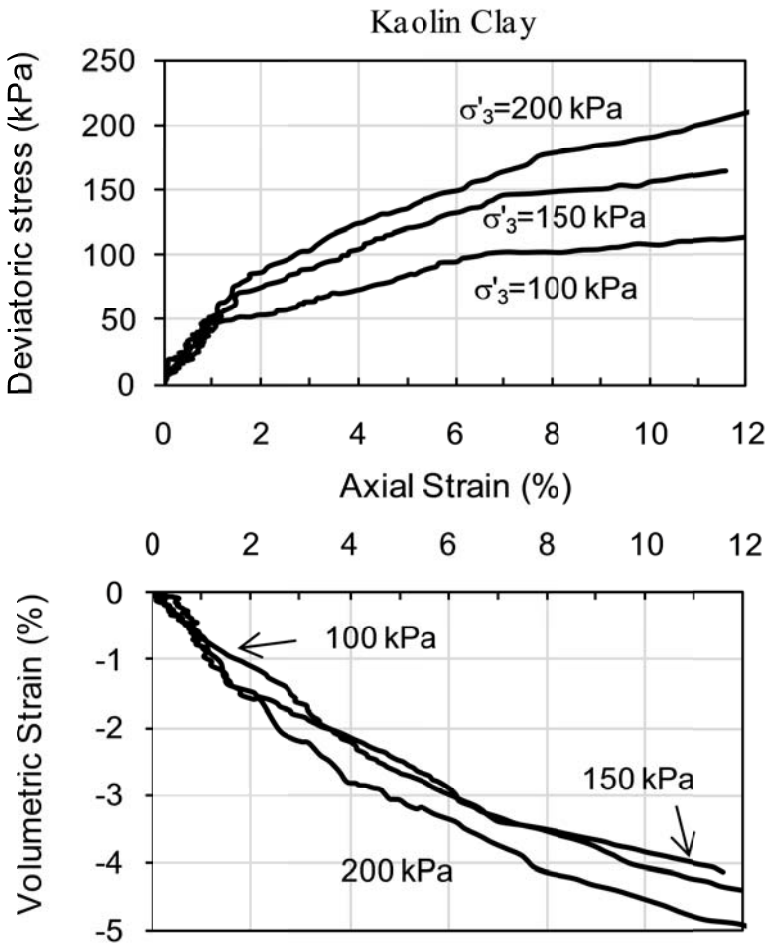

Fig.5.1 Deviatoric stress and volumetric strain versus axial strain for unreinforced/control specimen at confining pressures of 100 kPa, 150 kPa, and 200kPa

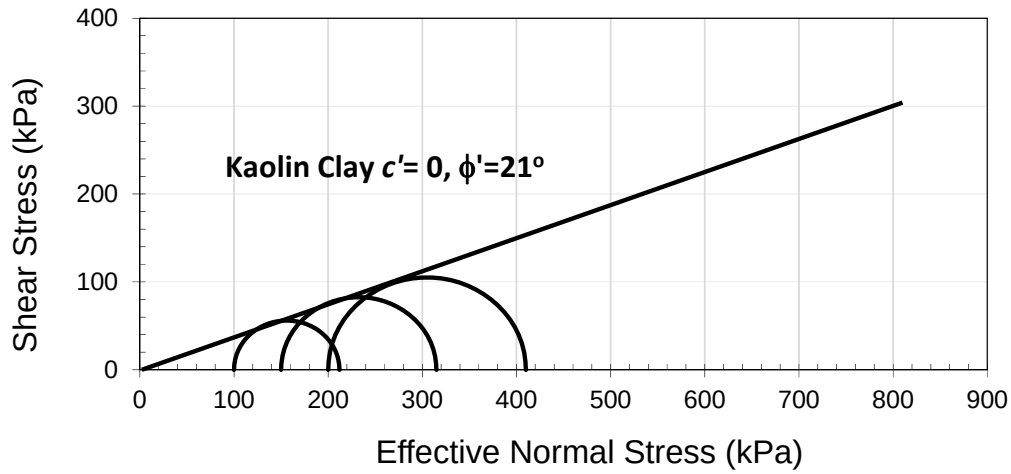

Fig. 5.2 Mohr Coulomb effective stress failure envelope for control/unreinforced Kaolin specimens

5.2.2. Kaolin Specimens Reinforced with Sand Columns

Results obtained from the triaxial tests conducted on kaolin specimens reinforced with partially and fully penetrating encased and ordinary sand columns are presented in Table 5.1 and in Figs. 5.3 to 5.7, which include pictures of the modes of failure and graphs showing the variation of the deviatoric stress and volumetric strain with axial strain. The results were analyzed to investigate the effect of relevant parameters such as column penetration ratio H_c/H_s, area replacement ratio A_c/A_s, and confining pressure on the improvement in the drained shear strength and the effective strength parameters of the clay. It should be noted that in all the discussion presented below, it was assumed that the sand column and the surrounding clay act as a single element with homogeneous distributions of stresses and strains.

5.2.2.1. Modes of Failure

For samples that were reinforced with partially penetrating columns, the mode

of failure was characterized by bulging of the clay specimen. The bulging was slight and relatively uniform along the height in samples reinforced with ordinary columns. For partially penetrated encased columns, the bulging was significant and concentrated in the lower-half of the clay specimen. As an illustration, photographs showing the degree of bulging in samples with partially penetrating 2-cm ordinary columns at different confining pressures are shown on Fig. 5.3. The bulging is evident in the samples tested at confining pressures of 100 kPa and 150 kPa, but was non-existent for the higher confining pressure of 200 kPa. The concentration of bulging at the lower half of the sample for samples reinforced with encased partially penetrating 3-cm sand columns is shown on Fig. 5.4 for the three confining pressures respectively.

Table 5.1. Test Results for Kaolin specimens inserted with frozen sand columns

Test No.	Confining pressure σ_3, (kPa)	Diameter of sand column (mm)	Area replacement ratio: A_c/A_s (%)	Column Penetration Ratio: H_c/H_s	Height of Sand Column: Hs (cm)	Deviatoric stress @ failure (kPa)	Volume strain (%)	E_{sec} @ 1% axial strain (kPa)	Increase in deviatoric stress (%)
1		0	0	0	-	112.0	-4.41	4260	-
2		20	7.9	0.75	10.65	116.4	-4.21	3800	3.9
3		20	7.9	1.0	14.2	131.7	-3.93	4050	17.6
4		20 (ESC)	7.9	0.75	10.65	119.0	-4.15	3420	6.3
5	100	20 (ESC)	7.9	1.0	14.2	160.0	-3.91	2580	42.9
6		30	17.8	0.75	10.65	133.0	-3.64	3754	18.8
7		30	17.8	1.0	14.2	169.7	-2.34	7630	51.5
8		30 (ESC)	17.8	0.75	10.65	154.0	-3.63	4230	37.5
9		30 (ESC)	17.8	1.0	14.2	206.0	-3.07	5300	83.9
10		0	0	0	-	165.0	-4.15	4780	-
11		20	7.9	0.75	10.65	163.3	-4.67	3190	-1.0
12		20	7.9	1.0	14.2	173.6	-4.17	4360	5.2
13		20 (ESC)	7.9	0.75	10.65	169.2	-4.04	4380	2.5
14	150	20 (ESC)	7.9	1.0	14.2	204.0	-4.02	4150	23.6
15		30	17.8	0.75	10.65	193.0	-3.92	3765	17.0
16		30	17.8	1.0	14.2	237.0	-3.57	8580	44.2
17		30 (ESC)	17.8	0.75	10.65	198.0	-4.05	4469	20.0
18		30 (ESC)	17.8	1.0	14.2	269.0	-3.15	8100	63.0
19		0	0	0	-	210.0	-4.93	5240	-
20		20	7.9	0.75	10.65	209.0	-5.21	4725	-0.5
21		20	7.9	1.0	14.2	203.0	-5.02	3600	-3.3
22		20 (ESC)	7.9	0.75	10.65	223.0	-4.50	6220	6.2
23	200	20 (ESC)	7.9	1.0	14.2	266.0	-4.95	5480	26.7
24		30	17.8	0.75	10.65	262.6	-3.72	6100	25.0
25		30	17.8	1.0	14.2	311.9	-3.27	7030	48.5
26		30 (ESC)	17.8	0.75	10.65	250.0	-3.70	7932	19.0
27		30 (ESC)	17.8	1.0	14.2	319.0	-3.12	7320	51.9

Fig.5.3 Example of external and internal modes of failure of test specimens (Hc/Hs = 0.75 and Ac/As = 7.9%, ordinary)

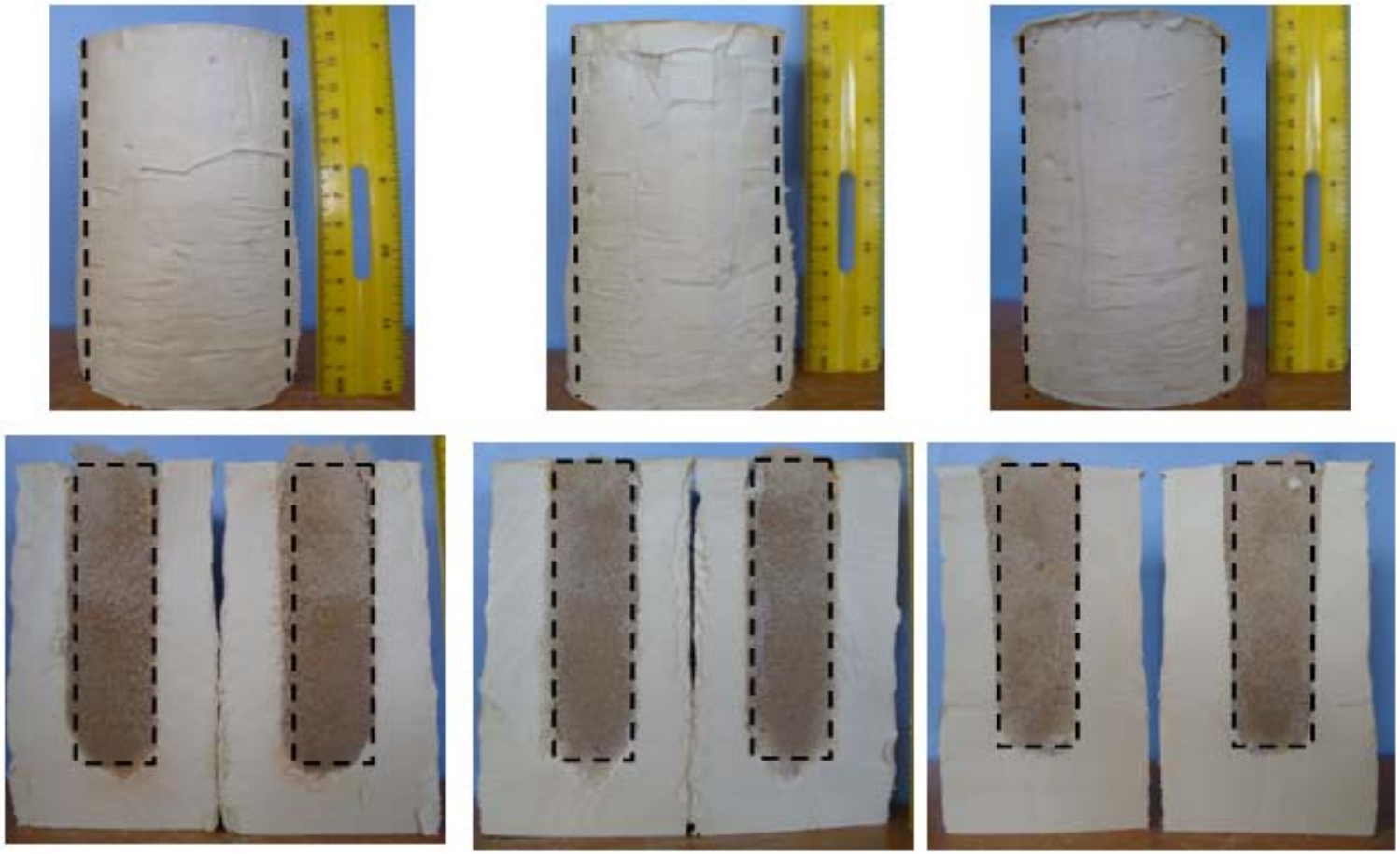

Fig.5.4 Example of external and internal modes of failure of test specimen (Hc/Hs = 0.75 and Ac/As = 17.8% encased).

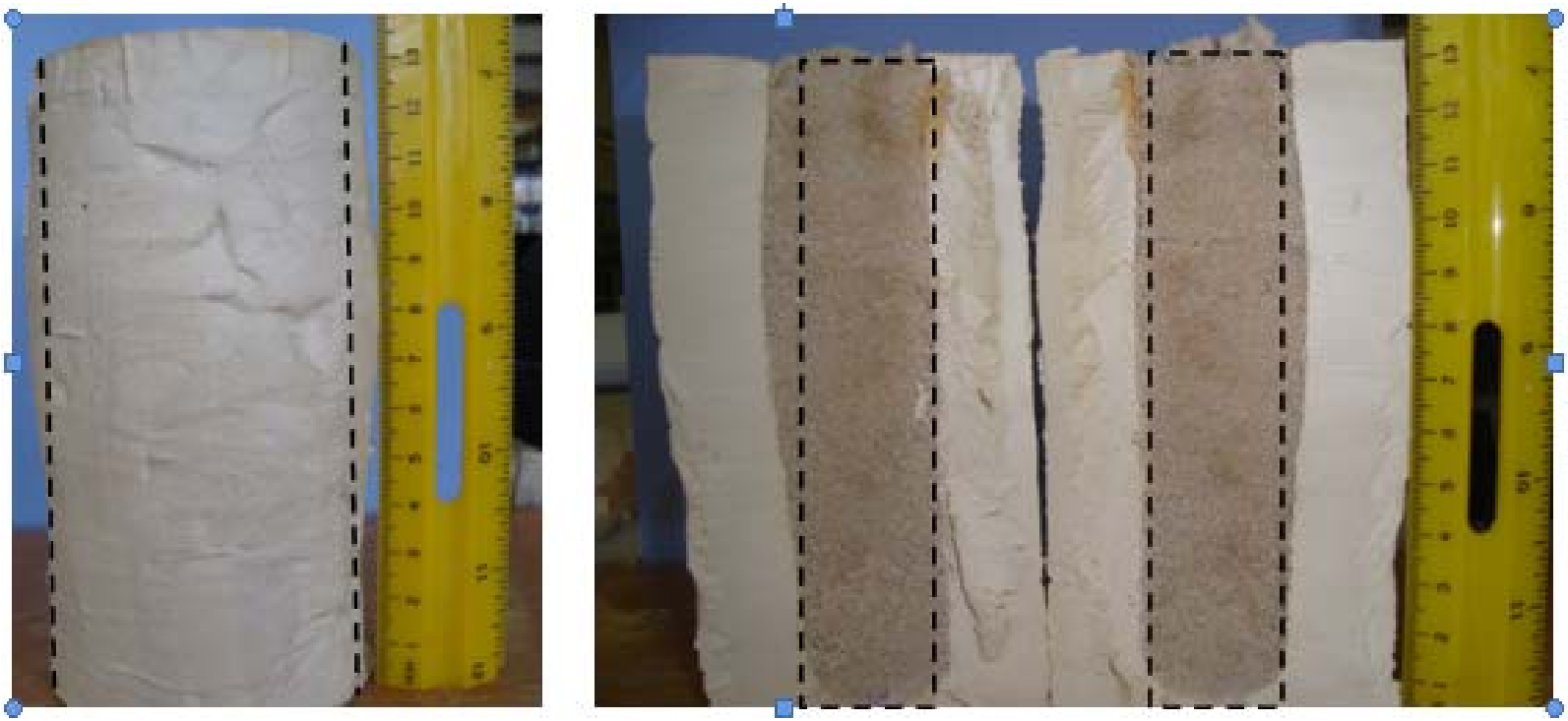

Fig..5.5 Example of external and internal modes of failure of test specimen (Hc/Hs = 1.0 and Ac/As = 17.8% encased).

These observations agree with findings from previous studies (Hughes and Withers 1974, Sivakumar et al. 2004 and Najjar et al. 2010) which indicate that for partially penetrating columns of short lengths, the stresses at the base of the column generally exceed the bearing capacity of the soil leading to a premature bearing capacity failure in the unreinforced lower portion of the specimen. For samples reinforced with fully penetrating columns, bulging was more concentrated in the upper half of the sample, (Fig. 5.4) with the degree of bulging decreasing significantly for encased columns.

To investigate the mode of failure of sand columns, the same test specimens were split along their vertical axes to expose the columns and the surrounding clay (Figs. 5.3, 5.4, and 5.5). For samples reinforced with ordinary partially penetrating sand columns, the sections shown in Fig. 5.3 indicate that the upper portion of the sand columns (length of about 1.5 times the column diameter) exhibited bulging of different levels, with the sample tested at 150 kPa exhibiting the most noticeable bulge. It is also worth noting that the sand column of the sample tested at 200 kPa exhibited a clear shearing displacement at about 2/3 of the column length. When partially penetrating columns were encased, the sand columns did not exhibit any noticeable bulging despite the fact that the clay specimens bulged in the lower half during drained shear (Fig. 5.4). For samples reinforced with fully penetrating ordinary columns, the bulging of the column was in line with the bulging observed for the corresponding clay specimens (Fig. 5.5).

5.2.2.2. Stress-Strain Behavior

The variation of the deviatoric stress and volumetric strain with the axial strain is presented in Figs. 5.6 and 5.7 for tests conducted with area replacement ratios of 7.9%

and 17.8% respectively. The stress-strain curves exhibited consistent increases in deviatoric stresses with strains as the samples were sheared towards critical state conditions. To define failure, the deviatoric stresses will be considered to have leveled out at an axial strain of 12%, which is the maximum strain that was measured in the drained tests. The measured volumetric strains were all contractive. For all confining pressures, the negative volumetric strains were reduced significantly when 3-cm diameter sand columns (A_c/A_s=17.8%) were inserted in the soft clay (see Table 5.1). As expected, this reduction in contractive behavior was more significant for tests involving fully penetrating sand columns, which are expected to be more dilative compared to partially penetrating columns. For tests involving the smaller area replacement ratio (A_c/A_s=7.9%), the volumetric strains that were measured in samples that were reinforced with partially and fully penetrating sand columns were similar to those measured in the control specimens, indicating that the inclusion of sand columns did not have any effect on the tendency for volume change, suggesting that the behavior is governed by the unreinforced part of the clay specimen.

5.2.2.3. Effect of Sand Columns on Deviatoric Stress at Failure

The percent improvement in the deviatoric stress at failure for the series of tests involving area replacement ratios of 7.9% and 17.8% is presented in Table 5.1 and plotted versus the initial effective confining pressure in Fig. 5.8. Results indicate that the use of ordinary 2-cm diameter sand columns (area replacement ratio=7.9%) did not result in notable increases in the deviatoric stress at failure except for the case with a confining pressure of 100kPa where the control specimen resulted in a deviatoric stress

at failure of 112kPa and the reinforced specimen with a 2-cm diameter sand column resulted in a deviatoric stress at failure of 131.7kPa (increase of 17.6%).

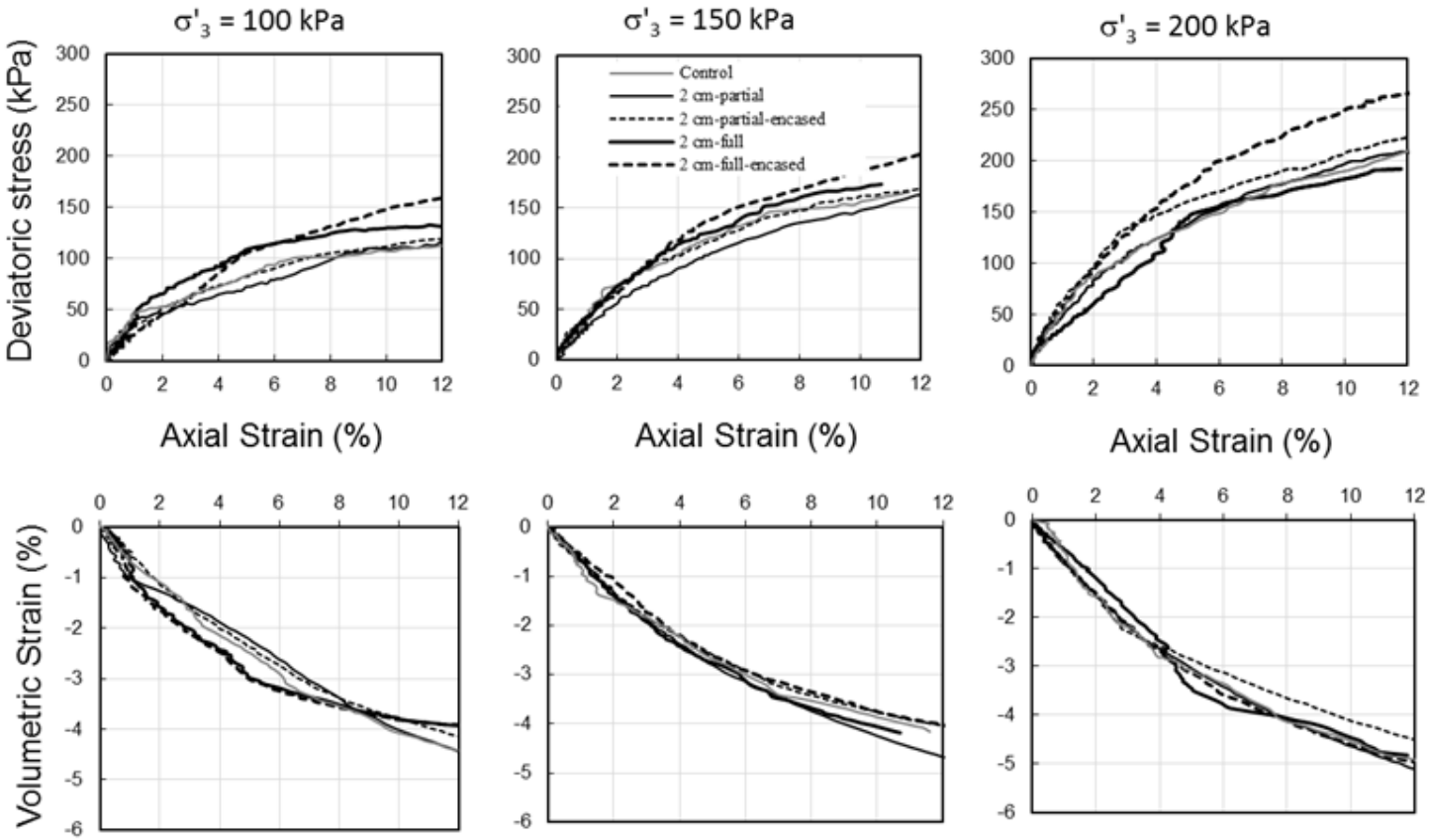

Fig. 5.6 Deviatoric stress and Volumetric strain versus axial strain for Kaolin specimen reinforced with 2-cm sand columns (Ac/As=7.9%)

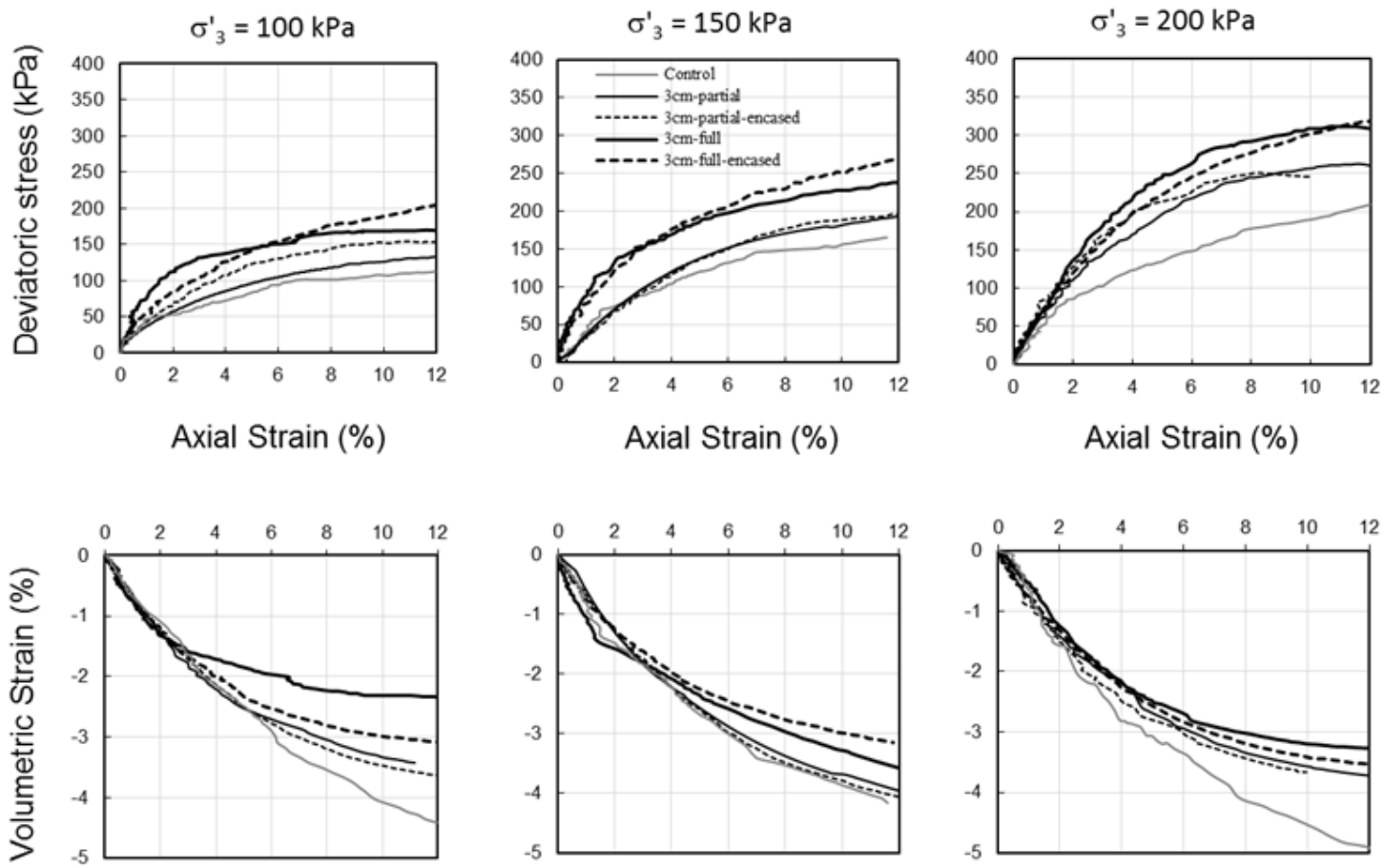

Fig. 5.7. Deviatoric stress and Volumetric strain versus axial strain for Kaolin specimen reinforced with 3-cm sand columns (Ac/As=17.8%)

For specimens reinforced with encased 2-cm sand columns, increases in the deviatoric stresses at failure were observed for samples reinforced with fully penetrating columns only and at all confining pressures, with a maximum improvement of about 41.3% at a confining pressure of 100kPa, and improvements of about 25% for confining pressures of 150kPa and 200 kPa. For the higher area replacement ratio of 17.8%, improvements ranging from 31.2% to 51.5% were observed for samples reinforced with fully penetrating ordinary sand columns and from 17% to 25% for partially penetrating ordinary sand columns. For samples with encased columns, additional improvements in the deviatoric stress at failure were observed due to the encasement, with the improvement ranging from 51.9% to 83.9% for specimens reinforced with fully penetrating columns and from 19% to 37.5% for partially penetrating columns.

It should be noted that for the drained tests conducted in this study using encased columns, the percent improvement in the deviatoric stress at failure decreased as the initial effective confining pressure was increased from 100 kPa to 200 kPa. These findings could be explained by the results of triaxial tests conducted by Wu and Hong (2009) on geotextile-encased and ordinary quartz sand specimens with diameters of 7cm and a height of 14cm compacted at 60% and 80% relative density. Three types of geotextile sleeves were used to encase the columns. Tests were conducted using dry sand at confining pressures of 20, 50, 100, 200, and 500 kPa. Test results indicated that the increase in the deviatoric stress of the sand specimen due to the encasement decreases with increases in confining pressure. The highest increase in deviatoric stress (13.8 times higher than the non-encased sand specimen for the strongest geotextile at 30% strain) was at 20 kPa pressure. At the highest confining pressure of 500 kPa, the increase was only 1.5 times that of the non-encased specimen.

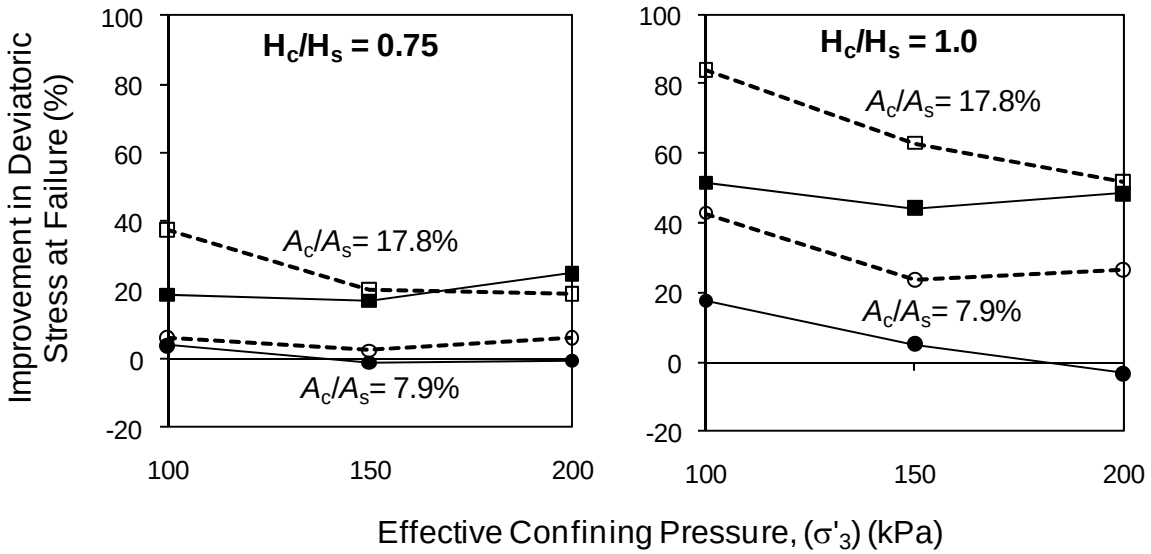

Fig. 5.8 Variation of improvement in deviatoric stress at failure with confining pressure (dotted lines for the encased sand columns)

5.2.2.4.Effect of Sand Columns on Volume Change

Measurements of the volumetric strains at failure were made for all tests and reported in Table 5.1. Results indicate that volumetric strains for samples that were reinforced with ordinary 2-cm sand columns ranged from 4% to 5% and were almost similar to the volumetric strains measured for the control clay specimens. Percent reductions in the volumetric strains were calculated and plotted on Fig. 5.9 versus the percent improvement in the deviatoric stress at failure. For 2-cm columns, percent reductions in volumetric strain were generally close to zero. For partially and fully penetrating non-encased sand columns, the near zero volumetric strain reductions were correlated with near zero improvements in deviatoric stress. However, for fully penetrating encased columns, no correlation was found between near-zero volumetric strain reductions and positive improvements in the deviatoric stresses at failure, which were found to be in the order of 25% to 43%.

For tests involving 3-cm sand columns, volumetric strains at failure generally decreased compared to control clay specimens. Measured volumetric strains ranged from about 3.6% to 4.0% for partially penetrating columns and 2.3% to 3.5% for fully penetrating columns. For tests conducted with 3-cm ordinary and encased columns at initial effective confining pressures of 150 kPa and 200 kPa, percent improvements in deviatoric stresses at failure were found to increase systematically with reductions in volumetric strains (Fig. 5.9b). For tests conducted at an effective confining pressure of 100 kPa, improvements in deviatoric stresses were found to increase with increasing reduction in volumetric strains. However, the relatively large improvements in strength that were observed for encased columns compared to ordinary columns for 100 kPa confining pressure were not associated with higher reductions in volumetric strains. These results, in addition to the results of the encased 2-cm columns, indicate that the additional improvement in strength due to the encasement is correlated more with the additional confinement and not to improvements in the tendency for volume change.

5.2.2.5. Effect of Sand Columns on the Drained Secant Modulus

A drained secant modulus $(E_{sec})_{1\%}$ defined at an axial strain of 1% was calculated for each test by dividing the deviatoric stress measured at an axial strain of 1% by the corresponding strain. Results of the calculated values of $(E_{sec})_{1\%}$ are presented in Table 5.1 and plotted in Fig. 5.10. For tests conducted using area replacement ratio of 7.9%, results indicated reductions in $(E_{sec})_{1\%}$ for partially and fully penetrating sand columns. The only exceptions were tests conducted with encased columns at a confining pressure of 200kPa, where slight increases in $(E_{sec})_{1\%}$ were observed. For tests conducted using area replacement ratios of 17.8%, increases in

$(E_{sec})_{1\%}$ were observed for fully penetrating columns at all confining pressures and for partially penetrating columns at a confining pressure of 200 kPa.

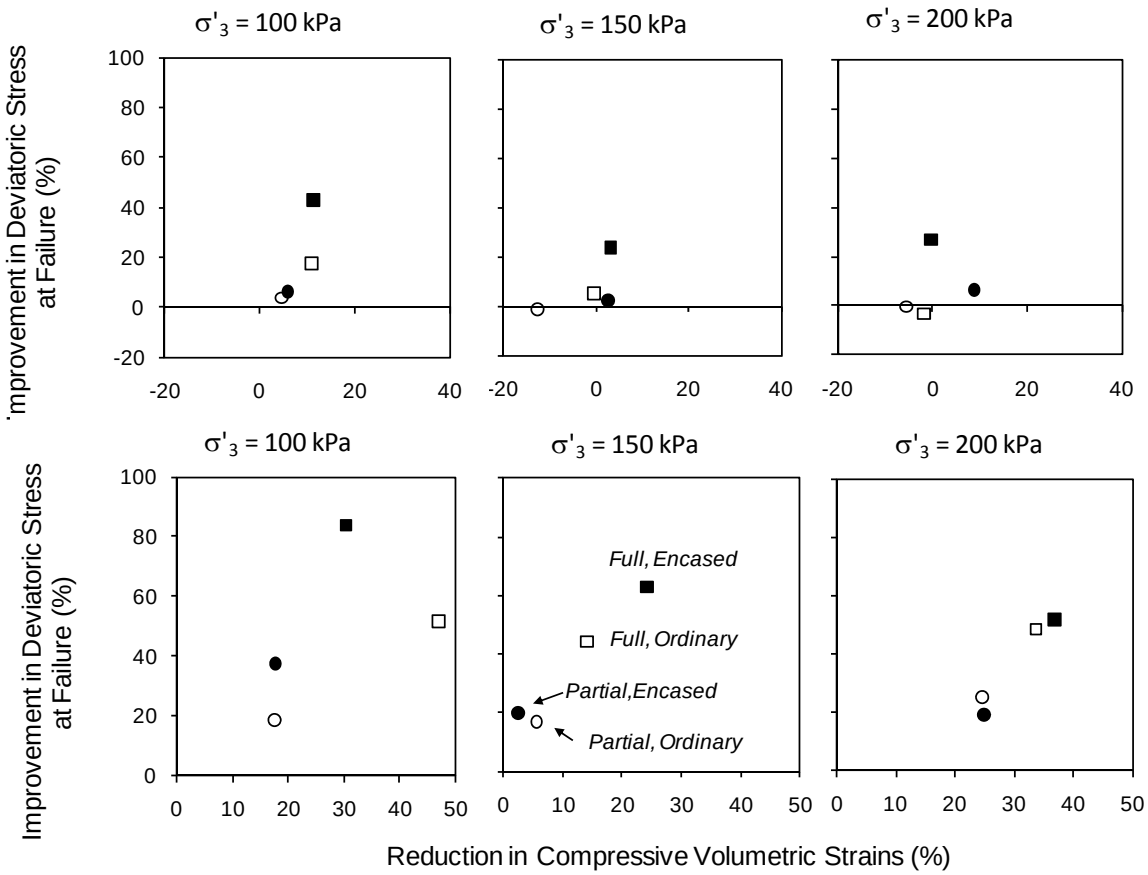

Fig. 5.9 Relationship between improvements in deviatoric stress and reduction in volumetric strains at failure for (a) Ac/As=7.9% and (b) Ac/As=17.8%

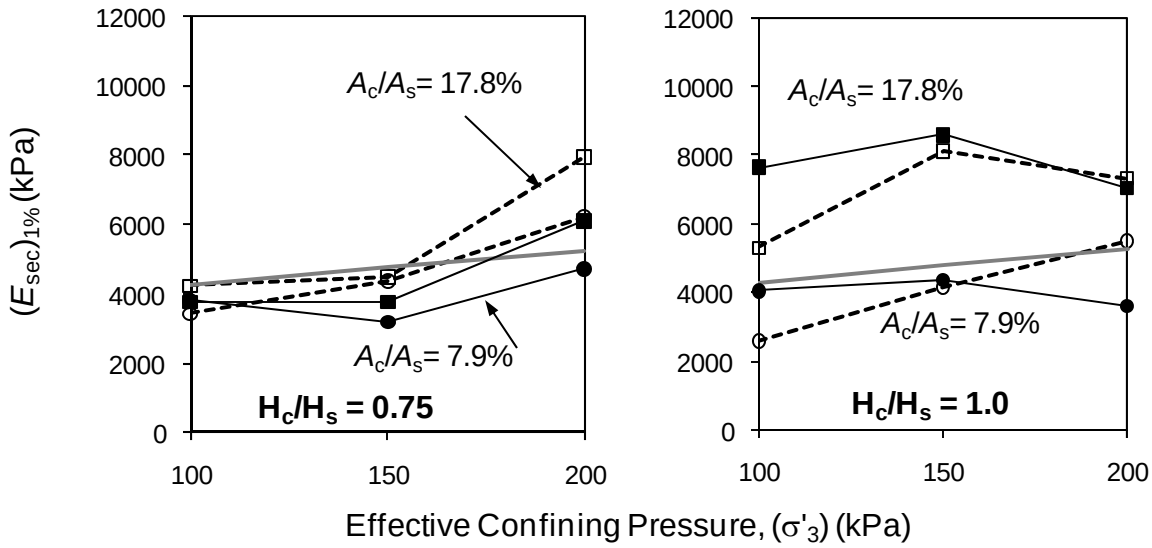

Fig. 5.10 Variation of (Esec)1% with effective confining pressure (dotted lines represent encased columns)

The response observed in Fig. 5.10 for clay/sand composites at low strain levels (as reflected in $(E_{sec})_{1\%}$) is quite complex, particularly with regards to the reduction observed in $(E_{sec})_{1\%}$ and the roles that partial penetration, presence of encasement, and confining pressure could have played with this regard. The installation of the sand column could also have contributed to the reduction in (E_{sec}) at small strains, where the response of the sand column could be affected negatively by any reduction in the contact stresses (confinement) between the column material and the surrounding clay due to column installation. The effects of installation are expected to be more critical for partially penetrating columns (reduced contact at the tip of the column) and relatively small effective confining pressures (lack of full contact at relatively small strains). More importantly, the different stress–strain properties of the clay and the sand could also influence (E_{sec}), particularly at the early stages of loading where sharing of load between the column and the clay initiates, and where the dilation of the column could result in a rapid loss of stiffness. At the early stages of loading, the column could accept a high proportion of the load

due to the large contrast in the stiffness between the column and the clay, but the contrast in stiffness is expected to decrease as the column dilates and transfers more of its load to the clay.

To investigate the dependency of the drained secant modulus on strain level, the variation of E_{sec} with strain at effective confining pressures of 100, 150, and 200 kPa is plotted on Fig. 5.11 for the control clay specimen and for specimens that were reinforced with encased and non-encased sand columns at an area replacement ratio of 17.8%. As expected, the curves on Fig. 5.11 indicate that the secant modulus for reinforced and control specimens decreases as the axial strain increases, reflecting the nonlinearity in the stress-strain response. Specimens that are reinforced with sand columns exhibit a sharp drop in the secant stiffness for strains that are less than 1% to 2%. After a strain of 2%, the stiffness decreases with strain at a decreasing rate.

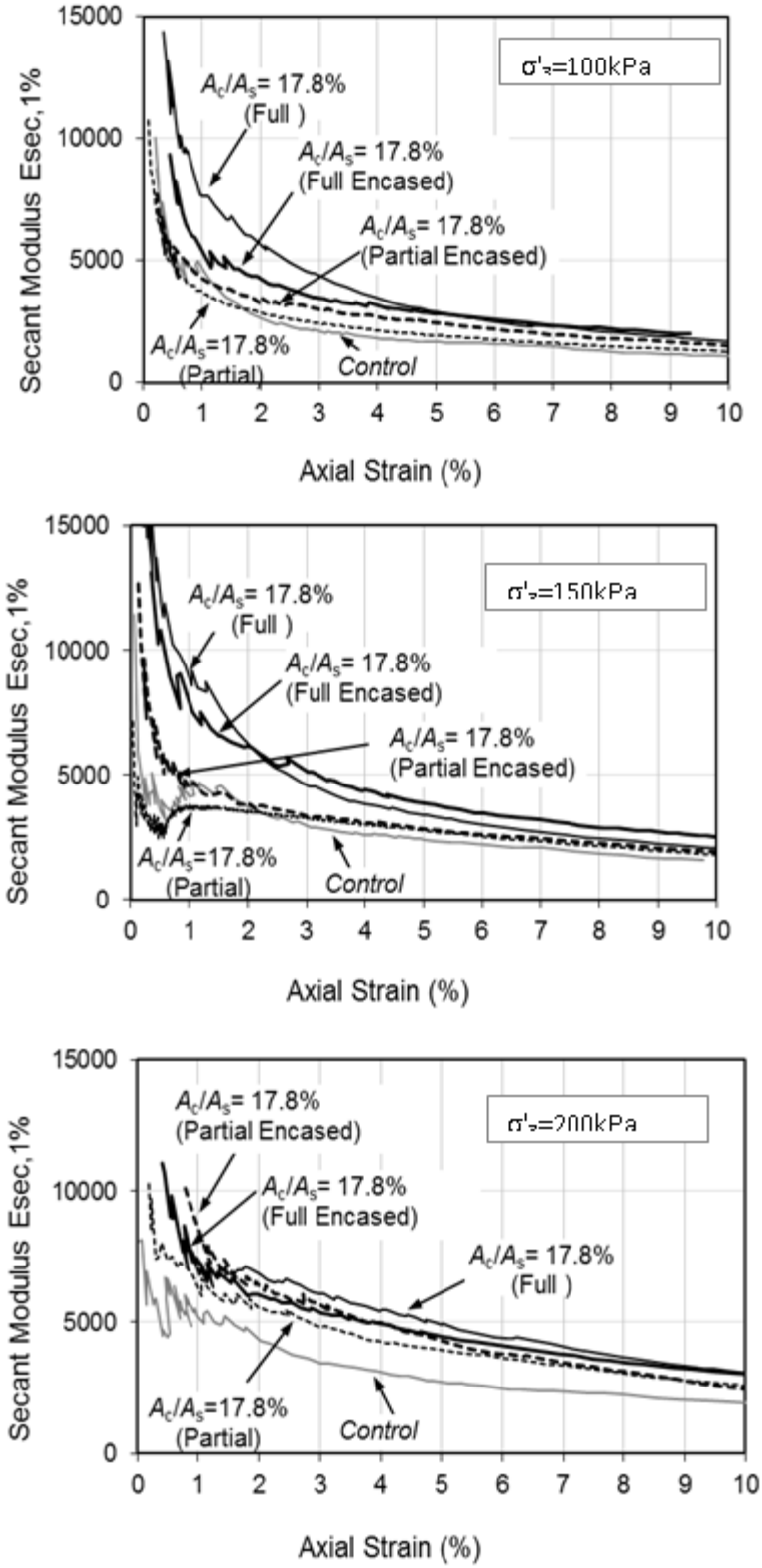

Fig. 5.11 Variation of (Esec) with strain for control and composite specimens

An attempt was made to predict the variation of E_{sec} of the reinforced clay specimen with strain using the curves representing E_{sec} of the control specimens and the sand specimens, and taking into consideration the area replacement ratio of 17.8%. This was achieved using the equilibrium equation $\sigma A=\sigma_c A_c+\sigma_s A_s$ presented by Baumann and Bauer (1974), where σ, σ_c and σ_s are the total average stress acting on the soil specimen, the total stress acting on the sand column, and the total stress acting on the surrounding clay, respectively and A is the cross-sectional area of the specimen. The stress in the sand column σ_c, and the stress in the surrounding clay σ_s, can be predicted at any strain level using (E_{sec}) of the sand specimen and the control clay specimen at that strain level, respectively. For an area replacement ratio of 17.8%, the stress acting on the composite specimen can be calculated based on the equilibrium equation presented above (Baumann and Bauer 1974) and used to back calculate a predicted (E_{sec}) for the composite sample at the desired level of strain. If this exercise is repeated for different levels of strain, a curve representing the predicted variation of (E_{sec}) with strain can be obtained.

For illustration, the predicted variation of (E_{sec}) with strain was determined for tests involving composite specimens reinforced at an area replacement ratio of 17.8% using ordinary fully penetrating sand columns for initial effective confining pressures of 100, 150, and 200 kPa (see Fig. 5.12). A comparison between measured and predicted curves indicates that the simplified model by Baumann and Bauer (1974) results in satisfactory predictions of the general trend of the variation of (E_{sec}) with strain, particularly for strains greater than 2%. A more elaborate analysis of the curves in Fig. 5.12 indicates that the predictions slightly under predict (E_{sec}) for strains greater than 1% to 2% for all confining pressures. Moreover, predicted values of (E_{sec}) were found to significantly overpredict the measured (E_{sec}) at small strains for the higher effective normal pressure of 200 kPa

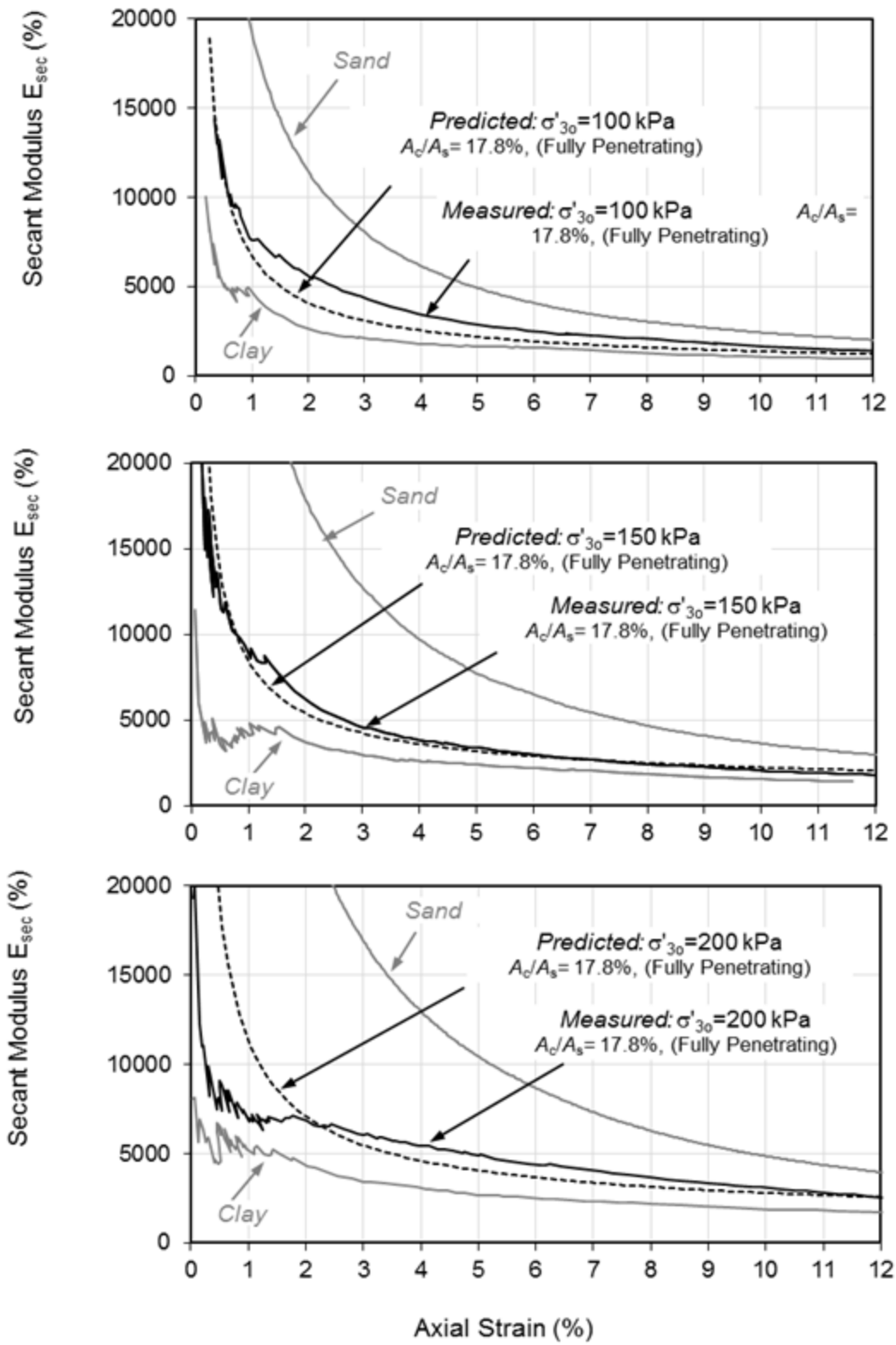

Fig. 5.12 Predicted and measured variation of (Esec) with strain for control and composite specimens (Hc/Hs=1, Ac/As=17.8%, ordinary)

Since the use of E_{sec} of the control and sand specimens in the Baumann and Bauer (1974) model resulted in representative predictions of the variation of (E_{sec}) with strain for the composite specimen, it is hypothesized that the stress concentration factors that are associated with the predictions would also be representative of actual stress concentration factors in the sand columns. As a result, the variation of the stress concentration factors with strain was evaluated and plotted in Fig. 5.13 for the three confining pressures. For relatively small strains (about 1%), results indicated that stress concentration factors generally increased from about 5 to 10, as the confining pressure increased from 100 to 200 kPa. The stress concentration decreases with axial strain to reach an asymptotic value of about 2 at strains of about 10 to 12%, with the asymptotic value being independent of confining pressure.

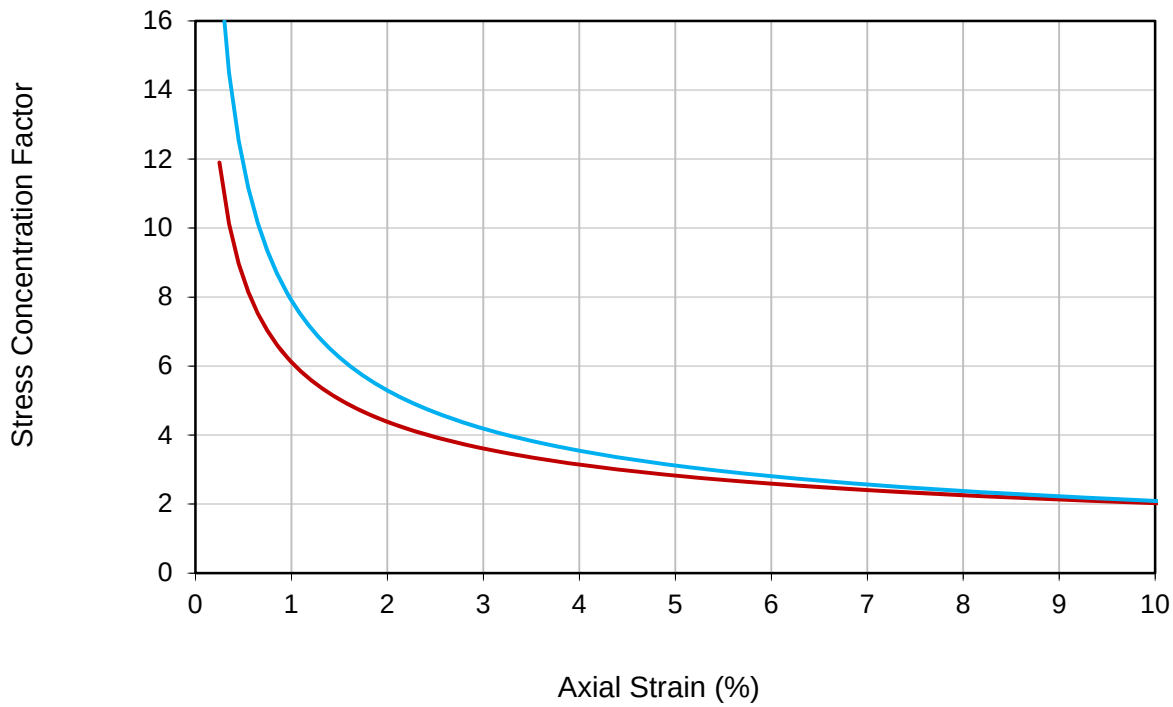

Fig. 5.13. Variation of predicted stress concentration factors with axial strain

5.2.2.6. Effect of sand columns on the Drained Shear Strength

Fig.5.14a-b shows the effective Mohr-Coulomb envelops corresponding to each combination of area replacement ratio and column penetration ratio analyzed in the present study, for non-encased and encased columns, respectively. The resulting shear strength parameters c' and ϕ' are summarized in Table 5.2.

The data in Table 5.2 indicates that the insertion of partially penetrating 2-cm sand columns didn't lead to a noticeable change/increase in the effective friction angle ϕ' and cohesion intercept c' of the composite soil. For fully penetrating 2-cm columns, non-zero effective cohesion intercepts c' of 15 kPa and 22 kPa, with associated effective friction angles ϕ' of 16° and 21°, were observed for ordinary and encased columns respectively. For the case involving ordinary columns, the non-zero c' and the reduced ϕ' reflect the improvement observed in the deviatoric stress at the lower confining pressure of 100 kPa and the lack of improvement at higher confining pressures. On the other hand, the non-zero c' of 15 kPa and the unimproved ϕ' of 21° are expected given previous research which shows that encasing sand columns with geosynthetics of different strengths results in non-zero cohesive intercepts which increase as the strength of the fabric increases (Wu and Hong 2009), with the increases in c' being associated with no improvements in the friction angle ϕ'.

For samples reinforced with 3-cm ordinary columns, the friction angle ϕ' was found to increase to 23° and 26° (compared to 21° for the control clay) for cases involving partially penetrating and fully penetrating sand columns, respectively. The increases in ϕ' were not associated with any increases in the effective cohesion intercept c'. On the other hand, samples that were reinforced with 3-cm encased columns showed no improvements in the friction angle compared to the control specimens, but were associated with non-zero c' values of 15 kPa and

34 kPa for cases involving partially penetrating and fully penetrating sand columns, respectively. To get a visual description of the effect of the encasement on the shear strength envelops the Mohr circles at failure and the associated Mohr-Coulomb envelopes for the tests conducted with 3-cm sand columns are shown on Fig. 5.15 for partially and fully penetrating columns. The envelops for the ordinary columns showed consistent increases in the friction angle, while the envelops for the encased columns were parallel to, but higher than, the envelop of the control clay specimens

Table 5.2. Effective shear stress failure parameters

Column Diameter (cm)	Column Penetration Ratio	c' (kPa)	ϕ' (deg)
0	0	0.0	21.0
2	0.75	0.0	20.6
2	1	22	16.0
2(ESC)	0.75	0	21.0
2(ESC)	1	15.0	21.0
3	0.75	0.0	23.0
3	1	0	26.0
3(ESC)	0.75	15.0	21.0
3(ESC)	1	34.0	21.0

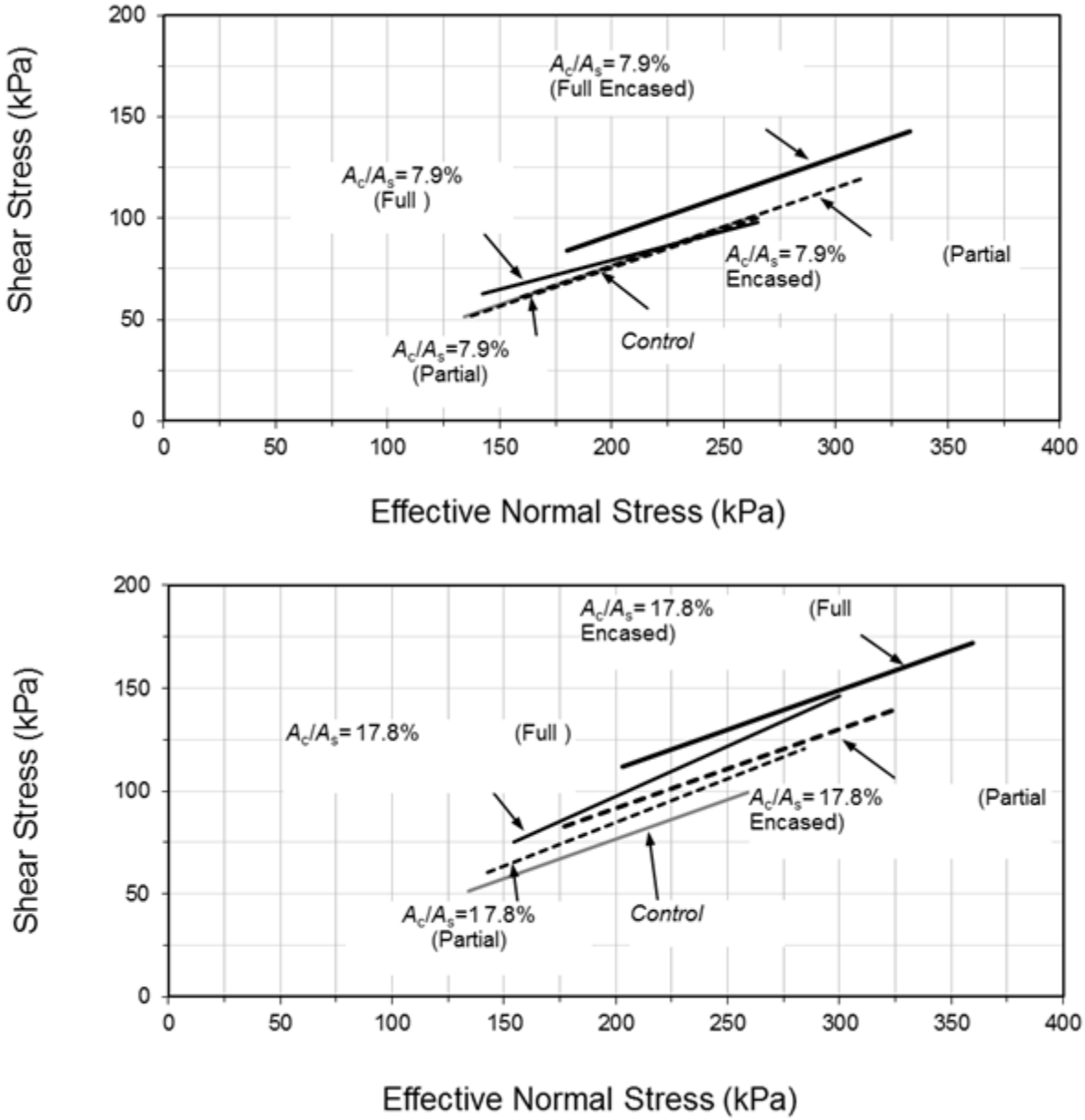

Fig. 5.14 Drained failure envelopes for unreinforced and reinforced kaolin specimens

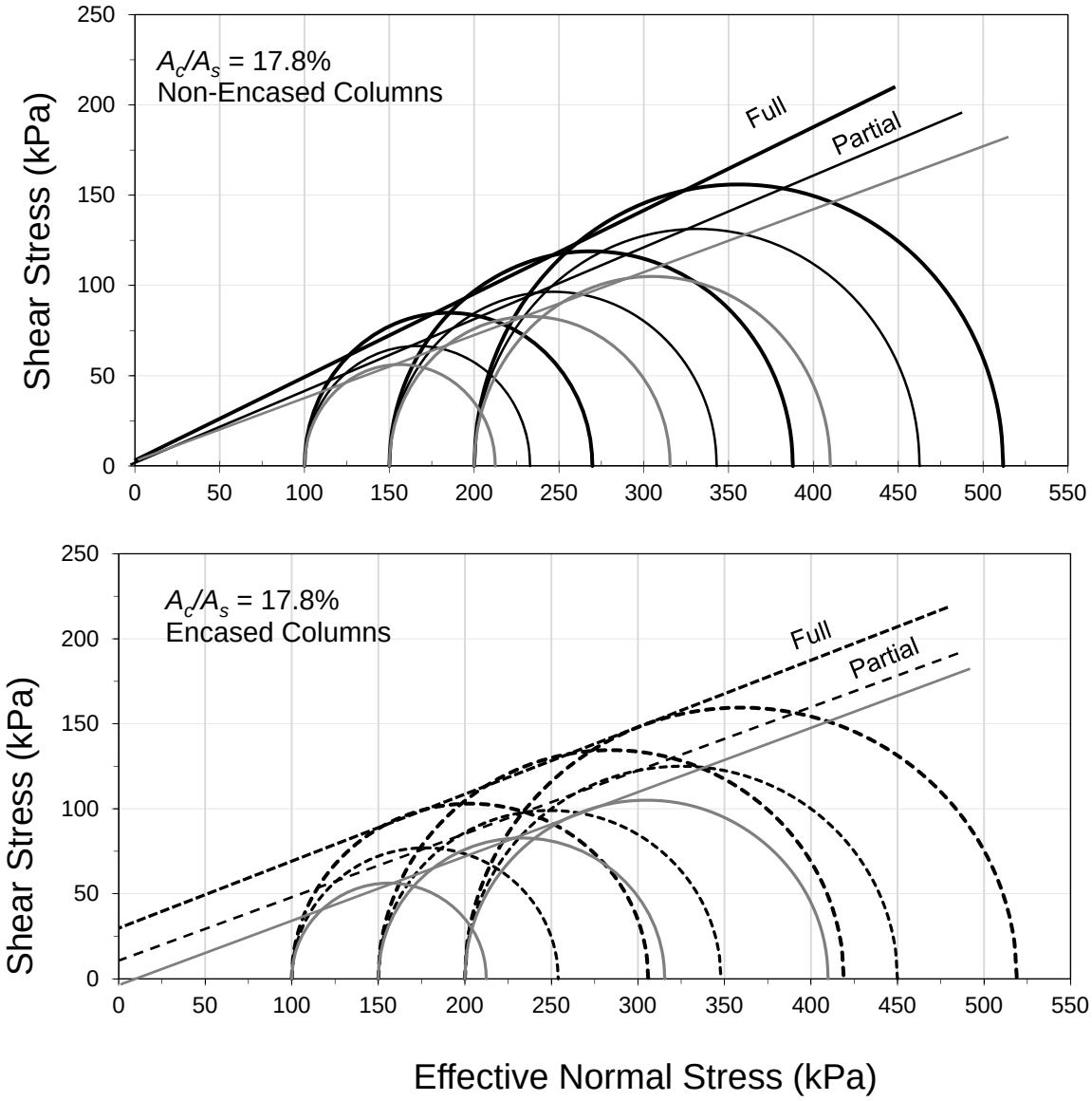

Fig. 5.15 Mohr-Coulomb envelopes for the 3-cm sand columns for partially and fully penetrating columns

5.3. Summary of Main Findings

Based on the results of 27 consolidated drained triaxial tests that were conducted in this experimental research study, the following conclusions can be drawn with regards to the effect of sand columns on the drained response of soft clay:

1. Reinforcing normally consolidated soft kaolin specimens with sand columns at an area replacement ratio of 7.9% resulted in reductions in (Esec)1%, with the only exceptions being tests conducted with encased columns at a confining pressure of 200 kPa. For tests conducted using area replacement ratios of 17.8%, increases in (Esec)1% were observed for fully penetrating columns at all confining pressures and for partially penetrating columns at a confining pressure of 200 kPa.

2. The inclusion of 3-cm sand columns in the clay reduced appreciably the contractive volumetric strains of the clay specimens, with the reduction being more significant for tests involving fully penetrating sand columns, which are expected to be more dilative compared to partially penetrating columns. No significant reductions in volumetric strains were observed for samples reinforced with the 2-cm columns. For cases involving ordinary columns, a correlation was observed between reductions in volumetric strains and increases in deviatoric stresses at failure. Such a correlation was not present in samples with encased columns.

3. An investigation of the variation of the drained secant modulus (Esec) with strain indicated that the secant modulus for reinforced and control specimens decreases as the axial strain increases, with specimens that are reinforced with sand columns exhibiting a sharp drop in the secant stiffness for strains that are less than 1% to 2%. After a strain of 2%, the secant stiffness decreases with strain at a decreasing rate. An analysis indicates that the equilibrium equation presented in Baumann and Bauer (1974) could be utilized together with data from tests

conducted on the control clay and control sand specimens to provide representative predictions of the variation of Esec with strain given a certain area replacement ratio.

4. The use of ordinary 2-cm diameter sand columns did not result in notable increases in the deviatoric stress at failure except for the case of fully penetrating columns with a confining pressure of 100 kPa (increase of 17.6%). When the 2-cm columns were encased, the improvement at 100 kPa increased to 41.3%, while improvements in the order of 25% were observed for confining pressures of 150 and 200 kPa. For the higher area replacement ratio of 17.8%, improvements ranging from 31.2% to 51.5% were observed for samples reinforced with fully penetrating ordinary columns and from 17% to 25% for partially penetrating ordinary columns. For samples with encased columns, additional improvements in the deviatoric stress at failure were observed due to the encasement, with the improvement ranging from 51.9% to 83.9% for specimens reinforced with fully penetrating columns and from 19% to 37.5% for partially penetrating columns.

5. For clay specimens that were reinforced with partially penetrating 2-cm sand columns, the effective friction angle ϕ' and the apparent cohesion c' were not significantly affected by the presence of the sand columns. For fully penetrating 2-cm columns, non-zero c' values were observed and were associated with unchanged or slightly reduced ϕ' values compared to the control clay specimens. The non-zero c' values reflect the improvements in deviatoric stresses at failure at the lower confining pressure of 100 kPa compared to the higher confining pressures of 150 and 200 kPa.

6. For the larger area replacement ratio of 17.8% improvements in ϕ' were observed for ordinary columns (ϕ' increased from 21o for the control clay to 23o for partially penetrating columns to 26o for fully penetrating columns), while improvements in c' were observed for

encased columns (c’ values increased from 0 kPa for control samples to 15 kPa for partially penetrating columns to 34 kPa for fully penetrating columns). These results of encased columns are in line with previous research which shows that encasing sand columns with geosynthetics results in non-zero cohesive intercepts (Wu and Hong 2009), with the increases in c’ being associated with no improvements in the friction angle ϕ'.

CHAPTER 6

COMPARISON BETWEEN DRAINED AND UNDRAINED TESTS

6.1. Introduction

This chapter explores the effects of drainage and rate of loading on the load response of soft clays that are reinforced with sand columns. To achieve this objective, the results of the current comprehensive laboratory testing program that consisted of 27 consolidated drained (CD) triaxial tests will be compared to the results reported in Najjar et al. (2010) and which were based on a series of consolidated undrained (CU) tests that were identical to their drained counterparts. The clay specimens had diameters of 7.1 cm and heights of 14.2 cm and were reinforced with encased and ordinary sand columns with diameters of 2 or 3 cm and were constructed as fully or partially penetrating in the clay specimen. Tests were conducted at effective confining pressures of 100, 150, and 200 kPa.

6.2. Test Results

The results for the drained and undrained test cases are compiled and presented in Table 6.1. These results are analyzed in this chapter to determine the effect of the drainage condition on the load response of the soft clay. In the analysis, emphasis is placed on the improvement in the deviatoric stress at failure, generation of excess pore pressure and its relation to the tendency for volume change, and on the improvement in stiffness and shear strength parameters. In all the plots presented in this chapter, results from undrained tests are represented by dashed lines, while results from drained tests are represented by solid lines.

Table 6.1 Comparison between Drained (this study) and Undrained (Najjar et al. 2010) Results

Test No.	Confining pressure σ_3, (kPa)	Drainage	Diameter of sand column (mm)	Area replacement ratio: A_c/A_s (%)	Column Penetration Ratio: H_c/H_s	Deviatoric stress @ failure (kPa)	Excess pore water pressure (kPa)	Volume strain (%)	E_{sec} @ 1% axial strain (kPa)	Increase in deviatoric stress (%)
1		Undrained	0	0	0	64.7	61.3	-	4150	-
2		Undrained	20	7.9	0.75	71.4	57.3	-	4220	3.9
3		Undrained	20	7.9	1	73.2	51.2	-	4390	13.1
4		Undrained	20 (ESC)	7.9	0.75	76.2	58.0	-	4762	17.8
5		Undrained	20 (ESC)	7.9	1	105.2	58.9	-	5132	62.6
6		Undrained	30	17.8	0.75	77.8	48.9	-	4597	20.2
7		Undrained	30	17.8	1	113.4	42.7	-	5853	75.3
8		Undrained	30 (ESC)	17.8	1	129.6	42.8	-	7150	100.3
9	100	Drained	0	0	0	112.0	-	-4.41	4260	-
10		Drained	20	7.9	0.75	116.4	-	-4.21	3800	3.9
11		Drained	20	7.9	1	131.7	-	-3.93	4050	17.6
12		Drained	20 (ESC)	7.9	0.75	119.0	-	-4.15	3420	6.3
13		Drained	20 (ESC)	7.9	1	160.0	-	-3.91	2580	42.9
14		Drained	30	17.8	0.75	133.0	-	-3.64	3754	18.8
15		Drained	30	17.8	1	169.7	-	-2.34	7630	51.5
16		Drained	30 (ESC)	17.8	0.75	154.0	-	-3.63	4230	37.5
17		Drained	30 (ESC)	17.8	1	206.0	-	-3.07	5300	83.9
18		Undrained	0	0	0	84.2	95.1	-	6092	-
19		Undrained	20	7.9	0.75	97.7	88.9	-	6100	16.0
20		Undrained	20	7.9	1	100.5	87.8	-	6368	19.4
21		Undrained	20 (ESC)	7.9	0.75	102.0	85.4	-	6402	21.1
22		Undrained	20 (ESC)	7.9	1	120.1	76.8	-	6093	42.6
23		Undrained	30	17.8	0.75	113.6	78.1	-	6697	34.9
24		Undrained	30	17.8	1	147.8	65.2	-	8624	75.5
25		Undrained	30 (ESC)	17.8	1	158.8	67.8	-	8045	88.6
26	150	Drained	0	0	0	165.0	-	-4.15	4780	-
27		Drained	20	7.9	0.75	163.3	-	-4.67	3190	-1.0
28		Drained	20	7.9	1	173.6	-	-4.17	4360	5.2
29		Drained	20 (ESC)	7.9	0.75	169.2	-	-4.04	4380	2.5
30		Drained	20 (ESC)	7.9	1	204.0	-	-4.02	4150	23.6
31		Drained	30	17.8	0.75	193.0	-	-3.92	3765	17.0
32		Drained	30	17.8	1	216.4	-	-3.57	8580	31.2
33		Drained	30 (ESC)	17.8	0.75	198.0	-	-4.05	4469	20.0
34		Drained	30 (ESC)	17.8	1	269.0	-	-3.15	8100	63.0
35		Undrained	0	0	0	110.2	130.9	-	7637	-
36		Undrained	20	7.9	0.75	121.0	120.3	-	7904	9.8
37		Undrained	20	7.9	1	131.7	112.1	-	7996	19.5
38		Undrained	20 (ESC)	7.9	0.75	123.9	121.1	-	8144	12.5
39		Undrained	20 (ESC)	7.9	1	149.3	115.7	-	8228	35.5
40		Undrained	30	17.8	0.75	144.2	107.8	-	8983	29.2
41		Undrained	30	17.8	1	184.5	89.4	-	10103	67.4
42		Undrained	30 (ESC)	17.8	1	206.6	86.5	-	11407	87.5
43	200	Drained	0	0	0	210.0	-	-4.93	5240	-
44		Drained	20	7.9	0.75	209.0	-	-5.21	4725	-0.5
45		Drained	20	7.9	1	203.0	-	-5.02	3600	-3.3
46		Drained	20 (ESC)	7.9	0.75	223.0	-	-4.50	6220	6.2
47		Drained	20 (ESC)	7.9	1	266.0	-	-4.95	5480	26.7
48		Drained	30	17.8	0.75	262.6	-	-3.72	6100	25.0
49		Drained	30	17.8	1	311.9	-	-3.27	7030	48.5
50		Drained	30 (ESC)	17.8	0.75	250.0	-	-3.70	7932	19.0
51		Drained	30 (ESC)	17.8	1	319.0	-	-3.12	7320	51.9

6.2.1. Analysis for Control Kaolin Specimens

The variations of the deviatoric stress, pore pressure, and volumetric strain with axial strain are plotted on Fig. 6.1 for the control clay specimens. The stress-strain curves for the undrained tests indicate that the deviatoric stresses reached their maximum values at axial strains that are generally less than 5%. On the other hand, the stress-strain curves for the drained tests exhibited consistent increases in deviatoric stresses with strains as the samples were sheared towards critical state conditions. Moreover, the deviatoric stresses at failure (assuming failure at 12% strain) were found to be consistently greater in drained tests compared to undrained tests (almost twice in magnitude), irrespective of the level of the confining pressure . On the other hand, the stress-strain response indicates that the control clay exhibited higher stiffness at the onset of loading compared to drained tests.

The differences in the observed stress-strain response could be explained by observing the variations in the pore water pressure (for undrained tests) and volumetric strain (for the drained tests) as shearing progressed. The measured volumetric strains in the drained tests were all contractive and consistent with the positive pore pressures witnessed in the corresponding undrained tests. The positive volumetric strains during shearing result in a decrease in the void ratio of the drained clay specimens leading to a strain hardening behavior. The positive pore water pressures on the other hand result in a decrease in the effective confining pressure of the undrained specimen resulting in an early peak in the deviatoric stress. These results are expected for normally consolidated clays that are sheared in a triaxial setup under drained and undrained conditions, respectively.

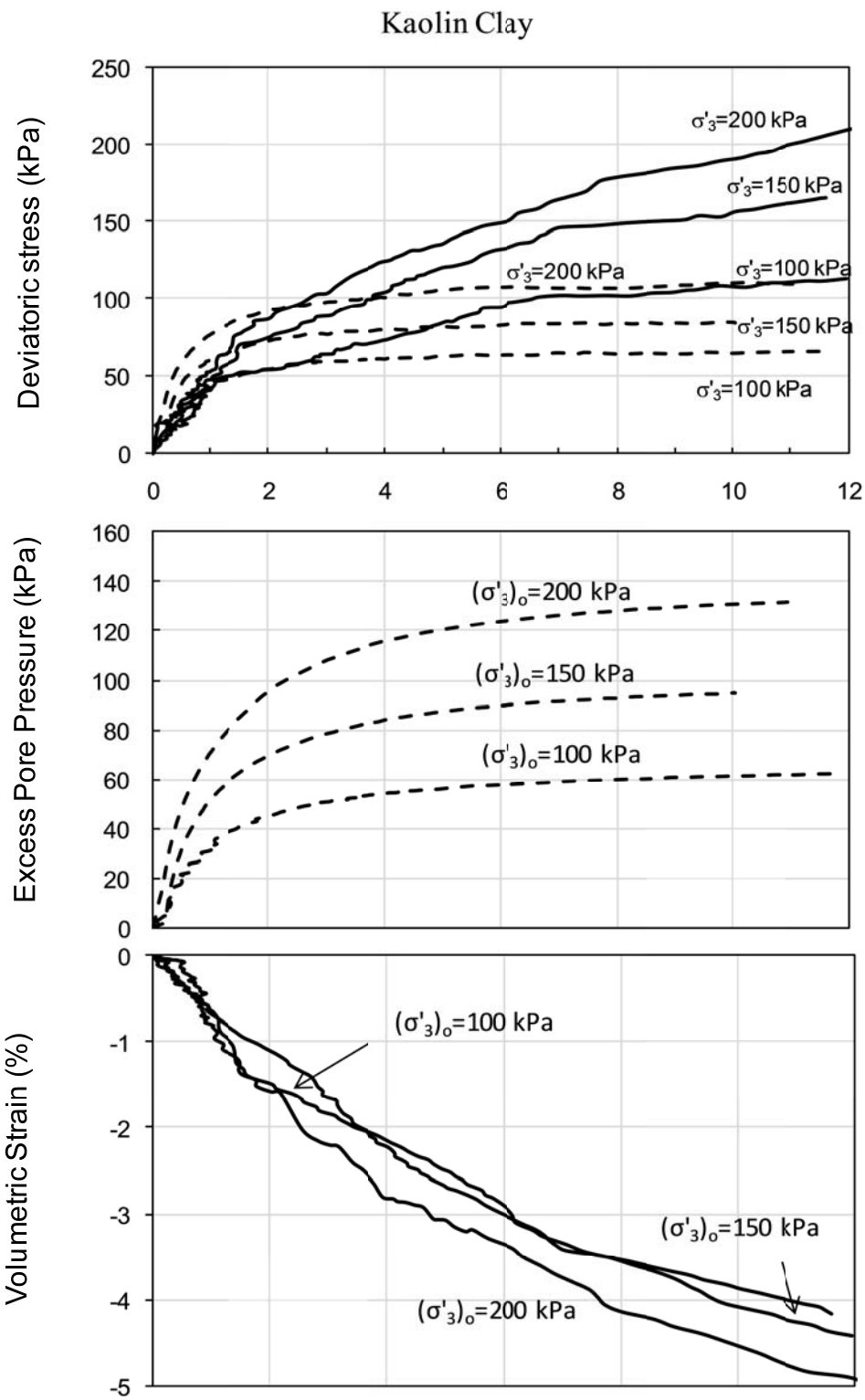

Fig. 6.1 Deviatoric stress, excess pore pressure, and volumetric strain versus axial strain for control clay (Dotted lines indicate undrained tests and solid lines indicate drained tests).

The effective Mohr circles and the corresponding effective Mohr-Coulomb failure envelops for the drained and undrained tests are plotted on Fig. 6.2 for comparison. Interestingly, results on Fig. 6.2 indicate that the effective friction angle ϕ' was about 26° for the undrained tests and 21° for the drained tests, while the effective cohesive intercept c' was equal to zero for both types of tests. The difference in the calculated friction angles from the CD tests and the CU tests with pore pressure measurement could be considered to be significant and is attributed to two main issues: (1) The difference in the mean effective confining pressure at failure between the drained and undrained tests (about 3 to 4 times greater in drained tests compared to undrained tests), and (2) the difference in the rate of loading between the drained and undrained tests (strain rate equal to 0.25% per hour for drained tests and 1% per hour for undrained). Although the two effects are expected to result in an increase in the effective friction angle for undrained tests compared to drained tests, the difference seems to be higher than expected and will lead to some complications in the analysis of the reinforced clay specimens as will be seen in later sections of this chapter.

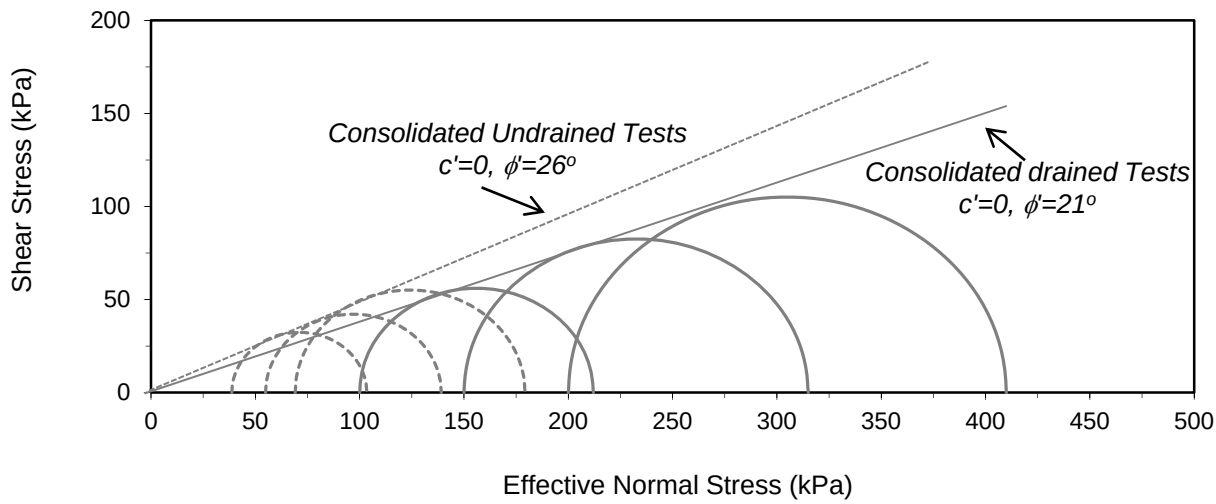

Fig. 6.2 Comparison between Mohr-Coulomb failure envelops for control clay specimens from CD and CU triaxial tests.

6.2.2. Analysis for Ottawa Sand Specimens

The variations of the deviatoric stress, pore pressure, and volumetric strain with axial strain are plotted for the medium dense (relative density of about 44%) sand specimens on Fig. 6.3. The stress-strain curves for the drained tests indicate that the deviatoric stresses reached their maximum values at relatively small axial strains (about 2%) as the specimens dilated significantly during shearing. On the other hand, the stress-strain curves for the undrained tests exhibited consistent increases in deviatoric stresses with strains up to an axial strain of about 6% where the deviatoric stresses leveled out. The stress-strain behavior of the undrained tests were associated with the generation of negative pore pressures which increased in magnitude significantly at the onset of loading and leveled out at an axial strain of about 6%. The relatively large negative pore pressures that were generated in the undrained tests coupled with the dilative response that was observed in the drained tests reflect the significant dilative nature of the Ottawa sand at a relative density of 44%, which is the density used to construct the sand columns in the testing program.

The effective Mohr circles and the corresponding effective Mohr-Coulomb envelops for the drained and undrained tests for Ottawa sand are plotted on Fig. 6.4 for comparison. Results on Fig. 6.4 indicate that the effective friction angle ϕ' was about 33° for the undrained tests and 35° for the drained tests and the effective cohesive intercept c' was equal to zero for both types of tests. The difference between the measured effective friction angles could be attributed to the mean effective stresses at failure which were an order of magnitude greater for the undrained tests (due to the generation of negative excess pore pressures in the undrained specimens as indicated in Fig. 6.4).

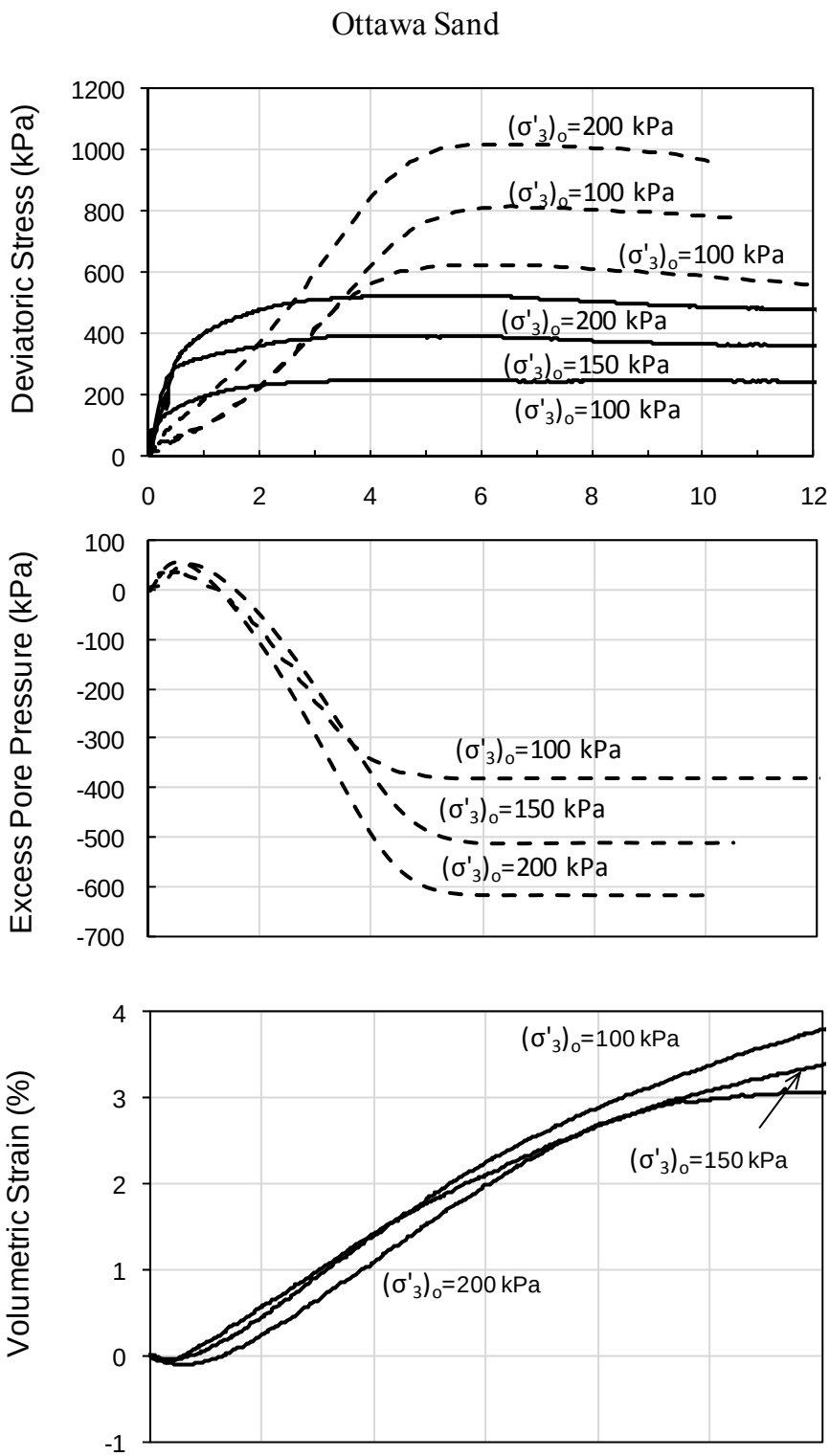

Fig.6.3 Deviatoric stress, excess pore pressure, and volumetric strain versus axial strain for Ottwa sand (Dotted lines indicate undrained tests and solid lines indicate drained tests).

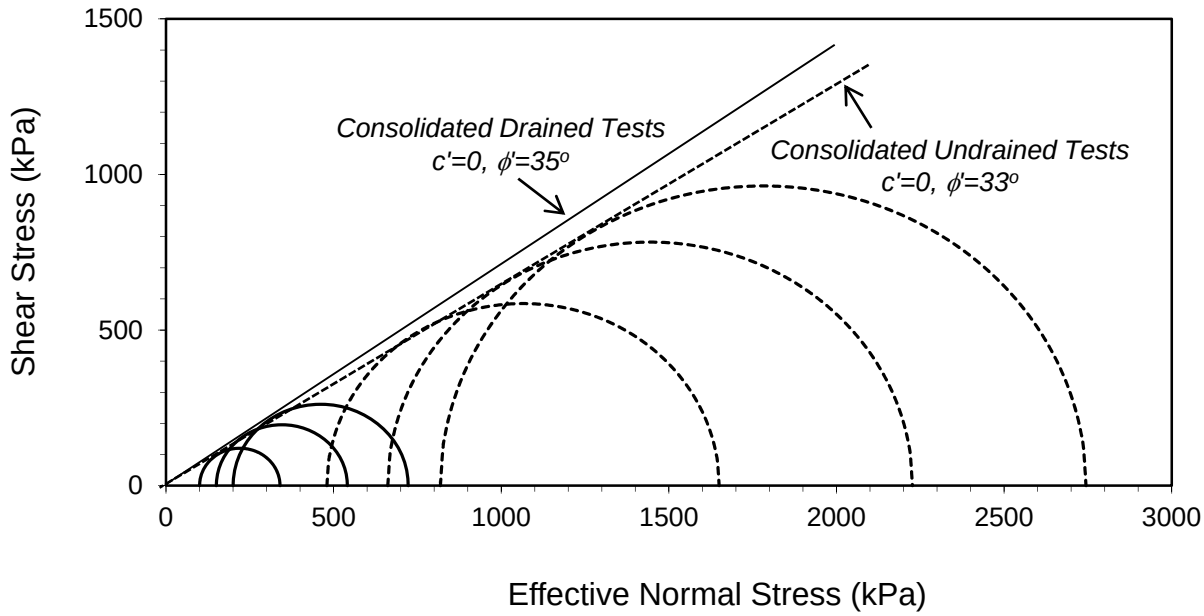

Fig.6.4 Comparison between Mohr-Coulomb failure envelops for Ottawa sand specimens from CD and CU triaxial tests.

6.2.3. Undrained and Drained Response for Clay Reinforced with Ordinary Sand Columns

6.2.3.1. Comparison between the Stress Strain Behavior

The variation of the deviatoric stress, excess pore pressure, and volumetric strain with axial strain is presented in Figs. 6.5 and 6.6 for clay samples that were reinforced with partially penetrating and fully penetrating ordinary sand columns, respectively. Results are presented for drained and undrained tests on the same figures to allow for a direct comparison between the load response at initial effective confining pressures of 100, 150, and 200 kPa.

Results for specimens reinforced with partially penetrating columns (Fig. 6.5) indicate that for the small area replacement ratio A_c/A_s of 7.9%, no improvements in the load-carrying capacity were observed in the drained tests, while slight improvements were observed for undrained tests. On the other hand, results pertaining to the higher area replacement ratio of 17.8% indicated improvements in the load-carrying capacity of the clay specimens for both drained and undrained tests.

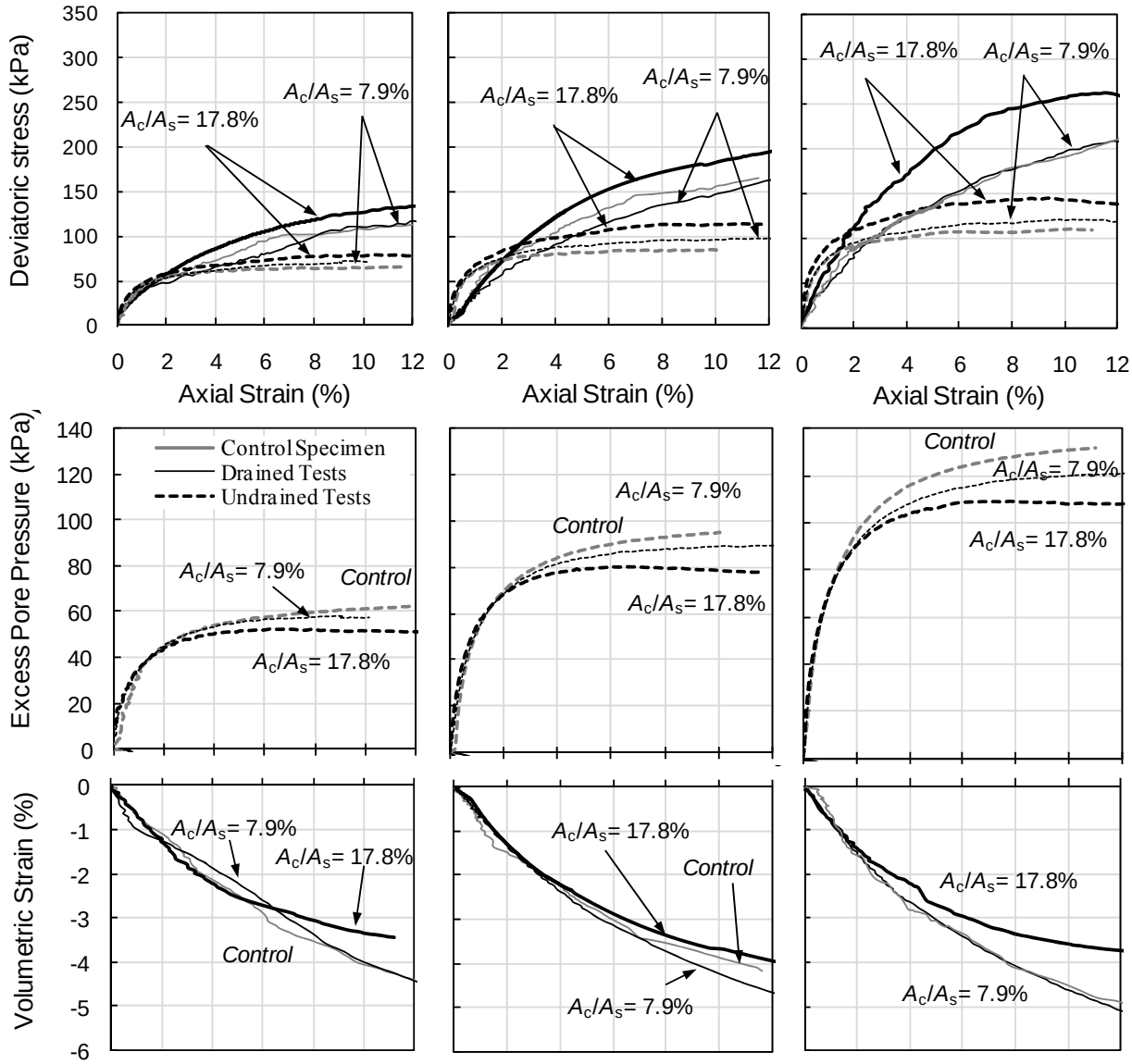

(a) $\sigma'_{3.o}$=100 kPa (b) $\sigma'_{3.o}$=150 kPa (c) $\sigma'_{3.o}$=200 kPa

Fig.6.5 Comparison between the variation of the deviatoric stress, excess pore pressure, and volumetric strain with axial strain for drained and undrained loading conditions (ordinary sand columns, partial penetration).

The lack of any improvement in the load response in the drained tests for samples with A_c/A_s of 7.9% was associated with no change in the volumetric strain in reference to the control clay specimens. On the other hand, test specimens with an A_c/A_s of 17.8% exhibited reductions in the magnitude of the contractive volumetric strains in association with the improvements observed in the drained load response. For the undrained tests, the improvement that was

observed in the load response for both area replacement ratios was associated with a reduction in the excess positive pore pressure in comparison to the control clay specimens. This reduction in positive pore pressures was found to be higher for samples reinforced with a higher area replacement ratio of 17.8% and was associated with larger improvements in the load response. It is worth noting that for all samples at all initial effective confining pressures, the load-carrying capacities that were observed in the drained tests were higher than the load-carrying capacities that were observed for the undrained counterparts. This is related to the fact that the control clay specimens in the drained tests exhibited a higher load capacity compared to the control undrained tests as indicated in Fig. 6.1.

Results for specimens reinforced with fully penetrating columns (Fig. 6.6) indicated similar tendencies to those witnessed for partially penetrating columns. For example, no improvements in the load-carrying capacity and no changes in the volumetric strains were observed in the drained tests for A_c/A_s of 7.9%, except for the test conducted at a confining pressure of 100 kPa. For the undrained tests with an A_c/A_s of 7.9%, slight improvements in the load-carrying capacity were observed and were associated with decreases in the generation of excess positive pore pressures. On the other hand, results pertaining to the higher area replacement ratio of 17.8% indicated significant improvements in the load-carrying capacity of the clay specimens for both drained and undrained tests, with the improvements being clearly associated with decreases in the magnitudes of the volumetric strains in drained tests and in the excess positive pore pressures in the undrained tests. The decrease in the excess positive pore water pressure and contractive volumetric strains during shear could be attributed to the significant tendency for dilation in the 3-cm diameter sand column compared to the 2-cm diameter sand columns and the control specimen.

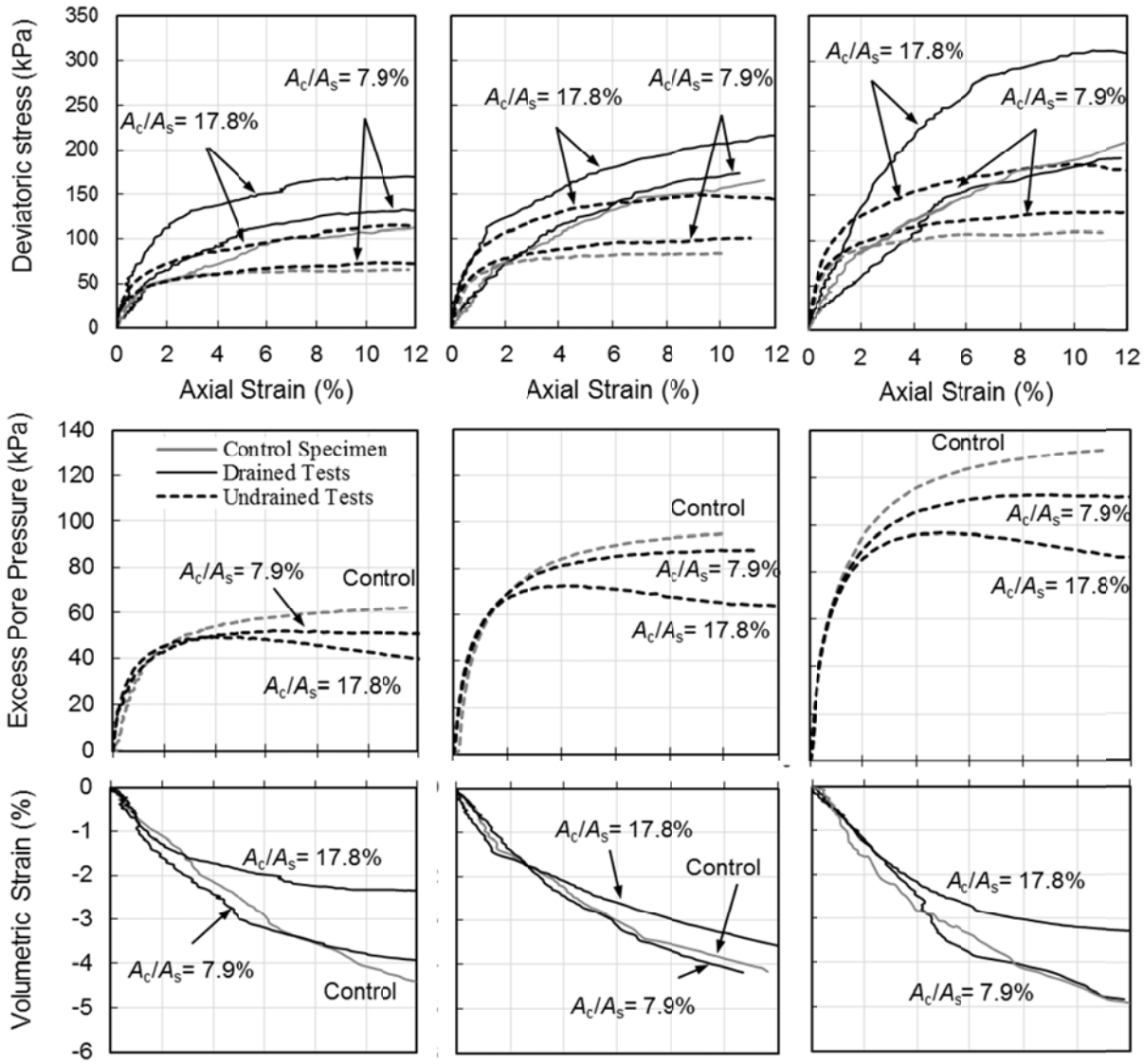

Fig. 6.6 Variation of deviatoric stress and volumetric strain with axial strain (ordinary sand columns, full penetration)

6.2.3.2. Comparison between the Deviatoric Stress at Failure

The percent improvements in the deviatoric stress at failure for both drained and undrained tests are plotted versus the initial effective confining pressure in Fig. 6.7a and 6.7b for clay samples that were reinforced with partially penetrating and fully penetrating ordinary sand columns, respectively.

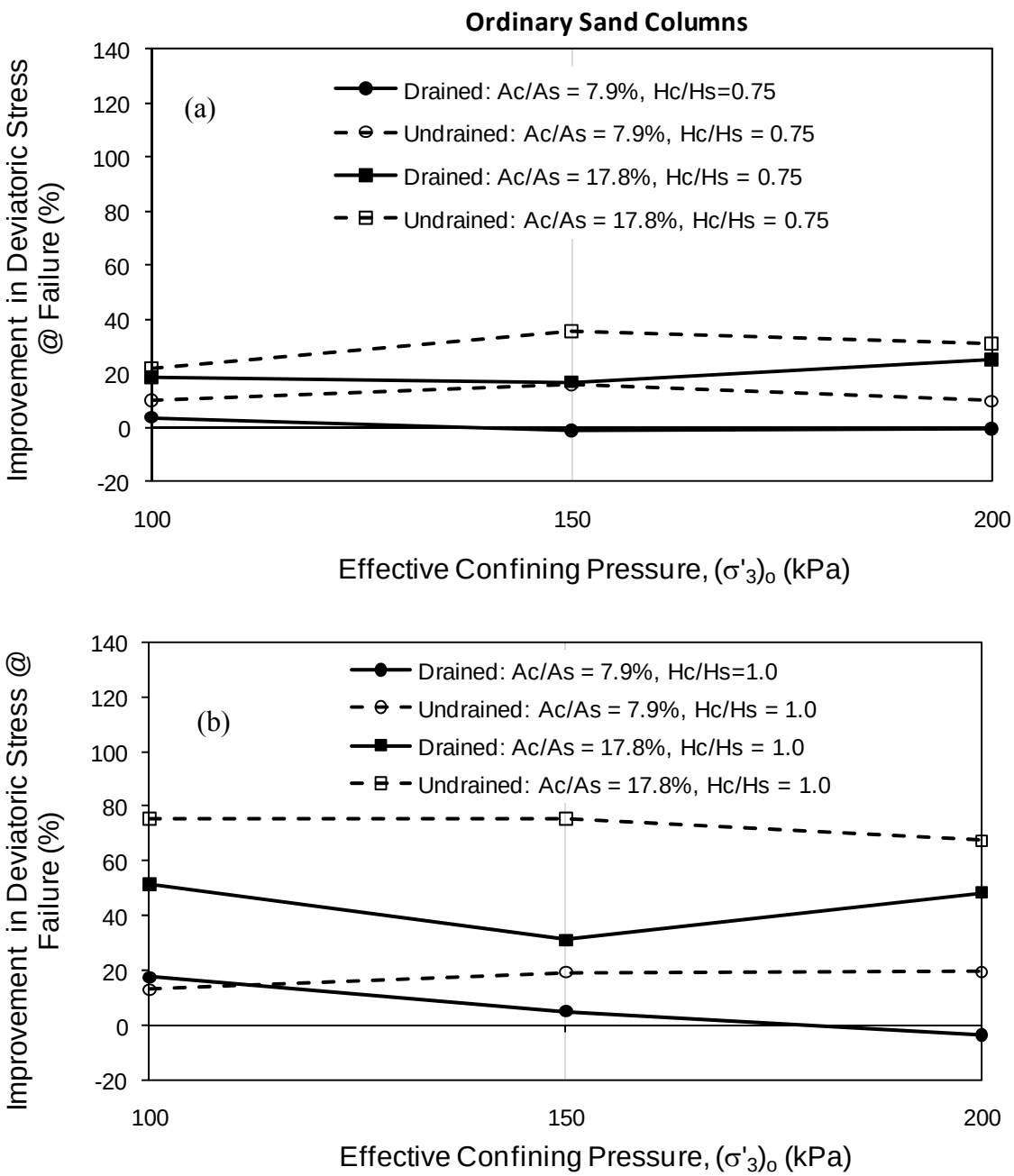

Fig. 6.7 Improvement in the deviatoric stress at failure for (a) partially penetrating ordinary sand columns and (b) fully penetrating ordinary sand columns for drained and undrained tests.

For the undrained tests, results in Figs. 6.7a and 6.7b indicate that the increase in the deviatoric stress at failure for partially penetrating columns ranged from 4 to 16% for A_c/A_s=7.9% and from 20 to 35% for A_c/A_s=17.8%. For the corresponding drained tests, the respective improvements

ranged from 0 to 3% for A_c/A_s=7.9% and from 17 to 25% for A_c/A_s=17.8%. For samples reinforced with fully penetrating columns, the results of the undrained tests indicated that the increase in the deviatoric stress at failure ranged from 13 to 20% for A_c/A_s=7.9% and from 67 to 75% for A_c/A_s=17.8%. For the corresponding drained tests, the respective improvements ranged from 0 to 17% for A_c/A_s=7.9% and from 31 to 51% for A_c/A_s=17.8%.

An analysis of the results presented in Figs. 6.7a and 6.7b indicates that the percent improvement in the deviatoric stress at failure for the undrained tests was consistently higher than the improvement observed for the drained tests. This observation could lead to the conclusion that sand columns are more efficient at increasing the load-carrying capacity of soft clays in an undrained setting than in a drained setting. It should be noted though that the percent improvement in the deviatoric stress at failure was calculated for the drained and undrained tests on reinforced specimens in reference to the drained and undrained response of the control clay, respectively. Results on Figs. 6.5 and 6.6 indicate that although the percent improvement in the deviatoric stress at failure was higher for undrained tests, the absolute values of the deviatoric stress at failure were still much higher for drained tests, signifying that the drained load response could likely represent an upper bound in the shear strength of the reinforced clay specimens analyzed in this study. For a given area replacement ratio, the drained strength of the clays was found to be consistently greater in magnitude than the undrained strength. This indicates that in field applications involving the use of sand columns in soft clays, it is expected that the drained shear strength which will govern the behavior of the reinforced clay for long-term conditions would likely be greater than the undrained shear strength which governs the stability of the reinforced clay in the short term. These results would need to be confirmed with further tests in future research studies.

6.2.3.3. Comparison between the Effective Shear Strength Parameters

The effective shear strength parameters that were obtained from drained and undrained tests on samples tested at effective confining pressures of 100, 150 and 200 kPa are presented in Table 6.2 for comparison. The corresponding Mohr coulomb failure envelopes are shown in Figs. 6.8 and 6.9 for clay specimens reinforced with ordinary 2-cm and 3-cm diameter sand columns, respectively.

For specimens that were reinforced with partially penetrating 2-cm ordinary sand columns, very little improvements in the load carrying capacity were observed compared to control clay specimens. This translated into effective shear strength parameters (c' and ϕ') that were relatively similar to the control specimens (see Table 6.2 and Fig. 6.8a). For specimens that were reinforced with fully penetrating 2-cm ordinary sand columns (see Table 6.2 and 6.8b), c' and ϕ' resulting from the undrained tests were also similar to the parameters of the undrained control clay, despite the fact that average improvements in the order of 18% were observed in the deviatoric stresses at failure. This could be explained by the fact that the improvements in deviatoric stresses at failure were offset by decreases in excess pore pressure at failure for the reinforced specimen, resulting in c' and ϕ' that were more or less unchanged compared to the undrained control specimens. Finally, results of the drained tests that were conducted on fully penetrating 2-cm sand columns indicated a reduction in the effective friction ang ϕ' and an increase in c' in comparison to the control clay specimen (ϕ' decreased from 21° to 16° and c' increased from 0 kPa to 22 kPa). These results reflect the decreasing trend in the percent improvement in deviatoric stress at failure with increasing effective confining pressure as indicated for drained fully penentrating 2-cm specimens in Fig. 6.7b (improvement decreased from 18% to 0% as confining pressure increased from 100 to 200 kPa).

Table 6.2 Comparison between effective shear strength parameters for clay specimens reinforced with ordinary sand columns and tested under drained and undrained conditions.

Drainage Condition	Type of Column	Column Penetration Ratio	Area Replacement Ratio (%)	c' (kPa)	ϕ' (deg)
Drained	-	-	-	0.0	21.0
Drained	Ordinary	0.75	7.9	0.0	20.6
Drained	Ordinary	1	7.9	22	16.0
Drained	Ordinary	0.75	17.8	0.0	23.0
Drained	Ordinary	1	17.8	0.0	26.0
Undrained	-	-	-	0.0	26.3
Undrained	Ordinary	0.75	7.9	4.4	23.7
Undrained	Ordinary	1	7.9	1.0	25.3
Undrained	Ordinary	0.75	17.8	0.0	25.9
Undrained	Ordinary	1	17.8	11.9	23.6

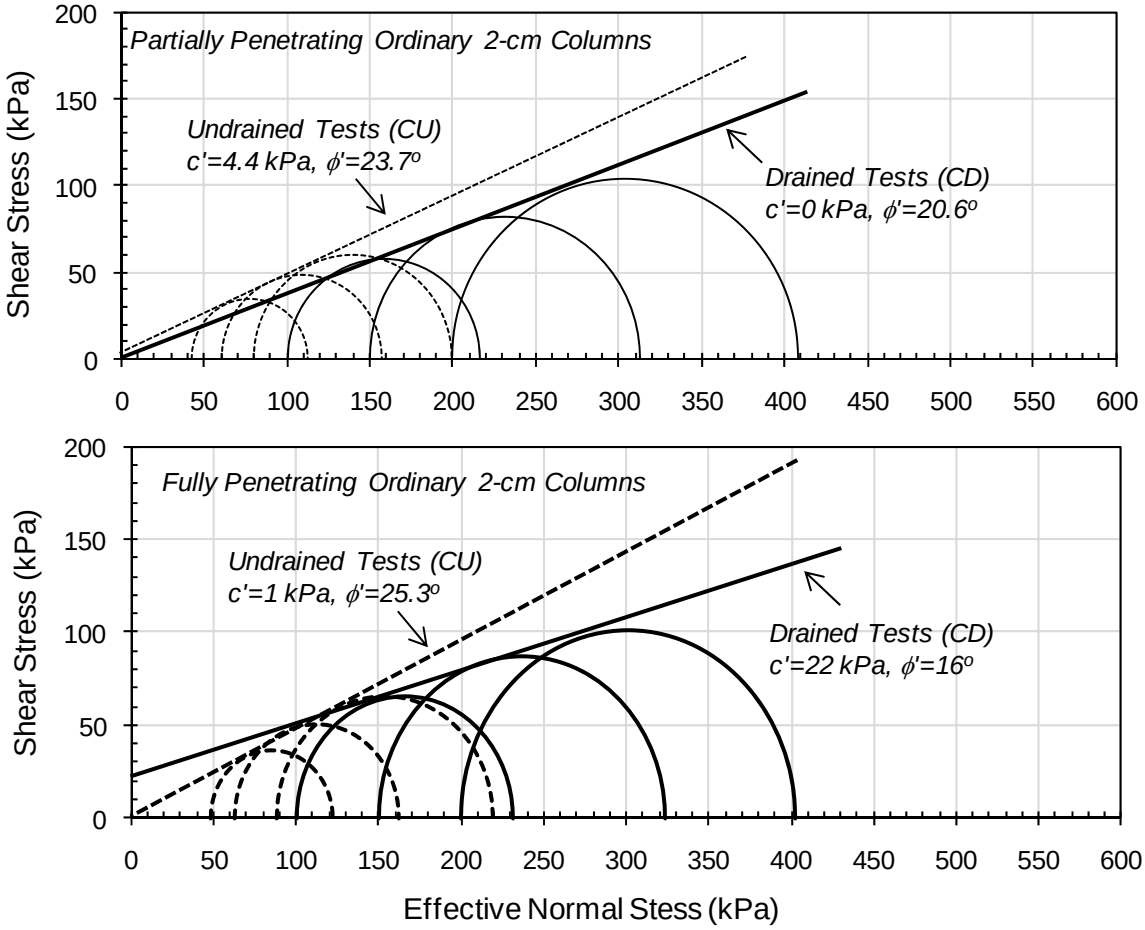

Fig. 6.8 Mohr-Coulomb failure envelopes (samples with ordinary 2-cm sand columns).

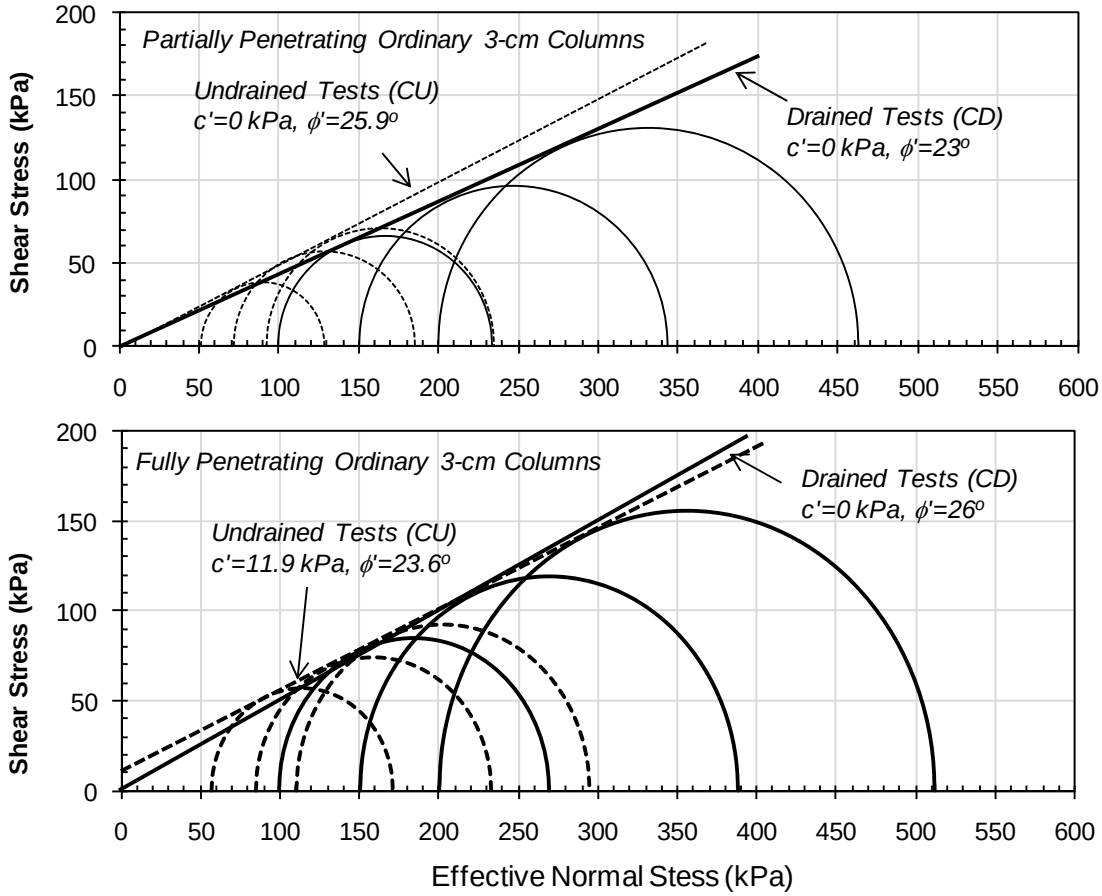

Fig. 6.9. Mohr-Coulomb failure envelopes (samples with ordinary 3-cm sand columns).

For specimens that were reinforced with partially penetrating 3-cm ordinary sand columns, no improvements were observed in c' and ϕ' for the undrained tests ($c' = 0$, $\phi' = 26^o$), and slight improvements were observed in ϕ' for drained tests ($\phi' = 23^o$ compared to $\phi' = 21^o$ for control clay). The lack of improvement in c' and ϕ' for the undrained tests does not reflect the 30% average improvement in the deviatoric stress at failure that was observed in Fig. 6.7b, the reason being the associated reduction in pore pressure witnessed in these tests. For specimens that were reinforced with fully penetrating 3-cm sand columns, an increase in c' (from 0 to 12

kPa) and a slight reduction in ϕ' (from 26° to 24°) were observed in the undrained tests. For the drained tests, c' remained equal to zero and ϕ' increased appreciably (from 21° to 26°).

A thorough analysis of the results in Table 6.2 and in Figs. 6.8 and 6.9 leads to the following observations with regards to the difference between the effective shear strength parameters that were inferred from drained and undrained tests on identical samples:

1. The major difference in the inferred values of ϕ' for the control clay specimens from drained (ϕ' = 21°) and undrained tests (ϕ' = 26°) adds a level of complexity to the analysis of the effective strength envelops of the reinforced clay.
2. Irrespective of the difference in the ϕ' of the control clay, the utilization of c' and ϕ' solely (ex. Table 6.2) as a basis for comparing the effective shear strength envelops from drained and undrained tests might not be indicative of the differences in the results. This is due to the fact that the resulting c' and ϕ' from drained and undrained tests in identical samples are not derived from the same range of effective stress, with the range of mean stresses in undrained tests being 2 or 3 times smaller than the range of the stresses in the drained tests.
3. Based on point 2 above, it is observed that differences in the failure envelops from drained and undrained tests tend to become smaller as the differences in the mean effective stresses between drained and undrained tests become smaller. This is shown clearly in the tests conducted using 3-cm columns (Fig. 6.9) where the increase in the deviatoric stresses and the decrease in the excess pore pressures at failure in the undrained tests were significant enough to push the Mohr circles to higher stresses. For these tests (especially the fully penetrating 3-

cm column), the difference between the drained and undrained Mohr-Coulomb failure envelops becomes smaller for a wide range of effective normal stresses.

6.2.3.4. Comparison between Secant Young's Modulus

A secant Young's modulus $(E_{sec})_{1\%}$ defined at an axial strain of 1% was calculated for each test by dividing the deviatoric stress measured at an axial strain of 1% by the corresponding strain. Results of the calculated values of $(E_{sec})_{1\%}$ for drained and undrained tests are presented in Table 6.1 and plotted in Fig.6.10 versus the initial effective confining pressure for comparison. For the undrained tests involving partially penetrating 2-cm (A_c/A_s=7.9%) and 3-cm (A_c/A_s=17.8%) columns, no improvements were observed in the values of $(E_{sec})_{1\%}$ for all confining pressures. For fully penetrating columns, results indicate that the average improvement in the secant undrained Young's modulus $(E_{sec})_{1\%}$ for effective confining pressures of 100 kPa, 150 kPa, and 200 kPa was about 5% for an area replacement ratio of 7.9% and about 38% for area replacement ratios of 17.8%.

Interestingly, results of the drained tests conducted with an area replacement ratio of 7.9% exhibited a reduction in $(E_{sec})_{1\%}$ at all confining pressures. Similarly, samples that were reinforced with an area replacement ratio of 17.8% using partially penetrating columns also exhibited a reduction in $(E_{sec})_{1\%}$ confining pressures of 100 kPa and 150 kPa. On the other hand, results of tests conducted on specimens with the higher area replacement ratio of 17.8% and fully penetrating columns exhibited a consistent increase in $(E_{sec})_{1\%}$, reaching about 80% for confining pressures of 100 kPa and 150 kPa, and about 34% for a confining pressure of 200 kPa. The reduced efficiency of the sand columns in providing improvement in stiffness at high confining pressures (200 kPa) is not clear at this time, but could be due to a possible reduction in the lateral

confinement of the sand column during shear at the initial stage of loading of the composite specimens.

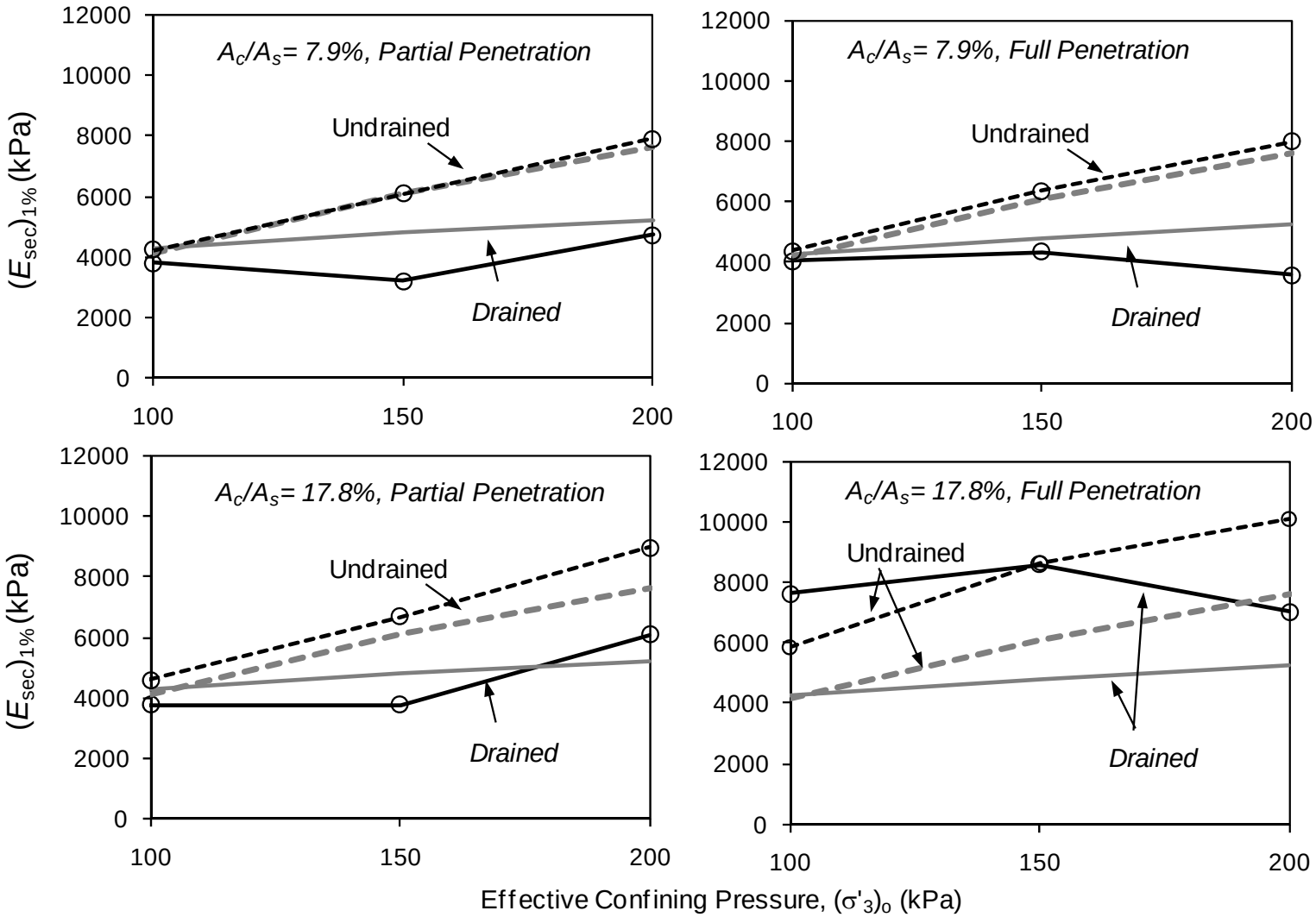

Fig.6.10 Variation of (Esec)1% with effective confining pressure for samples reinforced with ordinary sand columns

A comparison between $(E_{sec})_{1\%}$ values that are obtained from identical drained and undrained tests indicates that except for test cases with a confining pressure of 100 kPa, the stiffness of the specimens as indicated by $(E_{sec})_{1\%}$ was larger for the undrained tests. The results can be explained by noting that the dependency of $(E_{sec})_{1\%}$ of the control clay tests on the initial effective confining pressure in the undrained tests was much stronger than the dependency of $(E_{sec})_{1\%}$ in the control drained tests on confining pressure. As the effective confining pressure increased from 100 kPa to 200 kPa, $(E_{sec})_{1\%}$ in the undrained control tests increased from 4150 kPa to 7637 kPa, whereas the corresponding increase in the drained control tests was from 4260 kPa to 5240 Kpa.

6.2.4. Undrained and Drained Response for Clay Reinforced with Encased Sand Columns

6.2.4.1. Comparison between the Stress Strain Behavior

The variation of the deviatoric stress, excess pore pressure, and volumetric strain with axial strain is presented in Figs. 6.11 and 6.12 for clay samples that were reinforced with partially penetrating and fully penetrating encased sand columns, respectively. As with the ordinary columns, results for specimens reinforced with partially penetrating columns (Fig. 6.11) indicate that for the small area replacement ratio A_c/A_s of 7.9%, no improvements in the load-carrying capacity were observed in the drained tests, while slight improvements were observed for undrained tests. On the other hand, results pertaining to the higher area replacement ratio were only available for the drained tests and indicated significant and consistent improvements in the load-carrying capacity of the clay specimens for all confining pressures.

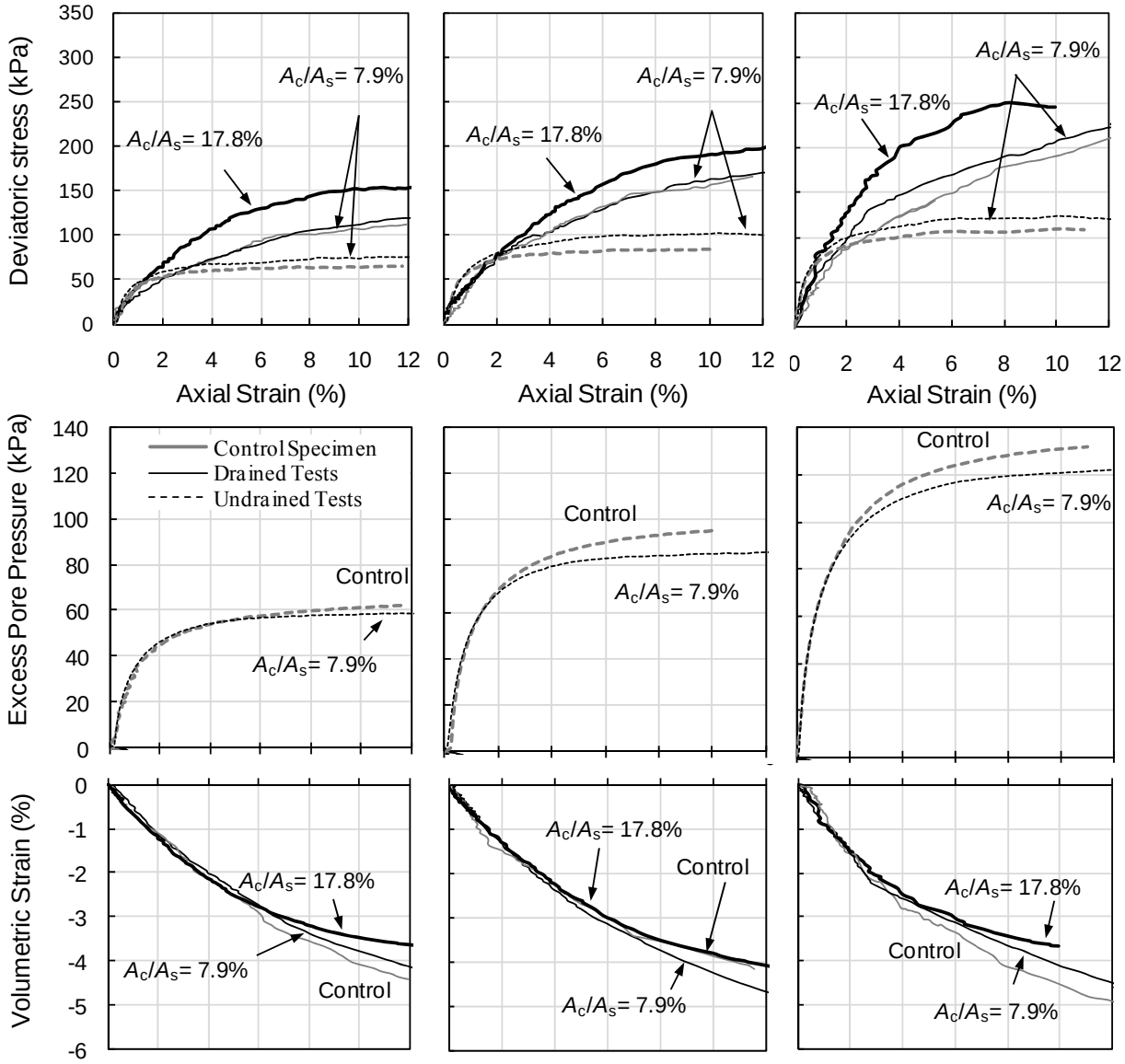

Fig. 6.11 Comparison between the variation of the deviatoric stress, excess pore pressure, and volumetric strain with axial strain for drained and undrained loading conditions (encased sand columns, partial penetration).

Results for specimens reinforced with fully penetrating columns (Fig. 6.12) indicated significant improvements in the load carrying capacity for all area replacement ratios for both drained and undrained tests. Of special interest is the improvement that was observed for the drained tests for specimens reinforced with the smaller area replacement ratio of 7.9%, which did not show any improvement when ordinary sand columns were used (Fig. 6.6). The encasement

of the sand columns with a geotextile allowed the samples to carry additional load at high strains by providing additional lateral confinement to the sand column. It is worth noting that the additional improvement in the drained load-carrying capacity for these samples was not associated with any additional decrease in contractive volumetric strains compared to samples reinforced with ordinary sand columns.

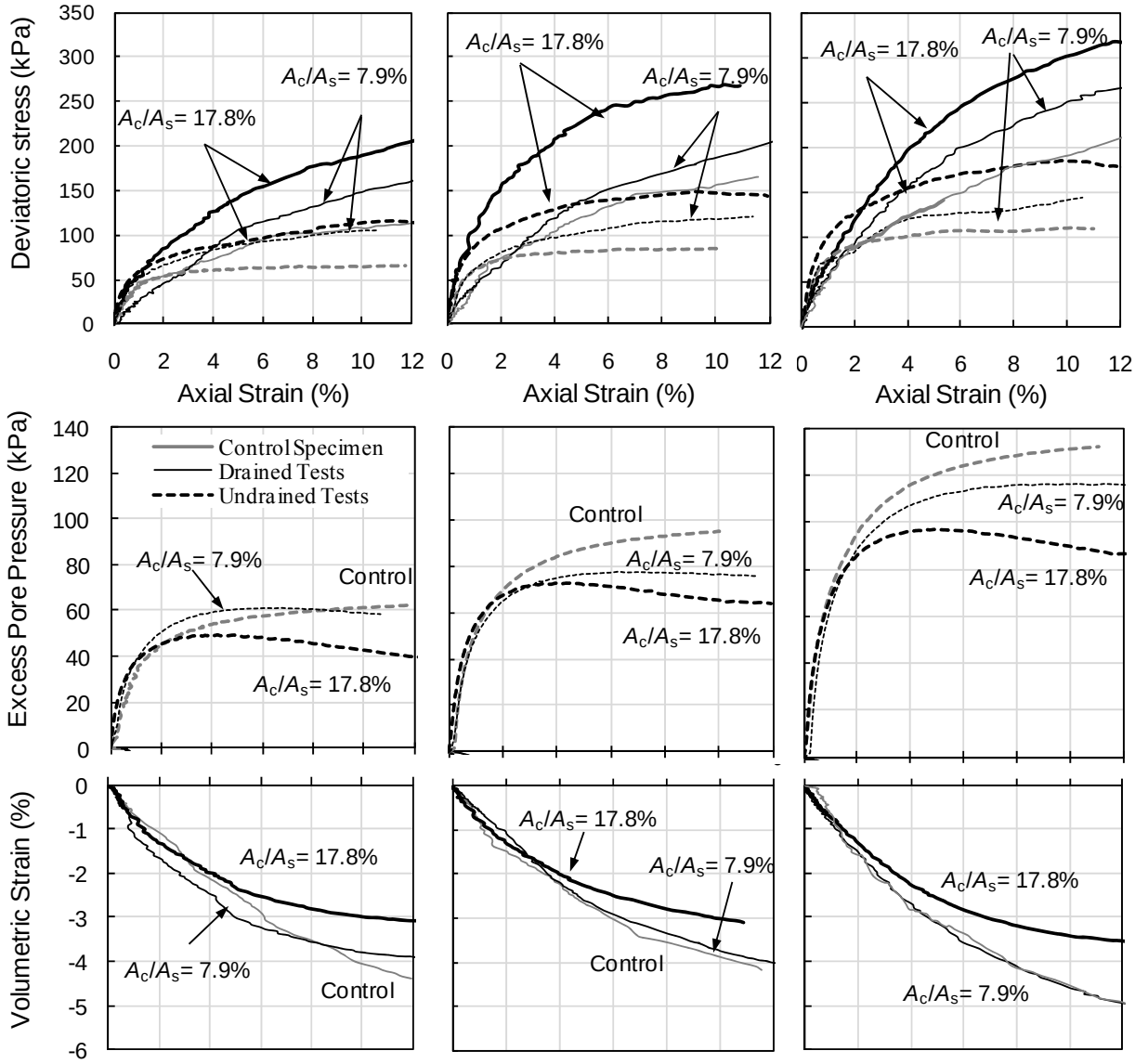

Fig. 6.12 Comparison between the variation of the deviatoric stress, excess pore pressure, and volumetric strain with axial strain for drained and undrained loading conditions (encased sand columns, full penetration).

6.2.4.2. Comparison between the Deviatoric Stress at Failure

The percent improvements in the deviatoric stress at failure for both drained and undrained tests are plotted versus the initial effective confining pressure in Fig. 6.13a and 6.13b for clay samples that were reinforced with partially penetrating and fully penetrating encased sand columns, respectively.

For the undrained tests, results in Figs. 6.13a and 6.13b indicate that the increase in the deviatoric stress at failure for partially penetrating columns ranged from 10 to 21% (compared to 4 to 16% for ordinary columns) for A_c/A_s=7.9%. For the corresponding drained tests, the respective improvements ranged from 2.5% to 6.3% (compared to 0 to 3% for ordinary columns) for A_c/A_s=7.9% and from 19 to 38% (compared to 17 to 25% for ordinary columns) for A_c/A_s=17.8%. For samples reinforced with fully penetrating columns, the results of the undrained tests indicated that the increase in the deviatoric stress at failure ranged from 35 to 62% (compared to 13 to 20% for ordinary columns) for A_c/A_s=7.9% and from 88 to 100% (compared to 67 to 75% for ordinary columns) for A_c/A_s=17.8%. For the corresponding drained tests, the respective improvements ranged from 23 to 43% (compared to 0 to 17% for ordinary columns) for A_c/A_s=7.9% and from 52 to 84% (compared to 31 to 51% for ordinary columns) for A_c/A_s=17.8%.

Results presented above indicate that encasing the sand column with a geotextile results in a consistent increase in the percent improvement in the deviatoric stress at failure for both drained and undrained tests compared to ordinary sand columns. The percent improvement in the deviatoric stress at failure for encased columns ranges from about 1.5 to 3.0 times the percent improvement observed for ordinary sand columns. It should be noted that for both drained and undrained tests, the maximum improvements in the deviatoric stresses at failure occurred at the

small confining pressure of 100 kPa, and these improvements decreased as the effective confining pressure was increased to 150 kPa and 200 kPa. Reasons behind this observed behavior were presented in detail in chapter 5.

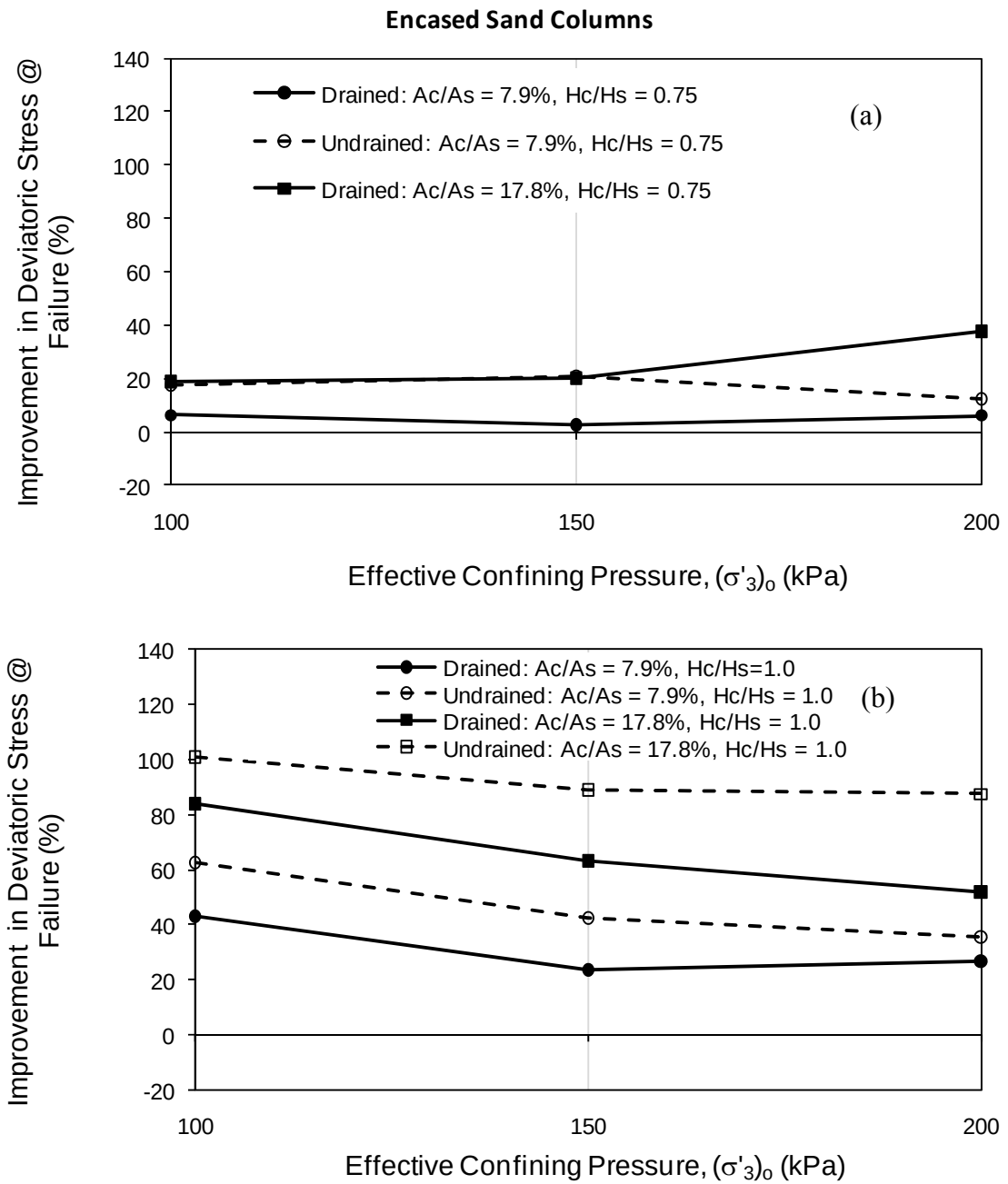

Fig. 6.13 Improvement in the deviatoric stress at failure for (a) partially penetrating encased sand columns and (b) fully penetrating encased sand columns for drained and undrained tests.

6.2.4.3. Comparison between the Shear Strength Parameters

The effective shear strength parameters that were obtained from drained and undrained tests on samples reinforced with encased columns and tested at effective confining pressures of 100, 150 and 200 kPa are presented in Table 6.3 for comparison. The corresponding Mohr coulomb failure envelopes are shown in Figs. 6.14 and 6.15 for clay specimens reinforced with encased 2-cm and 3-cm diameter sand columns, respectively.

For specimens that were reinforced with partially penetrating 2-cm encased sand columns, very little improvements in the load carrying capacity were observed compared to control clay specimens. This translated into effective shear strength parameters (c' and ϕ') that were relatively similar to the control specimens (see Table 6.3 and Fig. 6.14a).

For specimens that were reinforced with fully penetrating 2-cm ordinary sand columns (see Table 6.3 and 6.14b), reductions in the effective friction angle ϕ' and increases in the apparent effective cohesive intercept c' were observed for the undrained test (ϕ' decreased from 26° to 18.5^{o} and c' increased from 0 kPa to 22 kPa) in comparison to the undrained control clay specimen. For the drained tests, ϕ' remained constant at 21° while c' increased from 0 kPa to 15 kPa. The increase in c' is expected and is generally related to the presence of the encasement which resulted in higher improvements in deviatoric stresses at failure at lower confining pressures as indicated in Fig. 6.14b. It is worth noting that despite the apparent differences in ϕ' and c' for the drained and undrained tests, a visual inspection of the Mohr Coulomb failure envelops on Fig. 6.14b indicates that the envelops for the drained and undrained tests are very close to each other and almost identical over a wide range of effective normal stresses. This observation is significant given the large difference that was observed for the drained and undrained envelops of the control clay specimens.

Table 6.3 Comparison between effective shear strength parameters for clay specimens reinforced with encased sand columns and tested under drained and undrained conditions.

Drainage Condition	Type of Column	Column Penetration Ratio	Area Replacement Ratio (%)	c' (kPa)	ϕ' (deg)
Drained	-	-	-	0.0	21.0
Drained	Encased	0.75	7.9	0.0	21.0
Drained	Encased	1	7.9	15	21.0
Drained	Encased	0.75	17.8	15	21.0
Drained	Encased	1	17.8	34	21.0
Undrained	-	-	-	0.0	26.3
Undrained	Encased	0.75	7.9	5.8	23.6
Undrained	Encased	1	7.9	22.3	18.4
Undrained	Encased	1	17.8	15.1	24.3

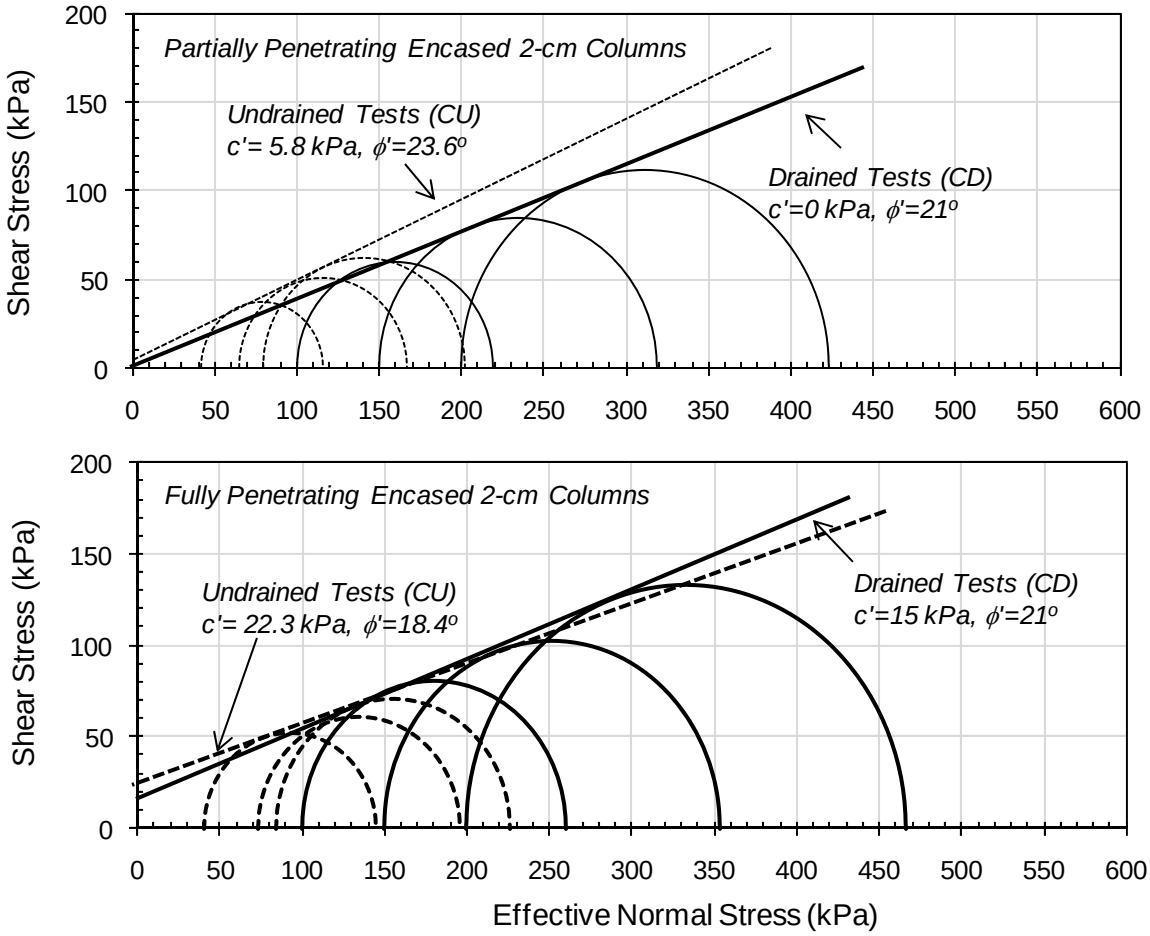

Fig. 6.14 Mohr-Coulomb failure envelopes (samples with encased 2-cm sand columns).

For specimens that were reinforced with partially penetrating 3-cm encased sand columns, no comparisons could be made between drained and undrained tests, since the undrained tests were not available. For specimens that were reinforced with fully penetrating 3-cm sand columns, an increase in *c'* was observed for both drained and undrained tests, with the increase in *c'* being higher for drained tests (*c'* increased from 0 to 34 kPa) compared to undrained tests (*c'* increased from 0 to 22 kPa). On the other hand, no change in the effective friction angle ϕ' was observed for the drained tests (ϕ' remained at 21°) and a very slight reduction in ϕ' was observed for the undrained tests (ϕ' reduced from 26° to 24°). Despite the apparent differences in ϕ' and *c'* for the drained and undrained tests, the envelops for the drained and undrained tests were observed to close to each other over a wide range of effective stresses.

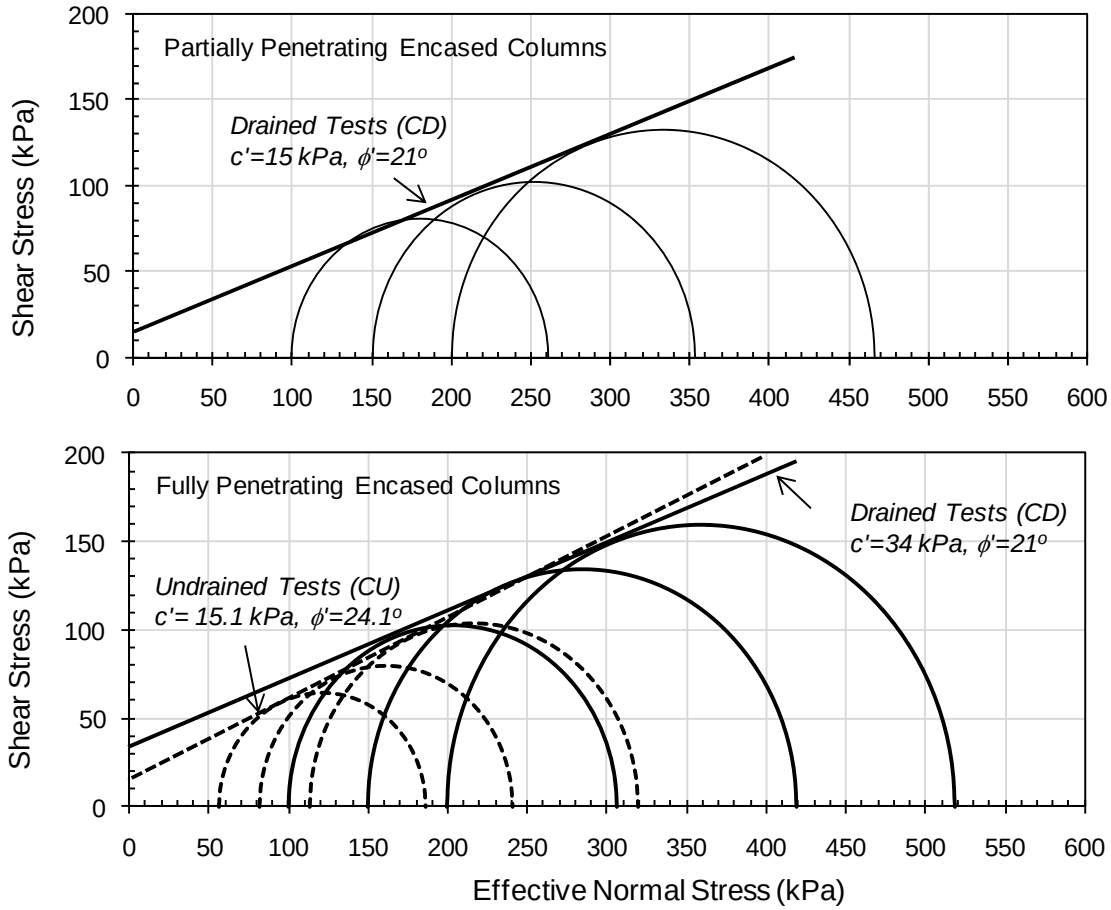

Fig. 6.15 Mohr-Coulomb failure envelopes (samples with encased 3-cm sand columns)

6.2.4.4. Comparison between Secant Young's Modulus

Calculated values of $(E_{sec})_{1\%}$ for drained and undrained tests using encased columns are presented in Table 6.1 and plotted in Fig. 6.16 versus the confining pressure for comparison. For the undrained tests involving partially and fully penetrating 2-cm (A_c/A_s=7.9%) columns, very minor improvements were observed in the values of $(E_{sec})_{1\%}$ for all confining pressures. For the drained tests involving partially and fully penetrating 2-cm (A_c/A_s=7.9%) columns, slight reductions in $(E_{sec})_{1\%}$ were observed for confining pressures of 100 kPa and 150 kPa, and very minor improvements were observed in $(E_{sec})_{1\%}$ at a confining pressure of 200 kPa.

For samples that were reinforced with partially penetrating 3-cm sand columns, no improvements were witnessed in the drained tests at confining pressures of 100 and 150 kPa and an improvement of about 50% in $(E_{sec})_{1\%}$ was observed for a pressure of 200 kPa. For samples that were reinforced with fully penetrating 3-cm columns consistent increases in $(E_{sec})_{1\%}$ were observed for the drained tests reaching about 80% for confining pressures of 100 and 150 kPa, and about 34% for a pressure of 200 kPa. For the undrained tests, an average improvement of about 50% was observed in the value of $(E_{sec})_{1\%}$ for the different confining pressures.

As mentioned in chapter 5 of this thesis, the complex response observed for $(E_{sec})_{1\%}$ for drained clay/sand composites could be attributed to the effects of sample preparation, where the response of the sand column could be affected negatively by any reduction in the contact stresses (confinement) between the column material and the surrounding clay due to column installation. This effect is magnified in drained tests (compared to undrained tests) since volume changes at the initial stages of loading are significant in drained test, especially for the sand column that is expected to dilate at relatively small strains and will start to transfer part of its load to the surrounding clay.

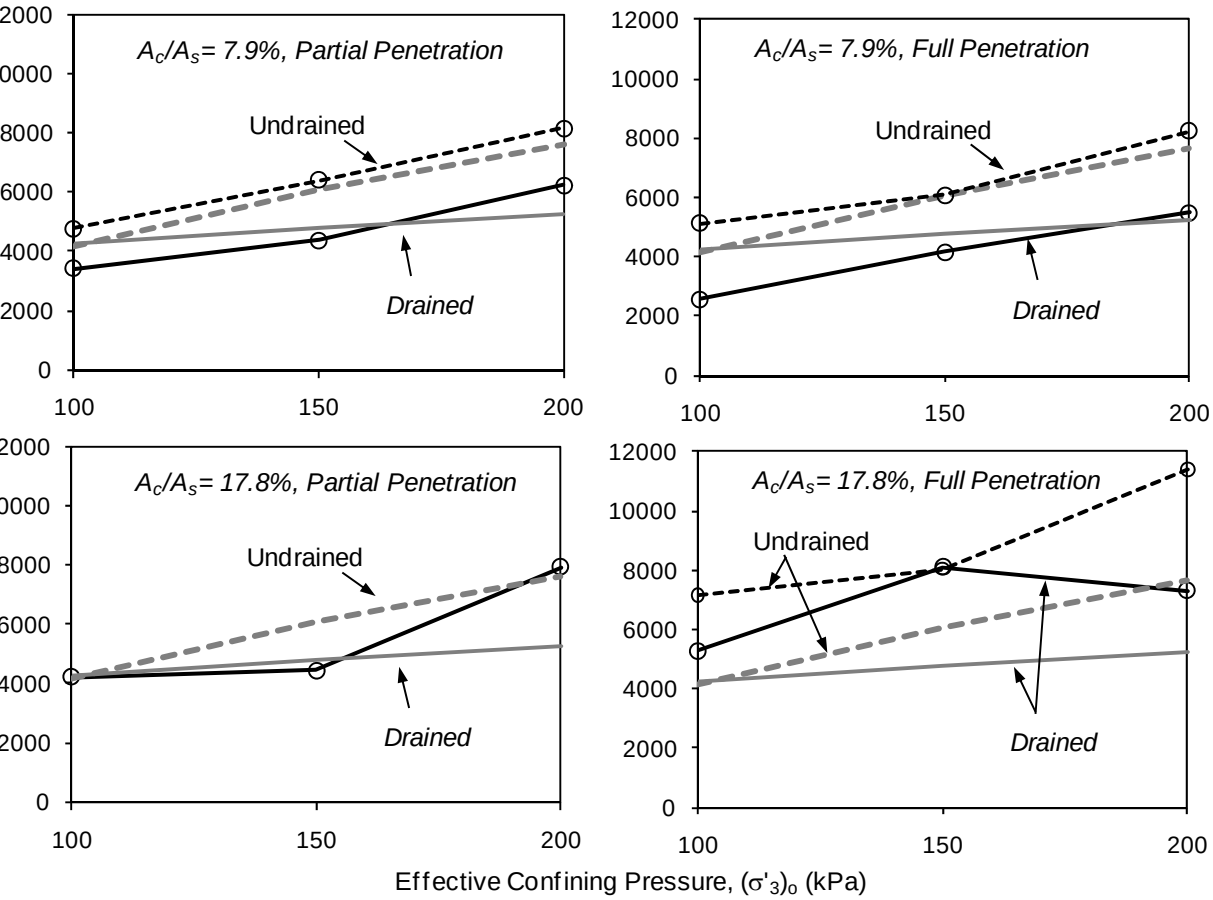

ation of (Esec)1% with effective confining pressure for samples reinforced with encased sand columns.

6.3. Summary of Main Findings

Based on a comparison between the 27 consolidated drained triaxial tests that were conducted in this experimental research study and 24 consolidated undrained triaxial tests that were reported in Najjar et al. (2010), the following conclusions can be drawn with regards to the difference in the drained and undrained load response of the composite clay:

1. For the control clay, a significant difference was observed in the effective friction angle ϕ' obtained from the CD tests ($\phi' = 21^o$) and the CU tests with pore pressure measurement ($\phi' = 26^o$). The difference could be attributed to the significant difference in the mean effective confining pressures at failure and the rate of loading between the drained and undrained tests. This difference was higher than expected and lead to some complications in the analysis of results of the reinforced clay specimens.

2. Based on a thorough analysis of the variation of the deviatoric stress, pore pressure, and volumetric strain with axial strain for ordinary and encased columns, and based on a quantitative analysis of the percent improvement in the deviatoric stresses at failure, it is concluded that:

- The percent improvement in the deviatoric stress at failure for the undrained tests was consistently higher than the improvement observed for the drained tests. This observation could lead to the conclusion that sand columns are more efficient at increasing the load-carrying capacity of soft clays in an undrained setting than in a drained setting.
- Although the percent improvement in the deviatoric stress at failure was higher for undrained tests, the absolute values of the deviatoric stress at failure were still much higher for drained tests, signifying that the drained load response could

likely represent an upper bound in the shear strength of the reinforced clay specimens analyzed in this study.

- This indicates that in field applications involving the use of sand columns in soft clays, it is expected that the drained shear strength which will govern the behavior of the reinforced clay for long-term conditions would likely be greater than the undrained shear strength which governs the stability of the reinforced clay in the short term.

3. An analysis of the effective Mohr-Coulomb failure envelops from drained and undrained tests indicated that:

- The use of 2-cm columns (partially and fully penetrating) does not generally result in any significant improvement in the effective failure envelops in reference to the control specimens. The only exception is the case involving fully penetrating encased columns, which exhibited an increase in c' and a more-or-less constant ϕ'.
- The use of 3-cm columns (partially and fully penetrating) resulted generally in improvements in the Mohr-Coulomb failure envelops, with the improvements being the most evident with fully penetrating encased columns.
- The utilization of c' and ϕ' solely as a basis for comparing the effective shear strength envelops from drained and undrained tests might not be indicative of the differences in the results, since c' and ϕ' from drained and undrained tests are not derived from the same range of effective stress.

- It is observed that differences in the failure envelops from drained and undrained tests tend to become smaller as the differences in the mean effective stresses between drained and undrained tests become smaller.

4. A secant Young's modulus $(E_{sec})_{1\%}$ defined at an axial strain of 1% was used as a basis for comparing the effect of drainage on the stiffness of the reinforced clay specimens. Results indicated that for specimens with a given area replacement ratio and a column penetration ratio, the undrained $(E_{sec})_{1\%}$ was generally found to be larger in magnitude than the drained $(E_{sec})_{1\%}$. In addition, the undrained $(E_{sec})_{1\%}$ exhibited consistent increases in reinforced specimens compared to control specimens. This was not the case for the drained $(E_{sec})_{1\%}$ which was found to decrease compared to the control specimens, especially for tests conducted at smaller confining pressures where the effects of column installation could have played a role in the reduction in $(E_{sec})_{1\%}$.

CHAPTER 7

CONCLUSIONS, RECOMMENDATIONS, AND FURTHER RESEARCH

7.1. Introduction

This chapter includes the main concluding remarks and observations resulting from the drained triaxial testing program conducted on 27 Kaolin specimens that were prepared from slurry, consolidated in a prefabricated 1-dimensional consolidometer, and reinforced with either ordinary or encased sand columns with different column penetration ratios (H_c/H_s= 0.75, and 1) and different area replacement ratios (A_c/A_s=7.9% and 17.8%). The data collected from the CD tests highlighted the effect of sand columns on the stiffness, drained shear strength, and the volumetric strain for the reinforced clay. An effort was also made to compare the load response of the drained tests with the response observed by Najjar et al. (2010) for identical samples that were tested under undrained conditions. Recommendations and further research works are also discussed in this chapter.

7.2. Conclusions

Based on the results of 27 consolidated drained triaxial tests that were conducted in this experimental research study, the following conclusions can be drawn with regards to the reliability of the testing procedure used and the effect of sand columns on the drained load response of soft clay, volumetric strains during drained loading, stiffness of reinforced clay, and effective shear strength parameters:

1. The specimen preparation method used in this study resulted in repeatable test specimens with acceptable variations in density for the clay specimens and the sand columns. The average and standard deviation of the bulk density of the clay were 16.13 kN/m^3 and 0.08 kN/m^3, respectively corresponding to an average void ratio of 1.34 and a standard deviation of 0.03. The average bulk density for the sand columns was found to be 19.4 kN/m^3 with a standard deviation of 0.12 kN/m^3. The relatively small variations observed in the densities of the kaolin clay and the sand columns indicated that friction in the 1-D consolidometers was minimal and that the specimen preparation procedure and the column preparation method were generally repeatable.

2. Reinforcing normally consolidated soft kaolin specimens with sand columns at an area replacement ratio of 7.9% resulted in reductions in $(E_{sec})_{1\%}$, with the only exceptions being tests conducted with encased columns at a confining pressure of 200 kPa. For tests conducted using area replacement ratios of 17.8%, increases in $(E_{sec})_{1\%}$ were observed for fully penetrating columns at all confining pressures and for partially penetrating columns at a confining pressure of 200 kPa.

3. The inclusion of 3-cm sand columns in the clay reduced appreciably the contractive volumetric strains of the clay specimens, with the reduction being more significant for tests involving fully penetrating sand columns, which are expected to be more dilative compared to partially penetrating columns. No significant reductions in volumetric strains were observed for samples reinforced with the 2-cm columns. For cases involving ordinary columns, a correlation was observed between reductions in volumetric strains and increases in deviatoric stresses at failure. Such a correlation was not present in samples with encased columns.

4. An investigation of the variation of the drained secant modulus (E_{sec}) with strain indicated that the secant modulus for reinforced and control specimens decreases as the axial strain increases, with specimens that are reinforced with sand columns exhibiting a sharp drop in the secant stiffness for strains that are less than 1% to 2%. After a strain of 2%, the secant stiffness decreases with strain at a decreasing rate. An analysis indicates that the equilibrium equation presented in Baumann and Bauer (1974) could be utilized together with data from tests conducted on the control clay and control sand specimens to provide representative predictions of the variation of E_{sec} with strain given a certain area replacement ratio.

5. The use of ordinary 2-cm diameter sand columns did not result in notable increases in the deviatoric stress at failure except for the case of fully penetrating columns with a confining pressure of 100 kPa (increase of 17.6%). When the 2-cm columns were encased, the improvement at 100 kPa increased to 41.3%, while improvements in the order of 25% were observed for confining pressures of 150 and 200 kPa. For the higher area replacement ratio of 17.8%, improvements ranging from 31.2% to 51.5% were observed for samples reinforced with fully penetrating ordinary columns and from 17% to 25% for partially penetrating ordinary columns. For samples with encased columns, additional improvements in the deviatoric stress at failure were observed due to the encasement, with the improvement ranging from 51.9% to 83.9% for specimens reinforced with fully penetrating columns and from 19% to 37.5% for partially penetrating columns.

6. For clay specimens that were reinforced with partially penetrating 2-cm sand columns, the effective friction angle ϕ' and the apparent cohesion c' were not

significantly affected by the presence of the sand columns. For fully penetrating 2-cm columns, non-zero c' values were observed and were associated with unchanged or slightly reduced ϕ' values compared to the control clay specimens. The non-zero c' values reflect the improvements in deviatoric stresses at failure at the lower confining pressure of 100 kPa compared to the higher confining pressures of 150 and 200 kPa.

7. For the larger area replacement ratio of 17.8% improvements in ϕ' were observed for ordinary columns (ϕ' increased from 21º for the control clay to 23º for partially penetrating columns to 26º for fully penetrating columns), while improvements in c' were observed for encased columns (c' values increased from 0 kPa for control samples to 15 kPa for partially penetrating columns to 34 kPa for fully penetrating columns). These results of encased columns are in line with previous research which shows that encasing sand columns with geosynthetics results in non-zero cohesive intercepts (Wu and Hong 2009), with the increases in c' being associated with no improvements in the friction angle ϕ'.

8. A comparison between the improvements observed in drained and undrained tests shows that the inclusion of sand columns in soft clays would increase the undrained strength of a clay more effectively than the drained strength. However, the drained strength at a given confining pressure was found to be consistently greater in magnitude than the undrained strength.

9. The above observation indicates that in field applications, the undrained strength of the composite system will likely govern the bearing capacity of the reinforced clay. This conclusion needs to be confirmed with further tests.

10. A comparison between $(E_{sec})_{1\%}$ from identical drained and undrained tests indicates that except for test cases with a confining pressure of 100 kPa, the stiffness of the specimens as indicated by $(E_{sec})_{1\%}$ was larger for the undrained tests, due to the stronger dependency of the undrained stiffness of the control clay specimens on the effective confining pressure. Interestingly, the values of $(E_{sec})_{1\%}$ for specimens with an area replacement ratio of 7.9% from drained tests exhibited a reduction in $(E_{sec})_{1\%}$, compared to control tests.

11. The utilization of c' and ϕ' solely as a basis for comparing the effective shear strength envelops from drained and undrained tests might not be indicative of the differences in the results, since c' and ϕ' from drained and undrained tests are not derived from the same range of effective stress. It is observed that differences in the failure envelops from drained and undrained tests tend to become smaller as the differences in the mean effective stresses between drained and undrained tests become smaller.

7.3. Recommendations

Based on the test results reported in this study, it can be concluded that reinforcement of soft normally consolidated clays with sand columns can significantly increase the stiffness and shear strength of the soft clay. The degree of improvement in the stiffness and drained shear strength can be enhanced by increasing the area replacement ratio of the column and extending the column length to full penetration. Results also show that encasing the columns with geotextile fabrics can increase their performance and will generally lead to increases in the stiffness and strength of the reinforced clay specimen.

For practical cases that involve the use of sand columns with similar properties to the

sand used in this study (friction angle of about 33 degrees) to improve the mechanical properties of normally consolidated clays that have similar index and strength properties to the Kaolin tested in this study ($S_u/\sigma'_v = 0.3$), it can be recommended based on the limited drained tests conducted in this study and based on the undrained tests reported in Najjar et al. (2010) that the clay be improved with sand columns having a length to diameter ratio of at least 6 at an area replacement ratio that is greater than 17.5% to ensure an improvement that is greater than 65% in the undrained shear strength. This improvement in the undrained shear strength can be relied on for improving the short term strength of the clay without compromising the long term drained strength of the unreinforced clay.

The limited tests that were conducted in this study on samples that were reinforced with sand columns that were encased with geotextile fabric did not allow for design recommendations to be specified. Generally, the results indicate that for practical cases, sand columns can be encased with geotextile fabrics to enhance the undrained shear strength and the stiffness of the reinforced clay material. This means that a target degree of improvement in undrained shear strength can be obtained by using shorter columns and/or smaller area replacement ratios provided that the sand columns be confined with a geotextile fabric. In this case, several parameters which include the strength of the fabric, the confining pressure, the strengths of the sand and the clay, and the geometry of the column are expected to affect the detailed design of reinforced clay system. The determination of the effect of all these parameters on the design of encased sand columns will require more research as proposed in the following section.

7.4. Further Research

- Perhaps the most relevant extension of the current work is conducting triaxial tests using different rates of loading while allowing drainage of the clay through the sand columns. This model would represent the actual drainage conditions in the field while maintaining a representative stress state that is similar to that of the field.
- Since the strength of the sand column is expected to be dependent on the density and shear strength of the granular material, it will be valuable for any future researcher to use a higher angle of friction for the column material to study its effect on the mechanical properties of reinforced soft clay. The results of such tests can be combined with the test results obtained in this research study to isolate the effect of the friction angle of the sand column on the degree of improvement.
- Most of the previous research works addressed the "foundation loading" concept, where the load is directly applied to the column. Hence, an important research study can involve adjusting and modifying the available "TruePath" automated triaxial equipment to allow loading of the column directly instead of loading the entire area in "uniform loading" as was done in the current research study. In that case, the ultimate load carrying capacity of the column can be checked and compared with the available column prediction strength capacity equations (ex. Hughes and Withers 1974).
- Conducting drained and undrained triaxial tests on samples that are reinforced at high area replacement ratio (around 30%) could provide a better representation of the area replacement ratios that are commonly used in practical field applications involving sand or stone columns.
- The effect of geotextile confinement can be further studied by encasing the sand columns

with geotextiles having different stiffnesses, so that the effect of the strength of the geotextile fabric can be studied and analyzed.

APPENDIX

1. DEVIATORIC STRESS AND VOLUMETRIC STRAINS VERSUS AXIAL STRAINS FOR PARTIALLY PENETRATING SAND COLUMNS

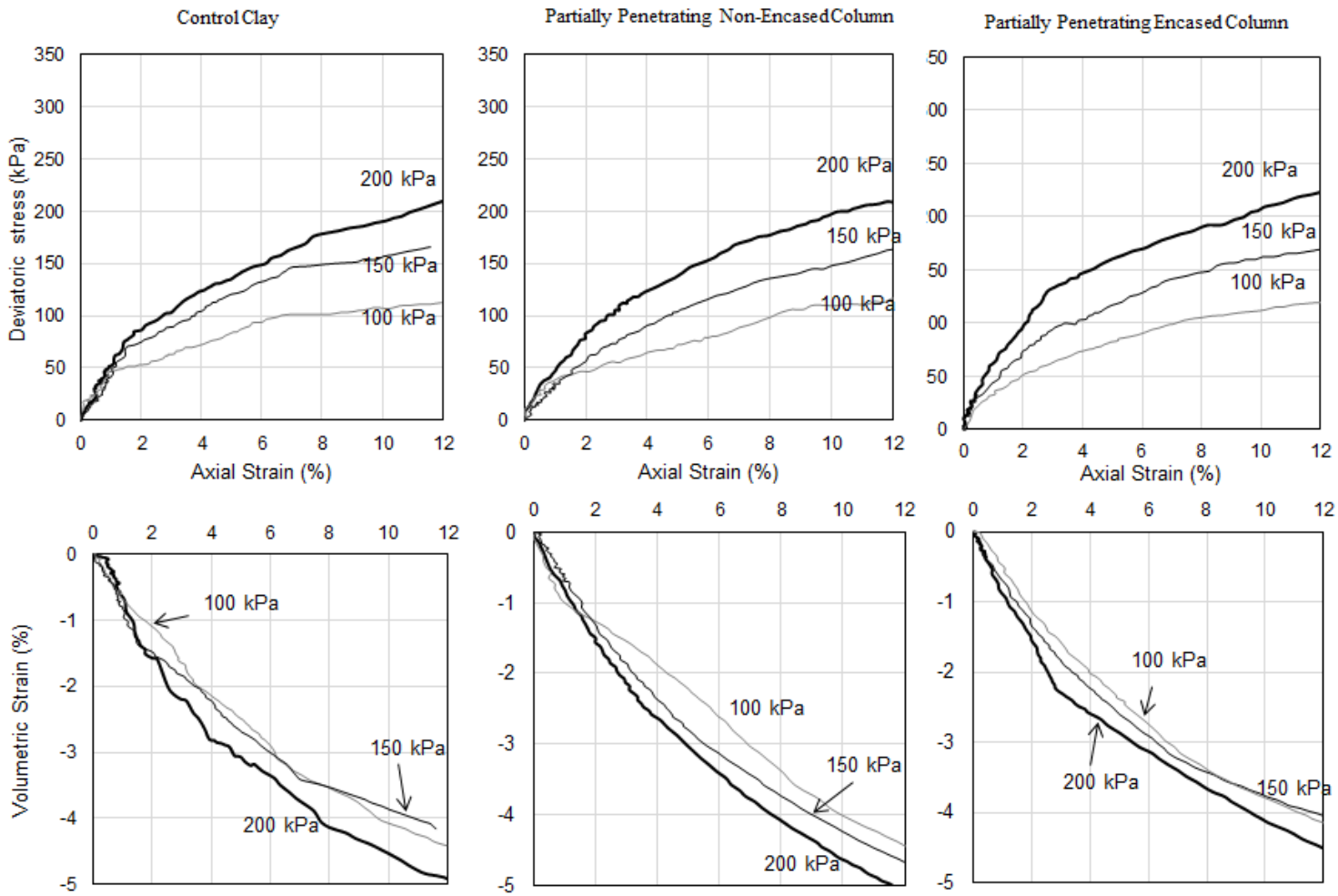

Fig.A.1 Deviatoric stress and volumetric strain versus axial strain for partially penetrating sand columns encased and non-encased for confining pressures of 100, 150 and 200kPa

2. DEVIATORIC STRESS AND VOLUMETRIC STRAINS VERSUS AXIAL STRAINS FOR FULLY PENETRATING SAND COLUMNS

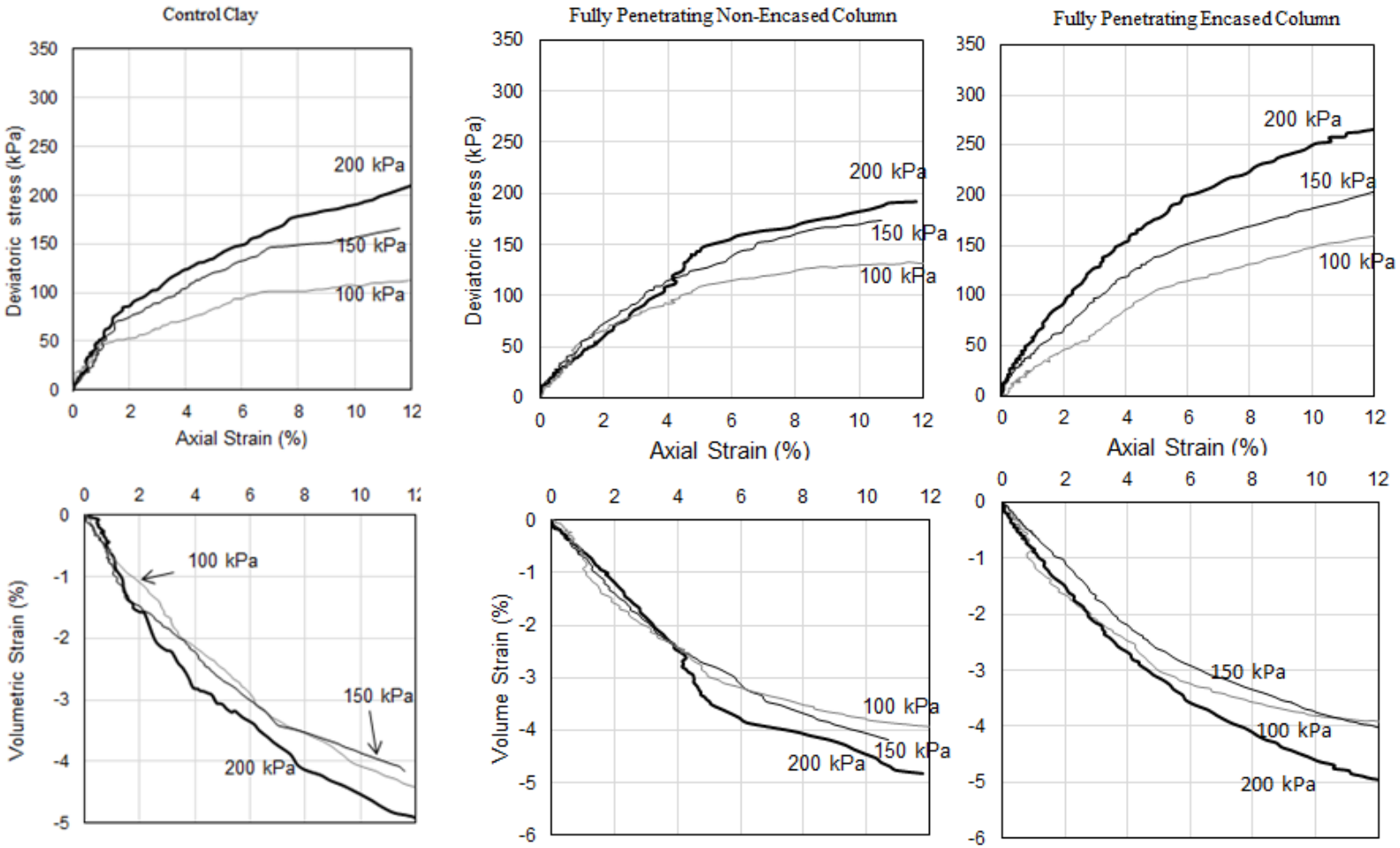

Fig.A.2 Deviatoric stress and volumetric strain versus axial strain for fully penetrating sand columns encased and non-encased for confining pressures of 100, 150 and 200kPa

REFERENCES

Alamgir, M., Miura, N., Poorooshasb, H. B., and Madhav. M. R. (1996), "Deformation analysis of soft ground reinforced by columnar inclusions" Computers and Geotechniques, Vol. 18, No. 4, pp. 267-290

Ambily, A. P., Gandhi, S. R., (2007), "Behavior of stone columns based on experimental and FEM analysis," Journal of Geotechnical and Geoenvironmntal Engineering, ASCE, Vol. 133, No. 4, April, pp. 405-415.

Andreou, P., Frikha, W., Frank, R., Canou, J., Papadopoulos, V., and Dupla, J. C. (2008), "Experimental study on sand and gravel columns in clay," *Ground Improvement*, Vol. 161, No. 4, pp. 189-198.

Ayadat, T. and Hanna, A. M. (2005), "Encapsulated stone columns as a soil improvement technique for collapsible soil," Ground Improvement, Vol. 9, No. 4, pp. 137-147.

Bauman, V. and Bauer, G. E. A. (1974), "The performance of foundations on various soils stabilized by the vibro-compaction method," Canadian Geotechnical journal, Vol. 11, No. 4, pp. 509-530.

Black, J., Sivakumar, V., Madhav, M. R., and McCabe, B. (2006), "An improved experimental set-up to study the performance of granular columns," Geotechnical Testing Journal, ASTM, Vol. 29, No. 3, pp. 193-199.

Black, J. V., Sivakumar, V., and McKinley, J. D. (2007), "Performance of clay samples reinforced with vertical granular columns," Canadian Geotechnical Journal, Vol. 44, February, pp. 89-95.

Black, J. V., Sivakumar, V., and Bell, A. (2011), "The settlement performance of stone column foundations," *Geotechnique*, Vol. 61, No. 11, pp. 909-922.

Cimentada, A., Da Costa, A., Canizal, J., and Sagaseta, C. (2011), "Laboratory study on radial consolidation and deformation in clay reinforced with stone columns," *Canadian Geotechnical Journal*, Vol. 48, pp. 36-52.

Fattah, M. Y., Shlash, K. T., and Al-Waily, M. J. M. (2011), "Stress Concentration Ratio of Model Stone Columns in Soft Clays," *Geotechnical Testing Journal*, ASTM, Vol. 34, No. 1, pp. 1-11.

Gniel, J. and Bouazza, A. (2009), "Improvement of soft soils using geogrid encased stone columns," *Geotextiles and Geomembranes,* Vol. 27, No. 3, pp. 167–175.

Hughes, J. M. O., and Withers, N. J. (1974), "Reinforcing of soft cohesive soils with stone columns," Ground Engineering, Vol. 7, May, No.3, pp. 42-49.

Juran, I., and Guermazi, A. (1988). "Settlement response of soft soils reinforced by compacted sand columns," *Journal of Geotechnical Engineering,* ASCE, Vol. 114, No. 8, pp. 930–943.

Kim, B. I. and Lee, S. H. (2005), "Comparison of bearing capacity characteristics of sand and gravel compaction pile treated ground," *Journal of Civil Engineering*, KSCE, Vol. 9, No. 3, pp. 197-203.

Malarvizhi, S. N. and Ilamparuthi, K. (2004), "Load versus settlement of claybed stabilized with stone and reinforced stone columns," Proceedings of Geo-Asia-2004, Seoul, Korea, pp. 322-329.

McKelvey, D., Sivakumar, V., Bell, A., and Graham J. (2004), "Modeling vibrated stone columns in soft clay," Proceedings of the Institute of Civil Engineers Geotechnical Engineering, Vol. 157, Issue GE3, pp. 137-149.

Muir Wood, D., Hu, W., and Nash, D. F. T. (2000), "Group effects in stone column foundations: Model tests," Geotechnique, Vol. 50, No. 6, pp. 689-698.

Murugesan, S. and Rajagopal, K. (2008), "Performance of Encased stone columns and design guidelines for construction on soft clay soils," *Proceedings of the 4th Asian Regional Conference on Geosynthetics*, June 17 - 20, Shanghai, China, pp. 729-734.

Murugesan, S. and Rajagopal, K. (2010), "Studies on the behavior of single and group of geosynthetic encased stone columns," *Journal of Geotechnical and Geoenvironmntal Engineering*, ASCE, Vol. 136, No. 1, pp. 129-139.

Najjar, S.S., Sadek, S., and Maakaroun, T. (2010), "Effect of sand columns on the undrained load response of soft clays", *Journal of Geotechnical and Geoenvironmental Engineering*, ASCE, Vol. 136, No. 9, pp. 1263-1277.

Narasimha Rao, S., Prasad, Y. V. S., and Hanumanta Rao, V. (1992), "Use of stone columns in soft marine clays," *Proceedings of the 45th Canadian Geotechnical Conference*, Toronto, Ont., Can. Canadian Geotechnical Society, October, pp. 9/1-9/7.

Shahu, J. T., and Reddy, Y. R., (2011), "Clayey soil reinforced with stone column group: model tests and analyses," *Journal of Geotechnical and Geoenvironmntal Engineering,* ASCE, Vol. 137, No. 12, pp. 1265-1274.

Sivakumar, V., McKelvey, D., Graham, J., and Hughus, D. (2004), "Triaxial tests on model sand columns in clay," Canadian Geotechnical Journal, Vol. 41, April, pp. 299-312.

Sivakumar, V., Jeludine, D. K. N. M., Bell, A., Glyn D. T., and Mackinnon, P. (2011), "The pressure distribution along stone columns in soft clay under consolidation and foundation loading," *Geotechnique*, Vol. 61, No. 7, pp. 613-620.

Wu, C. S. and Hong, Y. S. (2009), "Laboratory tests on geosynthetic-encapsulated sand columns," *Geotextiles and Geomembranes*, Vol. 27, pp. 107–120.